

PREDICTING POPULATION TRENDS UNDER ENVIRONMENTAL CHANGE: COMPARING METHODS AGAINST OBSERVED DATA

Fiona Elizabeth Bridget Spooner

A thesis submitted in partial fulfilment of the requirements for the degree of:

Doctor of Philosophy of

University College London 2019

Primary supervisor:

Prof. Richard G. Pearson

Secondary supervisor:

Dr Robin Freeman

I, Fiona Elizabeth Bridget Spooner, confirm that the work presented in this thesis is my own. Where information has been derived from other sources, I confirm that this has been indicated in the thesis

ABSTRACT

In this thesis I examine a range of approaches for predicting the impact of recent climate change and land use change on observed population trends. The thesis is split into three main parts. Firstly, I used linear mixed effects models to provide the first global assessment of the effects of environmental change on bird and mammal population trends. I find that populations have declined more rapidly in areas which have experienced rapid warming, this effect was more pronounced in bird populations.

Secondly, I built habitat suitability models for 16 mammal species to explore the relationship between predicted habitat suitability and population abundance. I explored the correlations between time-series of rates of change in habitat suitability and corresponding time-series of observed population growth rates. There was little evidence to support the idea that population growth rates are directly linked to habitat suitability. However, when lagged responses are considered there is a stronger positive relationship between changes in habitat suitability and population growth rates, highlighting the importance of biodiversity time-series.

Lastly, I built coupled niche-demographic (CND) models for three mammal species: Alpine ibex, brown bear and red deer. These are habitat suitability models linked with population models with dispersal mechanisms; they can be used to predict species abundance trends. CND models have been assumed have greater predictive accuracy than habitat suitability models, but there has been limited validation of CND model predictions against observed data. I found that CND models are an improvement on habitat suitability models. However, both sets of models perform relatively poorly. Simpler linear mixed effects models were able to provide more accurate estimates of average population growth. This suggests that

the high data requirements and computational resources needed to run CND models may be excessive, as currently, more parsimonious models provide better predictions of population growth rates.

IMPACT STATEMENT

In recent decades global biodiversity has faced multiple human-driven threats, leading to extinction rates being 1,000 times higher than expected. Two of the most significant threats to biodiversity are climate change and loss of habitat to anthropogenic land use. Both processes are anticipated to continue to threaten biodiversity for the foreseeable future. Understanding the patterns and processes of these threats on biodiversity is crucial to the effective conservation of populations and the consequent maintenance of ecosystem function. In this thesis I examined a range of approaches for predicting the impacts of recent climate change and land use change on observed animal population trends. I focussed on population trends of terrestrial birds and mammals, as these species tend to be well studied, and there is sufficient information available on them to build models across a spectrum of complexity.

In Chapter Two I analysed the recent impacts of climate change and land use change on observed bird and mammal population trends (1950-2005), providing the first global study of the impacts of recent environmental change on vertebrate population trends. I found that both bird and mammal population trends have declined fastest in locations where mean temperature has increased most rapidly, this effect is more noticeable in birds. This work has been published in a leading international peer reviewed journal and has been presented to a range of audiences, most notably a major international conservation conference. This work was also included in the Living Planet Report (2018), a biennial report produced by WWF which receives high levels of publicity. Additionally, this work was cited in a Scientific American article – “Trump to Curb Protections as Warming Endangers Species”.

This thesis also assesses the predictive accuracy of a novel modelling techniques by comparing predictions of population trends to observed population trends. There is potential for this technique to be used to estimate species extinction risk due to climate change, which would have major policy impact. However, this technique has not yet been validated against observed population trends and this is what I present in this thesis. The outputs of this work will be brought about through publication in high-impact journals.

ACKNOWLEDGEMENTS

First and foremost, I would like to thank my supervisors, Prof. Richard G. Pearson and Dr Robin Freeman for their support and guidance throughout the last four years. Their enthusiasm, ideas and knowledge have been invaluable, and without them this thesis this would not exist. I have been lucky to be part of two friendly and vibrant research groups, the Centre for Biodiversity and Environment Research at UCL and the Institute of Zoology. Both centres are filled with wonderful people who have ensured the last four years have passed by easily and enjoyably.

This thesis is entirely dependent on several open source datasets of software packages, so I would like to extend my gratitude to everyone that contributed to each of these. In particular, this thesis would not have been possible without the Living Planet database, which has been meticulously built and curated by many excellent people at the Indicators and Assessments Unit at the Institute of Zoology, to whom I am very grateful.

I'm thankful for my friends both inside and outside the office for providing advice and welcome escapes from PhD life. Special thanks to the Gigglegang, Sam Jones, Leejiah Dorward, Kate & Tom Harvey, Anthony Dancer, Paul Barnes, Dan Bayley, Sergio Henriques, Guilherme Fereira, Henry Ferguson-Gow, Heidi Ma, Harry Owen and Thalassa McMurdo Hamilton.

Finally, I would like to thank my amazing girlfriend Michaela who has been an incredible support every step of the way, and my family without whom I would not have started this PhD, let alone finished it.

TABLE OF CONTENTS

Predicting Population Trends Under Environmental Change: Comparing Methods Against Observed Data.....	i
Abstract.....	i
Impact Statement.....	iii
Acknowledgements.....	v
Chapter One: Introduction.....	1
Drivers of Biodiversity Loss.....	2
Habitat Loss.....	2
Climate Change.....	3
Interactions Between Climate Change and Habitat Loss.....	4
Measuring The Impacts of Environmental Change.....	5
Predicting Species Responses to Environmental Change.....	6
Habitat Suitability Models.....	6
Coupled Niche-Demographic Models.....	7
Validating Predicted Species Responses.....	8
Thesis Overview.....	9
Chapter Two: Rapid Warming is Associated with Population Decline Among Terrestrial Birds and Mammals Globally.....	12
Abstract.....	13
Introduction.....	13
Materials and Methods.....	16
Population Time Series Data.....	16
Climate Data.....	19
Land Use Data.....	19
Body Mass.....	20
Protected Areas.....	20
Linear Mixed Effects Models.....	21
Results.....	22
Discussion.....	27
Chapter Three: Predicting Population Trends from Habitat Suitability Models.....	33
Abstract.....	34
Introduction.....	34
Materials and Methods.....	38

Habitat Suitability Modelling.....	38
Observed Population Trends	43
Habitat Suitability Trends	44
Comparison of Habitat Suitability Trends and Population Trends	44
Results	45
Discussion.....	49
Chapter Four: Assessing the predictive ability of coupled niche-demographic models....	52
Abstract.....	53
Introduction	53
Materials and Methods	55
Habitat Suitability Models	56
Coupled Niche-Demographic Models.....	57
Model Assessment.....	62
Results	64
Discussion.....	70
Chapter Five: Discussion	76
Overview	77
Comparisons to the Literature	80
Drivers of Biodiversity Loss	80
Predicting Species Responses to Environmental Change	81
Caveats and Limitations	82
Data Limitations and Scale	83
Couple Niche-Demographic Model Limitations.....	85
Future Directions	86
Conclusions	87
References.....	89
Appendices.....	108
Model Averaging.....	108
Chapter Two Appendix	110
Future Projections.....	112
Including a Wider Set of Population Trends	115
Spatial Heterogeneity in the Data	119
Species Traits.....	121
Alternative Land Use Change Data	124

Chapter Three Appendix	130
Chapter Four Appendix	134
R Code Used For Coupled Niche-Demographic Models.....	138

CHAPTER ONE: INTRODUCTION

DRIVERS OF BIODIVERSITY LOSS

Over recent centuries, global biodiversity has faced increasing pressures from human activities, such as habitat fragmentation, introduction of non-native species, direct exploitation and climate change (Barnosky *et al.*, 2011). These human-induced threats have led to high rates of species extinctions which are estimated to be 1,000 times the background rate (De Vos *et al.*, 2015). Alongside extinctions, species have undergone substantial range losses (Ceballos & Ehrlich, 2002; Rodríguez, 2002; Thomas, 2004) and declines in abundance (Stuart *et al.*, 2004; Craigie *et al.*, 2010; WWF, 2018). Human impacts are pervasive; almost a third of protected areas are estimated to be under intense human pressure (Jones *et al.*, 2018), and increases in human footprint have been directly linked to increases in species extinction risk (Di Marco *et al.*, 2018). Biodiversity loss is having a profound impact on fundamental ecological processes, with the loss of ecosystem services costing >10% of the annual global gross product (IPBES, 2018). Species extinctions have caused declines in biomass production and decomposition rates (Hooper *et al.*, 2012); losses in marine biodiversity are associated with stock collapse and decreased water quality (Worm *et al.*, 2006); and habitat loss and land degradation are negatively impacting the well-being of 3.2 billion people (IPBES, 2018). Understanding the patterns and processes of the drivers of biodiversity loss is fundamental to providing effective conservation.

HABITAT LOSS

The primary driver of terrestrial species extinctions and population declines has been habitat loss and fragmentation (Millennium Ecosystem Assessment, 2005; Jetz, Wilcove, & Dobson, 2007; Vié, Hilton-Taylor, & Stuart, 2009), this is expected to continue throughout the twenty-first century (Sala, 2000). There is debate about the effect of habitat

loss on local species richness. It has been found that on average the effect of human induced habitat loss and fragmentation have decreased local species richness by 13.6% (Newbold *et al.*, 2015). However, it has also been found that over time local species assemblages have changed in composition, by becoming more homogenised, but there has not been a detectable decline in local species richness (Dornelas *et al.*, 2014).

Future land use change projections indicate that there will be multiple future extinctions in biodiversity hotspots (Jantz *et al.*, 2015) and that mammal population declines will be greatest in Africa and North America (Visconti *et al.*, 2011). Habitat loss threatens the continued provision of multiple simultaneous ecosystem services as this requires high species diversity (Cardinale *et al.*, 2012; Winfree *et al.*, 2018), because different species provide ecosystem functions at different places and different times (Isbell *et al.*, 2011). Habitat loss is thought to be the most prevalent cause of extinctions and population declines (Jetz, Wilcove and Dobson, 2007), however, anthropogenic climate change is increasingly considered to be an equal, if not more, important driver (Bellard, Bertelsmeier, Leadley, Thuiller, & Courchamp, 2012; Lemoine, Bauer, Peintinger, & Böhning-Gaese, 2007; Travis, 2003).

CLIMATE CHANGE

Between 1850 and 2005 average global surface temperatures increased by 0.61°C and are expected to increase by a further 0.3-0.7°C between 2016 and 2035 (IPCC, 2014). Climate change is a major global environmental threat and will be a key driver of biodiversity loss in the coming century (Brook *et al.*, 2009; Dawson *et al.*, 2011). Recent climate change has had significant ecological impacts (Parmesan, 2006), including changes in the distribution, abundance, demography and phenology of many species (Stevenson & Bryant, 2000; Walther *et al.*, 2002; Thomas *et al.*, 2004; Fordham *et al.*, 2013). Species distributions have shifted pole-ward at a median rate of 16.9km per decade and moved to higher elevations at

a median rate of 11m per decade (Chen *et al.*, 2011). Such changes have meant that some species, in particular those which are range restricted, are now at risk from extinction due to severe losses in climatically suitable habitat (Freeman, Scholer, Ruiz-Gutierrez, & Fitzpatrick, 2018; Parmesan, 2006).

Climate change has also influenced species abundance, a global meta-analysis showed that 80% of species have experienced abundance shifts in the direction predicted under climate change (Parmesan & Yohe, 2003). Additionally, climate change has been explicitly linked to population declines and extinction of range restricted amphibian species (La Marca *et al.*, 2005) and the abundance declines and local extirpations of high elevation tropical bird species (Freeman *et al.*, 2018). Climate change does not uniformly disadvantage all species. Warm-adapted bird species in Europe and the United States have increased in abundance since 1980, whereas cold-adapted species have declined (Stephens *et al.*, 2016). Similarly, abundances of warm-adapted European montane plant species have increased between 2000 and 2009, whilst cold-adapted species have declined (Gottfried *et al.*, 2012).

INTERACTIONS BETWEEN CLIMATE CHANGE AND HABITAT LOSS

Habitat loss and climate change are both major drivers of global biodiversity loss, and they do not act in isolation. Habitat loss is a major contributor to climate change, whilst climate change can exacerbate the impacts of habitat loss (IPBES, 2018). Meta-analyses have shown the effects of habitat loss and fragmentation are greatest in areas where maximum temperature is highest (Mantyka-Pringle, Martin and Rhodes, 2012). However, the mechanisms by which these two processes interact and the impact of this interaction on biodiversity is not well understood.

Habitat structure is an important determinant of meta-population dynamics and changes to land use can have impacts on habitat patch size and connectivity. This loss of connectivity can diminish the ability of a species to shift its distribution (Oliver and Morecroft, 2014), which is a common response of species to climate change (Chen *et al.*, 2011). This means that the impacts of climate change may be more severe where habitat loss has occurred. However, dry-adapted generalist species have been found to prosper in agricultural landscapes which have undergone climate warming (Frishkoff *et al.*, 2016).

MEASURING THE IMPACTS OF ENVIRONMENTAL CHANGE

Biodiversity loss is often measured in terms of species richness and extinctions, however these are relatively coarse units (Dirzo *et al.*, 2014; Selwood, Mcgeoch and Mac Nally, 2015). There can be significant population declines within an ecosystem, causing breakdown of ecosystem function, but this will not be reflected in measures of species richness if no species become locally extinct (Ceballos and Ehrlich, 2002). Extinction is a protracted process and species have often ceased to have any meaningful contribution to ecosystem function long before they become extinct (Säterberg, Sellman and Ebenman, 2013). Estimates of species richness can over-emphasise the contribution to ecosystem function of rare species and overlook declines of common species which may have a much greater impact (Winfrey *et al.*, 2015). However local animal population declines and changes in community composition can occur rapidly and have significant detrimental impacts on the ecosystems in which they occur (Dirzo *et al.*, 2014). In terms of measuring the services and function of an ecosystem, it is more useful to monitor population trends, rather than species richness (Ceballos and Ehrlich, 2002).

Despite its greater utility there are relatively few studies which use species abundance as the response metric when exploring the impacts of habitat loss and/or climate change on

biodiversity loss. This is because abundance is difficult and time-consuming to estimate compared to other metrics, such as occurrence (He and Gaston, 2000). Studies which have explored the effects of habitat loss and/or climate change on population trends are often limited to areas of greater data availability, for example Europe and North America (Lemoine *et al.*, 2007; Stephens *et al.*, 2016; Martay *et al.*, 2017). As a result, there has been no previous global multi-species assessment of the observed impacts of climate warming and habitat loss on population trends and this is what I address in Chapters Two and Three. I use the Living Planet database as a source of observed population trends. The Living Planet database is a long-term data set of population abundance data for vertebrate species (Loh *et al.*, 2005). There are currently records for >21,000 populations of 4,260 mammal, bird, reptile, amphibian and fish species from 1950-2017. The population trend data from the Living Planet database are taken from both grey and published literature, if certain criteria are fulfilled it is included in the database (for criteria see Loh *et al.*, 2005).

PREDICTING SPECIES RESPONSES TO ENVIRONMENTAL CHANGE

HABITAT SUITABILITY MODELS

A key area of ecological research is centred on predicting how species will respond to environmental change. A popular modelling approach, which has been used extensively to predict species responses to future change, is habitat suitability modelling (Thomas *et al.*, 2004). Habitat suitability models (which are synonymous with correlative niche models and species distribution models (Araújo & Peterson, 2012)) are used to statistically correlate species occurrence data with corresponding environmental variables. This is then used to identify statistically similar locations and estimate the distribution of suitable habitats (Kearney & Porter, 2004). This method of modelling is popular and well-established because habitat suitability models perform well at predicting species range

shifts in response to climate change (Araújo, Whittaker, Ladle, & Erhard, 2005). These models have low data requirements and the modelling process is relatively simple (Phillips, Dudík, & Schapire, 2004). Additionally, the outputs of habitat suitability models are easy to validate as there are an abundance of known species ranges to which predicted maps of suitable habitat can be compared (Ehrlén and Morris, 2015).

Species abundance is often assumed to be highest in the centre of a species range, which is also assumed to correspond to the centre of the species niche (Sagarin & Gaines, 2002). However, there is limited evidence to support this and empirical tests show results to be mostly inconsistent with theoretical expectations (Santini, Pironon, Maiorano, & Thuiller, 2018). A possible reason for the lack of congruence between reality and expectation is that both population trends and habitat suitability fluctuate over time, and there may be lagged responses of species abundances to changes in habitat suitability (Hylander and Ehrlén, 2013). I test this, for the first time, in Chapter Three by comparing time-series of population growth rates from the Living Planet database to time-series of modelled rates of change in habitat suitability.

COUPLED NICHE-DEMOGRAPHIC MODELS

Habitat suitability models have been criticised for over-simplifying the ecology of species distributions by overlooking factors such as species interactions, dispersal and population dynamics (Keith *et al.*, 2008; Brook *et al.*, 2009; Araújo & Peterson, 2012). There has been development of habitat suitability models to incorporate some of these ecological mechanisms. This has led to the creation of coupled niche-demographic models. These link habitat suitability models with demographic models, through incorporating population dynamics into the habitat suitability model and allowing species dispersal. These models

are more data intensive as it is necessary to parameterise the processes of survival, reproduction and dispersal (Brook *et al.*, 2009), each of which may vary stochastically and, or deterministically. The high data requirements of these models means that they are only be applicable to well-studied species (Fordham *et al.* 2013). Coupled niche-demographic models are becoming widely used (Jenouvrier *et al.* 2012; Fordham *et al.* 2013), and their superior performance to habitat suitability models has so far been assumed. Thus far, there has been limited work towards assessing the predictive accuracy of coupled niche-demographic models, because the necessarily detailed and complex observed datasets required for validation are rare (Fordham *et al.*, 2017; Zurell, Thuiller, Pagel, Sarmiento Cabral, *et al.*, 2016).

VALIDATING PREDICTED SPECIES RESPONSES

Virtual species data have been used to assess the predictive accuracy of a selection of dynamic range models of varying complexity, including coupled niche-demographic models. When used to predict under present day conditions, more complex models slightly outperformed simple habitat suitability models. However, under climate change all the complex models significantly outperformed habitat suitability models. (Zurell *et al.*, 2016). The only attempt at validating coupled niche-demographic models on observed data has been for 20 British bird species, comparing predicted range shifts to observed range shifts between 1970 and 2010 (Fordham *et al.*, 2017). Here, more complex coupled niche-demographic models tended to outperform simpler habitat suitability models. However, when static land use data were included there was little difference in the performance of the models.

A novel feature of coupled niche-demographic models is that they provide predictions of abundance, and when used to produce time-series they can predict population trends. These

predicted population trends can be used to estimate time to extinction, thereby predicting species extinction risk (Buckley *et al.*, 2010; Fordham *et al.*, 2012). However, it is not known how accurate these predictions of population trends are as they have yet to be validated against observed population trends. I address this in Chapter Four, using observed population trend data from the Living Planet database to assess the predictive accuracy of coupled niche-demographic models. Validation of the accuracy of these models against observed population trends is essential in order to improve predictions of the impacts of climate change on biodiversity, so that coupled niche-demographic models can be used to their full potential as a conservation management tool (Pacifi *et al.*, 2015).

THESIS OVERVIEW

In this thesis I present and evaluate techniques for predicting population trends of terrestrial mammal and bird species. I use a range of methods of varying levels of complexity and assess their predictive accuracy against observed population trend data from the Living Planet database. I begin this thesis with an introduction chapter, followed by three data chapters, ending with a discussion and conclusion chapter. In each chapter the ideas were conceived by Richard G. Pearson, Robin Freeman and me; I designed the research, collected and analysed the data; I led the writing with critical input from Richard G. Pearson and Robin Freeman.

Chapter Two. I performed a global analysis of the impacts of the rate of climate warming and the rate of conversion to anthropogenic land use on bird and mammal population trends. I gathered abundance time-series data for 987 populations of mammals and birds and calculated the average population growth rate for each population. I also extracted annual measures of mean temperature and anthropogenic land use cover at the site of each population and calculated the corresponding average rates of climate warming and

conversion to anthropogenic land use over the series of years each population trend covers. I also gathered species body mass data and data on protected area coverage of each of the populations. I used linear mixed effects models to determine the amount of variation in bird and mammal population trends that could be explained by the following factors: rate of climate warming (RCW), rate of conversion to anthropogenic land use (RCA), the interaction between RCA and RCW, species body mass and protected area coverage. This provides the first global study of the impacts of climate change and anthropogenic land use conversion on animal population trends. This chapter has been published in *Global Change Biology*: Spooner FEB, Pearson RG, Freeman R. Rapid warming is associated with population decline among terrestrial birds and mammals globally. *Glob Change Biol.* 2018; 24:4521–4531. <https://doi.org/10.1111/gcb.14361>.

Chapter Three. In this chapter I explored the relationship between predicted habitat suitability trends and observed population trends. I build habitat suitability models for 16 species and used these models to create annual maps of predicted habitat suitability across each species range. From these maps I extracted annual trends in habitat suitability at the location of 177 populations. I explored the correlations between rate of change in habitat suitability and population growth rates. I also investigated if correlations were higher when lagged responses of population growth rates to changes in habitat suitability were considered.

Chapter Four. In the final data chapter, I built coupled niche-demographic models for three species (red deer, brown bear and Alpine ibex) for which 17 population trends are available in the Living Planet database. These models were based upon the habitat suitability models from Chapter Three. Coupled niche-demographic models incorporate the ecological processes of population dynamics and dispersal into habitat suitability models. There has been limited validation of these models against observed trends to date. In this

chapter I assessed the performance of these models in two ways. Firstly, I compared the performance of coupled niche-demographic models to habitat suitability models. I correlated predicted population growth rates with observed population growth rates and compared these predictions to the correlations between rates of change in habitat suitability trends and observed population growth rates, which were calculated in Chapter Three. Secondly, I compared the predicted average population growth rates from both the coupled niche-demographic models and the best performing linear mixed effects model (Chapter Two) to the observed population growth rates.

CHAPTER TWO:
RAPID WARMING IS ASSOCIATED WITH
POPULATION DECLINE AMONG TERRESTRIAL
BIRDS AND MAMMALS GLOBALLY

ABSTRACT

Animal populations have undergone substantial declines in recent decades. These declines have occurred alongside rapid, human-driven environmental change, including climate warming. An association between population declines and environmental change is well established, yet there has been relatively little analysis of the importance of the rates of climate warming and its interaction with conversion to anthropogenic land use in causing population declines. Here I present a global assessment of the impact of rapid climate warming and anthropogenic land conversion on 987 populations of 481 species of terrestrial birds and mammals since 1950. I collated spatially referenced population trends of at least 5 years' duration from the Living Planet database and used mixed effects models to assess the association of these trends with observed rates of climate warming, rates of conversion to anthropogenic land use, body mass and protected area coverage. I found that declines in population abundance for both birds and mammals are greater in areas where mean temperature has increased more rapidly, this effect is more pronounced for bird populations. However, I do not find a strong effect of conversion to anthropogenic land use, body mass or protected area coverage. Our results identify a link between rapid warming and population declines, thus supporting the notion that rapid climate warming is a global threat to biodiversity.

INTRODUCTION

Global animal abundance has declined by 58% since 1970 (WWF, 2016). Key drivers of population declines include climate change and conversion of natural habitat to anthropogenic land uses, both of which have had major impacts on biological systems (Rosenzweig *et al.*, 2008; Newbold *et al.*, 2016) and are widely thought to be global threats to biodiversity (Thomas *et al.* 2004; Millenium Ecosystem Assessment 2005). The response of animal populations to these rapid environmental changes has not been consistent: some

populations have experienced increasing abundance and expanding distributions; conversely, other populations have suffered shrinking abundances and distributions (Frishkoff et al., 2016; La Marca et al., 2005; Thomas, Franco, & Hill, 2006). Declines in animal populations result in an erosion of ecosystem function and loss of ecosystem services (Ehrlich & Daily, 1993; Parmesan & Yohe, 2003; Thomas et al., 2006; Winfree et al., 2015).

It is well established that species have responded to climate warming through altitudinal and latitudinal shifts in distribution (Parmesan and Yohe, 2003) and with the advancement of phenological events (Root *et al.*, 2003). However, the effect of climate warming on animal abundance trends has been less well explored and multi-species studies have thus far been limited to Europe and North America. Martay et al. (2017) found that climate could explain significant country-level population declines in moths and increases in winged aphids across Great Britain, but found no group-wide trends for butterflies, birds or mammals. By contrast, it has been observed that warm-adapted butterflies and beetles in central Europe and warm-adapted birds across Europe and North America have had higher population growth rates under climate warming than those which are cold-adapted (Jiguet *et al.*, 2010; Bowler *et al.*, 2015; Stephens *et al.*, 2016). These trends may lead to a future divergence of population trends, with warm-adapted species increasing in abundance and cold-adapted species declining (Gregory *et al.*, 2009). To our knowledge there has been no previous global multi-species assessment of the observed impacts of climate warming on population trends. Furthermore, aforementioned studies have aggregated climate to country or range level, and population data are often aggregated to species level, which does not allow for population level variation in responses to climate warming.

Previous studies have shown that phenological and latitudinal shifts are greatest in areas that have experienced most warming (Rosenzweig *et al.*, 2008; Chen *et al.*, 2011). Natural

variability ensures that many populations can accommodate and respond to various types of change; however, local extinction occurs if the rate of climate warming exceeds the maximum possible rate of adaptive response (the adaptive capacity). To date, there have been no large-scale analyses exploring the relationship between the rate of climate warming (as opposed to the magnitude of warming) and animal population trends. I hypothesize that locations which have undergone faster climate warming will be locations where the threat to biodiversity is greatest and which have experienced more rapid population declines.

Habitat loss and fragmentation are known to be the primary drivers of biodiversity loss (Millennium Ecosystem Assessment 2005). Global studies have shown that the conversion of natural habitat to anthropogenic land uses leads to local declines in both species richness and abundance and that these declines are greater where conversion to anthropogenic land use has been greater (Newbold *et al.*, 2015). I therefore hypothesize that in areas where conversion to anthropogenic land use has been most rapid, there will be greater population declines.

Threats to biodiversity rarely act independently and can often have exacerbating interactions. In particular, the interaction between anthropogenic land use conversion and climate warming has been described as a ‘deadly anthropogenic cocktail’ (Travis, 2003) because habitat loss reduces the ability of species to adapt to climate change (for instance by inhibiting range shifts; Brook *et al.* 2008; Mantyka-Pringle *et al.* 2012; Oliver and Morecroft 2014). Little is known about how the interaction between climate warming and anthropogenic land use conversion varies across habitats or species (Root *et al.*, 2003; Brook, Sodhi and Bradshaw, 2008; Eglington and Pearce-Higgins, 2012; Oliver and Morecroft, 2014). Thus, this interaction remains a source of uncertainty when projecting future biodiversity trends (Sala, 2000). I therefore also hypothesize that there is an interaction between anthropogenic land use conversion and climate warming, such that the

greatest population declines will occur where there has been both rapid conversion to anthropogenic land use and climate warming.

I note that there are many other factors which may impact population trends, not least the positive impact of conservation effort (Young *et al.*, 2014) or the influence of species intrinsic traits (Lee & Jetz, 2011). Conservation efforts are often implemented through the creation and management of protected areas; thus, I hypothesize that population trends outside of protected areas will be more likely to be declining than those within them. Additionally, to account for the effect of species traits I explore the relationship between population growth rates and body mass, which is a correlate of many species traits (Brook, Sodhi and Bradshaw, 2008; Hilbers *et al.*, 2016). Recent research has shown there is a significant relationship between vertebrate body mass and extinction risk, such that heavier species of birds and mammals are likely to be more at risk of extinction (Ripple *et al.*, 2017). I therefore hypothesize that larger bodied birds and mammals are more likely to have declining populations.

I present a global study in which I spatially and temporally link observed changes in abundance for 987 populations of 481 species of birds and mammals (from 1950 to 2005) to changes in climate and land use. The combined historical, spatial and taxonomic coverage of the study allows the drawing out of generalizable trends on the impacts of recent anthropogenic environmental change on observed animal population trends.

MATERIALS AND METHODS

POPULATION TIME SERIES DATA

I obtained observed population trends from the Living Planet database (http://www.livingplanetindex.org/data_portal), which contains time series of annual population estimates for over 18,000 vertebrate populations observed during the period

1950-2015. The time series are collated from the scientific literature, online databases and grey literature (Collen *et al.*, 2009; McRae, Deinet and Freeman, 2017). To be included in the database there must be at least two years of population estimates and survey methods must be comparable for each year the population is estimated. Detailed criteria for inclusion in the database are outlined in Loh *et al.* (2005).

For each time series, the population count data were logged (base 10) so that it was possible to compare changes in population trends irrespective of their size (prior to this, zeros were replaced with 1% of the mean population count of the time series so that it was possible to log these values, following Collen *et al.* 2009). If the number of population counts within each time series was sufficient ($N > 6$) the time series was fit with a Generalized Additive Model (GAM). GAMs are more flexible than linear models and therefore more appropriate for fitting to population trends which can often be non-linear (Collen *et al.*, 2009). However, GAMs could not be fit reliably to time series where $N < 6$ data points, so for these time series I fit a linear regression. The smoothing parameter of each GAM was set to $\frac{N}{2}$, because this was found to be a suitable value for fitting the data well without overfitting to noise (Collen *et al.*, 2009). The fit of each linear regression or GAM to the population trends was assessed using R^2 .

For each time series, I calculated the average logged rate of population change ($\overline{\lambda_Y}$), or average lambda:

$$\lambda_y = \log_{10}\left(\frac{n_y}{n_{y-1}}\right) \quad \text{Eqn 1}$$

$$\overline{\lambda_Y} = \frac{1}{Y} \sum_0^n \lambda_y \quad \text{Eqn 2}$$

where n is the population estimate of a given year, y , and Y is the total number of years from the first to last population estimates.

I then filtered the data to only include populations that met the following five criteria: (i) the location is known (many of the population trends in the Living Planet database are nationally aggregated so cannot be spatially linked to environmental data); (ii) environmental data and body mass data were available; (iii) time series span five or more years (because longer time series will better reflect environmental changes); (iv) time series had $R^2 \geq 0.5$ when fit to the GAM or linear model (to ensure interpolated population estimates were reasonable); and (v) the population was recorded as being either inside or outside a protected area (any population recorded as both inside and outside a protected area was omitted).

After the populations were filtered based on these criteria, there were 987 remaining populations at 441 unique study sites (Figure 2.1). These populations were made up of 416 (42.1%) bird populations (292 species and 148 locations) and 571 (57.9%) mammal populations (189 species and 303 locations). This remaining subset had a mean time series length of 15.6 (± 9.2) years and population estimates for 55.1% of the years within each time series. Values for missing values were estimated using either log-linear interpolation or imputed from the GAMs.

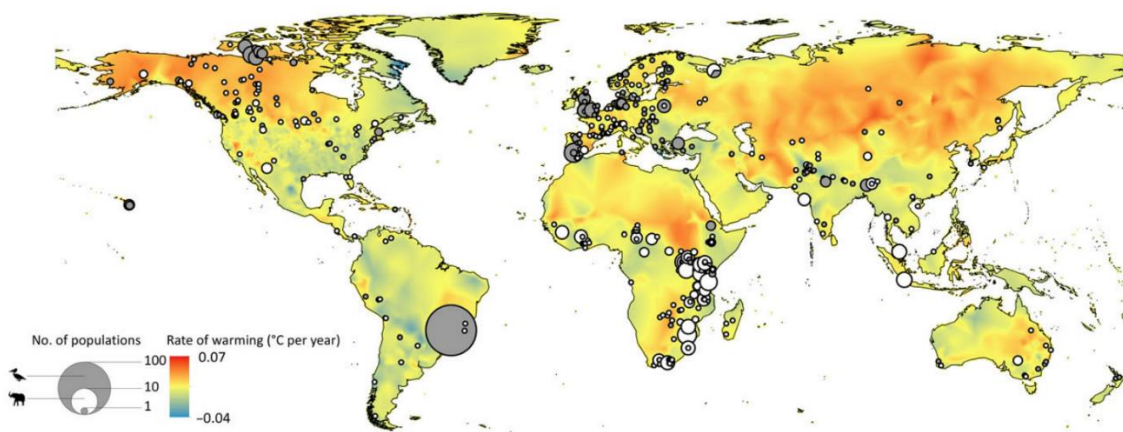


Figure 2.1 The points show the distribution and density of population time series used in the analysis. The black and white points signify bird and mammal populations respectively, where both classes are present the numbers of each are represented proportionally. 77.4% of the locations have one population. The base layer of the map shows the rate of temperature change, in degrees per year, between 1950 and 2005, based on analysis of the CRU TS v. 3.23 gridded time series data set (Harris *et al.*, 2014).

CLIMATE DATA

Global mean temperature data were gathered from the CRU TS v. 3.23 gridded time series (Harris et al. 2014; Figure 2.1), which provides monthly observations of land surface mean temperature at a spatial resolution of 0.5°. Monthly mean temperatures for the years 1950-2005 were extracted for the location of each observed population time series. The extracted temperatures were filtered to include only the years over which population estimates were available, and an average value was calculated for each year. A linear regression was then fit to those averages, the slope of which gives the annual rate of climate warming (RCW) over the period of observed population estimates.

LAND USE DATA

Global land use data were gathered from the HYDE database (Klein Goldewijk *et al.*, 2011), which provides decadal (1940-2000 & 2005) grid cell coverage of cropland and pasture at a spatial resolution of 0.083°. The percentage cover of cropland and pasture were summed to calculate percentage cover of anthropogenic land use in each cell. For each population time series, land use values were extracted for the years covered by the time series and averaged for a 0.25° x 0.25° grid around the cell containing each population (Figure 2.2). This was done to encapsulate landscape level change around each population. The decadal values of anthropogenic land use were linearly interpolated to annual values and from these values the average annual rate of conversion to anthropogenic land use (RCA) was calculated for each population time series, where positive values mean an increase in cropland or pasture cover.

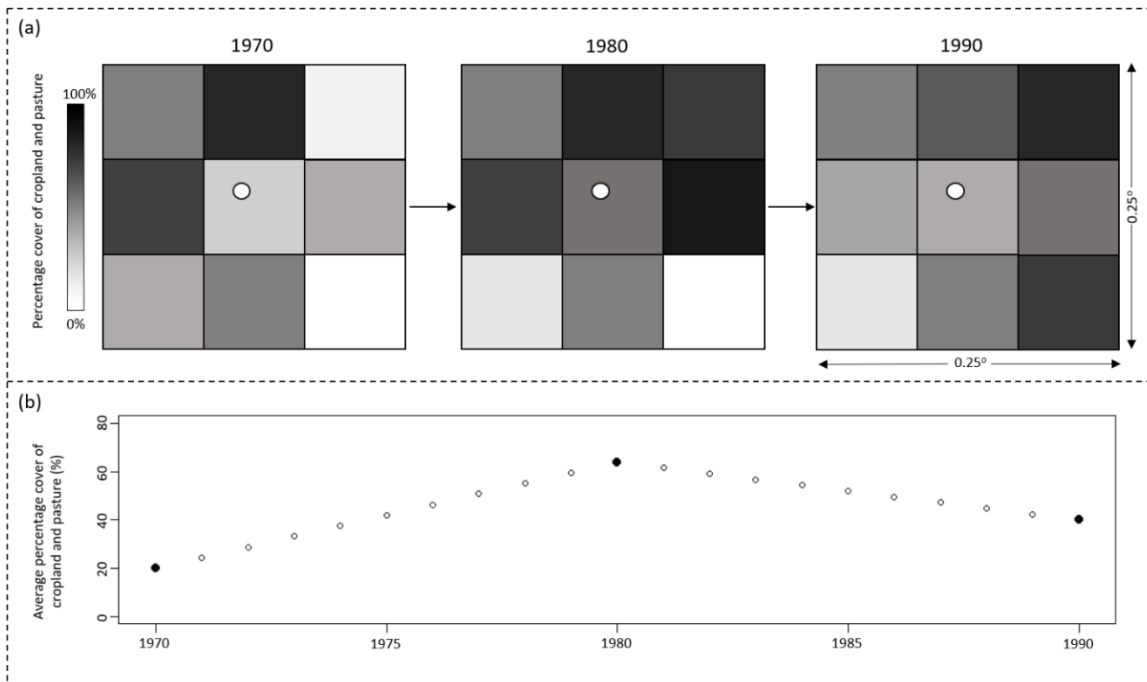


Figure 2.2 Illustration of how the rate of conversion to anthropogenic land use was calculated. (A) Example land use cover data for a population time series (1970-1990), where the white circle depicts the location of the population. Each grid of nine cells represents a decadal section of the HYDE data, which was cropped to the $0.25^\circ \times 0.25^\circ$ grid surrounding each population. (B) The average value of cropland and pasture percentage cover for each decadal grid (black circles) and the linearly interpolated annual values (hollow circles). For each population, I calculated the average annual change in percentage cover of cropland and pasture over the years for which I have population trend data (for this example population the value would be 1%).

BODY MASS

Adult body mass data for birds and mammals were extracted from the amniote life-history database (Myhrvold *et al.*, 2015). The body mass values were initially in grams and were logged (base 10) to normalise them. The values were then joined by species name to the corresponding Living Planet population time series. These body mass (BM) data were included as fixed effects in the candidate models.

PROTECTED AREAS

To account for the effect of protected areas on animal population trends I included protected area (PA) coverage as a binary fixed effect in the models. This information is available in the Living Planet Database.

LINEAR MIXED EFFECTS MODELS

I aimed to test the extent to which bird and mammal population trends could be explained by rates of climate warming and conversion to anthropogenic land use. However, it is likely that there will be important species- and site-specific effects that could mask the impacts of climate warming and conversion to anthropogenic land use. To account for this, I used linear mixed effects models which allow us to understand the magnitude and direction of the effect size of explanatory variables on the response variable. The inclusion of random effects allows for a varying intercept for every grouping factor, here ‘species’ and ‘site’, thus allowing for responses that are specific for species and site. Nineteen competing linear mixed effects models were constructed for the 987 populations, with the average logged rate of population change ($\overline{\lambda}_Y$) as the response variable and RCW, RCA, an interaction term between RCW and RCA, PA and BM as explanatory variables (Table 2.1). Species and study site were included as random effects in each of the models (Table 2.31). To facilitate comparison of effect size and the relative importance of each variable, the continuous fixed effects were scaled and centred by subtracting the mean and dividing by the standard deviation (Bates *et al.*, 2015).

Where there was no clear best performing model from the selection of competing models, the top models (where the cumulative sum of the AIC weights were ≤ 0.95) a conditional average and coefficients were taken from this model (Burnham and Anderson, 2002; Daskin and Pringle, 2018). The modelling process was carried out separately for birds and mammals because the life history characteristics of these two taxonomic groups differ enough for it to be expected that they will have different responses to environmental change.

Parameter	Description	Type of effect
<i>Species Name</i>	Species binomial, included to account for species specific responses	Random intercept
<i>Study Site</i>	Unique ID based on the coordinates of populations from Living Planet database, included to account for site specific effects	Random intercept
<i>Rate of Climate Warming (RCW)</i>	The rate of change in mean temperature per year, over the length of the population time series	Fixed
<i>Rate of Conversion to Anthropogenic Land Use (RCA)</i>	The rate of change in percentage cover of cropland and pasture per year, over the length of the time series	Fixed
<i>Body Mass (BM)</i>	Logged (base 10) body mass (g) of birds and mammals	Fixed
<i>Inside Protected Area (PA)</i>	A binary variable recording whether each population is inside or outside a protected area	Fixed

Table 2.1 Parameters used in linear mixed effects models.

All analyses were carried out using the statistical software R (R Core Team, 2018). The *plyr* (Wickham, 2011), *taRifx* (Friedman, 2014), *mgcv* (Wood, 2011) and *zoo* (Zeileis and Grothendieck, 2005) packages were used to format the population trend data. The *GISOperations* (Newbold, 2016), *raster* (Hijmans, 2016), *doParallel* (Microsoft Corporation and Weston 2015) and *reshape2* (Wickham, 2007) packages were used to format and extract the environmental data. The linear mixed effects modelling was undertaken using the *lme4* (Bates *et al.*, 2015) and *MuMIn* (Barton, 2016) packages.

RESULTS

The mixed effects models reveal a strong association between rapidly warming climates and declines in populations for both birds and mammals (Figure 2.3). This association is more than twice as strong in birds than in mammals.

In our analysis of the impact of RCA and RCW on bird and mammal populations I find (particularly in mammals) a variety of potential models with no clear ‘best’ model. I therefore took a model averaging approach, combining all models within a 95% confidence

set (Burnham and Anderson, 2002; Daskin and Pringle, 2018). I feel that this is a more conservative approach and, given the variability in potential effects within our analysis, more appropriate here. I have also explored using a $\Delta AIC < 6$, which is also recommended in the literature (Burnham and Anderson, 2002), and the difference in our results is negligible (e.g. difference in all coefficients $< 6.5\%$ see Appendices).

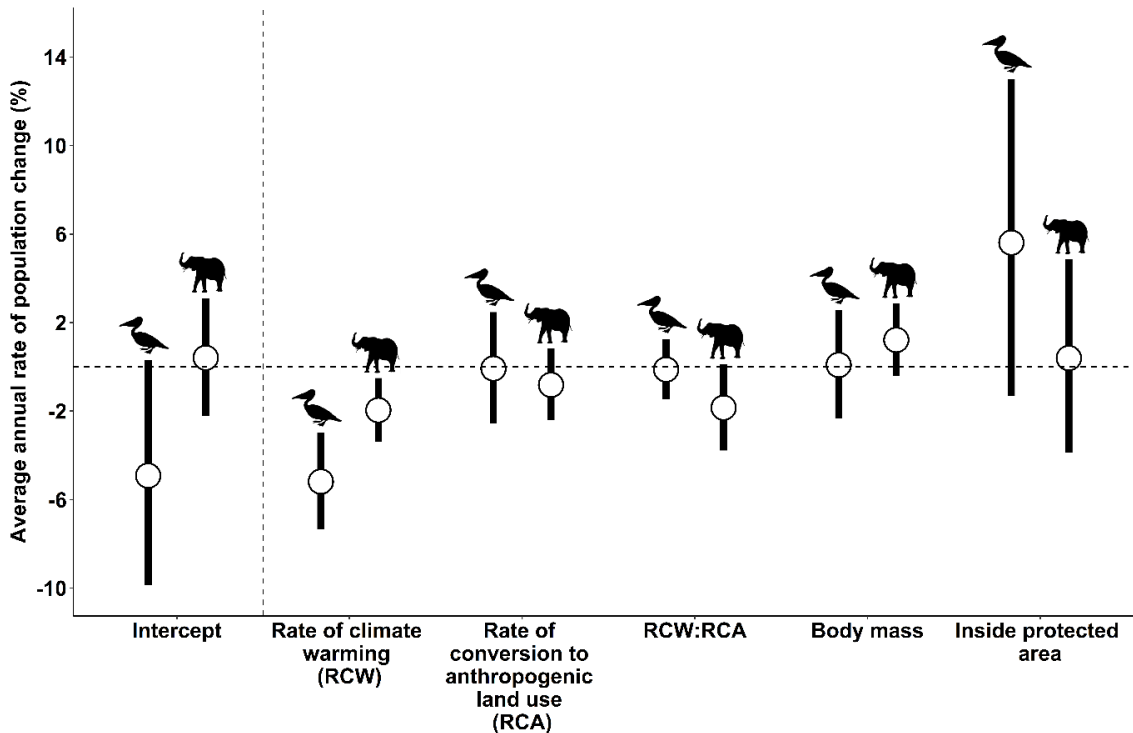


Figure 2.3 The distribution of the coefficients of the average models for bird and mammal populations. Circles show the estimated coefficient values for each variable and solid lines show the 2.5 - 97.5% confidence intervals. As the data were scaled and centred prior to modelling the intercept shows the distribution of modelled annual population growth rates outside of protected areas and with mean values for RCA, RCW and Body Mass (as the centre of these values, when scaled, is now zero). Another consequence of scaling and centring the data is that the coefficients show the change in annual population growth rate given a one standard deviation increase in each explanatory variable. For example, for bird populations an increase in the rate of mean temperature change of $0.07^{\circ}\text{C Y}^{-1}$ would lead to an average annual population decline of 5.09%. Confidence intervals that do not overlap with zero reveal a signal of either a positive or negative effect of a variable. Confidence intervals that overlap with zero show that within the averaged model an increase in a given variable has a mixture of both positive and negative effect sizes on the rate of population change across different populations.

The top performing models (based on ≤ 0.95 sum of Akaike weights) can be found in Table 2.2, with the full table of results in Table S2.1. All the explanatory variables feature within these top models, suggesting that each of these variables contribute to explaining variation in observed population trends.

In both the bird and mammal sets of competing models, I found that all the models containing RCW were within the top performing models, comprised of those where the cumulative sum of the Akaike weights was ≤ 0.95 . This suggests that these models are all useful and that RCW is the most important variable for explaining variation in both bird and mammal population trends.

Within the bird results there are two models where $\Delta AIC < 2$ (highlighted in Table 2.2). The top performing model, in terms of AIC, is made up of RCW and PA, followed by the model with only RCW. The top performing model explains a large amount of the variation in avian population trends: 8.2% is explained with the fixed effects (marginal R^2) and 78.6% is explained by the fixed and random effects (conditional R^2). This highlights the clear importance of these two variables in explaining bird population trends, which is also reflected in their relatively large effect sizes. I find that populations within protected areas tend to have less negative growth rates than populations outside of protected areas.

Within the mammal results there are six models where $\Delta AIC < 2$, between them containing each of the explanatory variables. This suggests that there are several quite different models that have a similar ability to explain variation in mammal population trends. The results for mammal populations are more complex than for bird populations; however, RCW is clearly an important variable, as evidenced by its presence in each of the six best models, its high relative variable importance (RVI) score of 0.95, and its large effect size. I found that the interaction term (RCW:RCA) was also an important variable in explaining population trends. This means that mammal populations that have experienced both high RCW and RCA tend to have more negative population growth rates. I also find that although the confidence intervals overlap zero, larger bodied mammals tend to have less negative population growth rates. The highest ranked model within the mammal data, in terms of AIC, was the model which contained, RCA, RCW, RCW:RCA, and body mass. The fixed effects of this model explain 2.8% (marginal R^2) of the variation in mammal population trends and 44.0% is explained with both the fixed and random effects (conditional R^2).

A. Results from Bird Population Trends										
<i>Model</i>	Δ AIC	Akaike Weight	Marg. R ²	Cond. R ²	Intercept	RCW	RCA	RCW:RCA	Body Mass	Inside Protected Area
<i>RCW+PA</i>	0.00	0.27	0.08	0.79	-6.12 (± 2.63)	-5.09 (± 1.17)				5.60 (± 3.50)
<i>RCW</i>	0.42	0.22	0.06	0.79	-3.38 (± 1.88)	-5.29 (± 1.17)				
<i>RCW+BM+PA</i>	2.06	0.10	0.08	0.79	-6.18 (± 2.69)	-5.10 (± 1.16)			0.12 (± 1.24)	5.62 (± 3.51)
<i>RCA+RCW+PA</i>	2.06	0.10	0.08	0.79	-6.13 (± 2.63)	-5.08 (± 1.17)	-0.11 (± 1.28)			5.62 (± 3.50)
<i>RCW+BM</i>	2.48	0.08	0.06	0.79	-3.40 (± 1.94)	-5.30 (± 1.17)			0.04 (± 1.25)	
<i>RCA+RCW</i>	2.48	0.08	0.06	0.79	-3.39 (± 1.88)	-5.29 (± 1.17)	-0.02 (± 1.29)			
<i>RCW*RCA+PA</i>	4.12	0.04	0.08	0.79	-6.12 (± 2.63)	-5.13 (± 1.22)	-0.11 (± 1.28)	-0.11 (± 0.69)		5.60 (± 3.51)
<i>RCA+RCW+BM+PA</i>	4.13	0.04	0.08	0.79	-6.19 (± 2.69)	-5.08 (± 1.17)	-0.12 (± 1.28)		0.13 (± 1.25)	5.64 (± 3.51)
<i>RCA*RCW</i>	4.51	0.03	0.06	0.79	-3.38 (± 1.88)	-5.35 (± 1.22)	-0.02 (± 1.29)	-0.14 (± 0.70)		
<i>Null Model</i>	22.48	<0.01	0.00	0.59	-1.23 (± 1.88)					
RVI						1.00	0.33	0.09	0.26	0.55
B. Results from Mammal Population Trends										
<i>Model</i>	Δ AIC	Akaike Weight	Marg. R ²	Cond. R ²	Intercept	RCW	RCA	RCW:RCA	Body Mass	Inside Protected Area
<i>RCA*RCW+BM</i>	0.00	0.17	0.03	0.44	0.68 (± 0.94)	-2.20 (± 0.73)	-0.75 (± 0.82)	-1.82 (± 1.02)	1.24 (± 0.82)	
<i>RCA*RCW</i>	0.12	0.16	0.02	0.45	0.38 (± 0.95)	-2.22 (± 0.73)	-0.55 (± 0.81)	-1.88 (± 1.02)		
<i>RCW</i>	1.05	0.10	0.01	0.42	0.38 (± 0.93)	-1.72 (± 0.68)				
<i>RCA+RCW+BM</i>	1.18	0.09	0.02	0.42	0.56 (± 0.93)	-1.71 (± 0.68)	-1.17 (± 0.78)		1.28 (± 0.81)	
<i>RCW+BM</i>	1.41	0.08	0.02	0.42	0.64 (± 0.93)	-1.71 (± 0.68)			1.06 (± 0.80)	
<i>RCA+RCW</i>	1.50	0.08	0.02	0.43	0.26 (± 0.93)	-1.73 (± 0.78)	-0.97 (± 0.68)			
<i>RCA*RCW+PA</i>	1.97	0.06	0.02	0.45	-0.36 (± 1.91)	-2.24 (± 0.73)	-0.58 (± 0.82)	-1.86 (± 1.02)		0.95 (± 2.10)
<i>RCA*RCW+BM+PA</i>	2.06	0.06	0.03	0.44	0.82 (± 2.08)	-2.20 (± 0.73)	-0.74 (± 0.82)	-1.83 (± 1.02)	1.27 (± 0.88)	-0.17 (± 2.25)
<i>RCW+PA</i>	2.93	0.04	0.01	0.42	-0.27 (± 1.88)	-1.74 (± 0.68)				0.40 (± 2.08)
<i>RCA+RCW+BM+PA</i>	3.24	0.03	0.02	0.42	0.62 (± 2.06)	-1.71 (± 0.68)	-1.17 (± 0.79)		1.29 (± 0.87)	-0.07 (± 2.25)
<i>RCA+RCW+PA</i>	3.28	0.03	0.02	0.45	-0.59 (± 1.90)	-1.75 (± 0.68)	-1.01 (± 0.78)			1.09 (± 2.09)
<i>RCW+BM+PA</i>	3.45	0.03	0.02	0.42	0.80 (± 2.07)	-1.70 (± 0.68)			1.09 (± 0.89)	-0.19 (± 2.25)
<i>Null Model</i>	3.69	0.03	0.00	0.39	-0.16 (± 0.92)					
<i>RCA+PA</i>	7.81	<0.01	<0.01	0.41	-0.23 (± 1.90)		-0.98 (± 0.78)			0.69 (± 2.09)
RVI						0.95	0.72	0.45	0.50	0.27

Table 2.2 Models included in the average model for explaining the growth rate of bird and mammal populations. The selection of models was based on a ≤ 0.95 cumulative sum of Akaike weights. The models are ranked in order of performance based on AIC, with higher ranking models listed towards the top of each table. Models within Δ AIC < 2 of the highest ranked models are highlighted with bold text and a grey background. A null model is included for comparison. RCW = annual rate of climate warming, RCA = annual rate of conversion to anthropogenic land use, BM = body mass, PA = population inside a protected area. The coefficient values have been transformed into percentage population change. According to the top ranked model for birds, an increase in RCW to rates expected under climate scenario RCP 8.5 (5-6°C, 2006-2100) would lead to an annual population decline of 3.85 - 4.65% in bird populations and 1.46 - 1.76% for mammal populations (for details see Appendices). RVI (relative variable importance) is the sum of Akaike weights over all models including the explanatory variable.

If I relax the criterion that R^2 for the linear regressions or GAMs must be > 0.5 for a population to be included in the study (see Methods), then the number of populations included in the analysis increases by 87% (total of 883 bird populations and 966 mammal populations) and the results of the mixed effects models remain similar (for details see Appendices). This suggests our findings are not only limited to the subset of the populations used in the primary analysis but are more broadly applicable across observed bird and mammal population trends. I also explored the effect of the heterogeneous distribution of population trends (Table S2.2).

There is less of a clear correlation between population trend and either body mass or RCA. The 95% confidence intervals of the coefficients for these variables overlap zero, meaning that across all the populations the effects of body mass and RCA can be both positive and negative. However, these results can be used to draw out trends in the data as they reflect the spread of the coefficients. For example, most mammal populations tend to increase with body mass, whereas the bird populations are more evenly distributed around zero (Figure 2.3).

DISCUSSION

The results reveal a strong association between rapid climate warming and declines of bird and mammal populations globally, showing that population declines have been greatest in areas that have experienced most rapid warming. The averaged model suggests that an increase in the rate of climate warming by one standard deviation (birds = 0.072°C per year, mammals = 0.079°C per year) leads to an increase in annual average population declines of 5.1% for birds and 2.0% for mammals (Figure 2.3). Although these rates are higher than the projected rates of warming under more pessimistic future scenarios (e.g., RCP 8.5, Riahi et al. 2011) I note that these projections are global averages and that within these

projections there will be regions, such as the Arctic (AMAP, 2017), which are likely to experience the higher rates of warming found within these models. Under this scenario (RCP 8.5) I would expect to see a 3.85 – 4.65% annual population decline in bird populations and 1.46 – 1.76% annual population decline in mammal populations (for details see Appendices). If the rate of climate warming continues to increase then I can expect greater bird and mammal population declines, these losses will be greatest at locations which experience most rapid climate warming (See Appendices, Figure S2.2). These findings echo aspects of previous global studies which suggest that future climate change will lead to large range contractions and increased species extinction risk (Thomas *et al.*, 2004; Jetz, Wilcove and Dobson, 2007).

I found the impact of rapid climate warming to be more pronounced for bird populations than mammal populations (Figure 2.3). This may be because climate change can lead to the desynchronization of bird breeding season and the peak resource availability (Stevenson and Bryant, 2000; Visser, Both and Lambrechts, 2004; Keogan *et al.*, 2018), whereas the seasonality of breeding in mammals is more flexible (Boutin and Lane, 2014). I note there are geographical differences in the representation of birds and mammals (Figure 2.1). Within the dataset there are populations of both classes in all continents except Antarctica, however, mammal populations dominate in Africa (59% of populations, 43% of sites) and bird populations in Europe (26% of populations, 45% of sites). This may contribute to the differences I see between the two groups in their response to RCW. It is also important to acknowledge that there is spatial bias in the dataset, there are relatively few sites in tropical forest habitat, particularly in South America and Southeast Asia. It is likely I would see a similar pattern in the results if there were data available from these regions. The RCW in tropical forests is relatively low (Corlett, 2011), however, species thermal niches tend to be narrower in the tropics meaning that the magnitude of their response to climate warming

may be greater (Freeman and Class Freeman, 2014). In particular, tropical montane species have undergone range contractions and declines in abundance associated with climate warming (Freeman et al 2018).

The interaction between RCA and RCW was an important variable in explaining mammal population trends, where it had a similar effect size to RCW (Table 2B). This suggests that mammal populations are likely to have suffered greater declines in areas where there has been both climate warming and rapid conversion to anthropogenic land use. I do not find an effect of the interaction between RCA and RCW for bird populations, this may be because the interaction is complex and context specific (Kampichler *et al.*, 2012); for example, logging and increased temperatures can lead to a decrease in transpiration and less rainfall (Bagley *et al.*, 2014), which may be devastating for many populations due to the drying of fuels and increased chance of fire and, or drought (Malhi *et al.*, 2008). However, conversion to agriculture and warmer breeding season temperatures may be beneficial to populations of warm-adapted generalist species (Karp *et al.*, 2018; Pearce-Higgins *et al.*, 2015). Additionally, it may be that historical land use change, which would not be captured by RCA, has altered the landscape so profoundly that it restricts species capacity to adapt to climate change (Benning *et al.*, 2002).

I did not find RCA to be an important variable when acting in isolation for either birds or mammals. The lack of a clear effect of RCA on bird populations may be because a large proportion (54.8%) are within protected areas and I find that bird populations within protected areas tend to have higher population growth rates than those outside. Within my dataset 60.3% of bird populations are made up of generalist species (here defined as having suitable habitat in more than one IUCN Level 1 habitat class), which may be more resilient to changing landscapes than specialist species. Conversion to agriculture does not uniformly disadvantage all bird species; for example, dry-adapted tropical species may

have higher abundance in agricultural landscapes (Karp *et al.*, 2018). However, I note that the ‘winners’ of conversion to agriculture tend to be in the minority (McKinney and Lockwood, 1999). As previously mentioned, there are comparatively few population trends from tropical forests. These areas are rich in biodiversity but also heavily threatened by conversion to anthropogenic land use (Wright, 2005). It may be that I would detect a larger effect size for RCA if there were more population trend data from tropical forests. The global effect of increased anthropogenic land use on populations has been identified in other global studies, such as the PREDICTS project (Newbold *et al.*, 2015), where finer resolution measures of local land use change were available.

Additionally, the effects of converting to anthropogenic land use are more likely to be detected at fine spatial resolutions (Pearson and Dawson, 2003; Heikkinen *et al.*, 2007), yet here I used relatively coarse resolution land use data. The coarse resolution of the data may be why I was unable to identify a clear effect of increasing anthropogenic land use on population trends at a global scale, despite it being a well-known driver of biodiversity loss (Millennium Ecosystem Assessment, 2005). I explored the impact of using an alternative land cover data set (ESA CCI; Bontemps *et al.*, 2013), which was available at a higher resolution but over a shorter time period. When using ESA CCI to quantify RCA I found that RCA and protected area coverage are important predictors for bird population trends. This finding suggests that the impacts of land use change on population trends are more detectable at higher spatiotemporal resolutions or that the impacts of climate change are more noticeable over longer time periods.

I do not find PA to be an important predictor for mammal population growth rates; however, I note that 84.6% of the mammal populations are from inside protected areas, making it difficult to capture the effect of protected areas. I also note that other studies have

shown the evidence of protected areas successfully conserving species populations is thus far inconclusive (Geldmann *et al.*, 2013).

Body mass was not an important predictor of population growth rates for bird populations. This may be because while greater extinction risk is positively linked with increased body mass (Ripple *et al.*, 2017), population declines, particularly of common species may not be captured by extinction risk criteria (Inger *et al.*, 2015). Within mammal populations I found that smaller bodied species were more likely to have declining populations than larger bodied species, although the confidence intervals overlap with zero, so caution must be taken with the interpretation of this result. However, I note that when a less restricted set of population trends are included (see Appendices), the confidence intervals around this result are tighter and no longer overlap with zero, although the effect size is not large. This finding goes against my hypothesis that larger bodied mammals would be more likely to have declining population trends and is contrary to the finding that larger mammals have higher extinction risk (Ripple *et al.*, 2017). This may be because the mammal data is dominated by populations within east African protected areas, where larger mammals may receive greater attention and conservation effort which could mean their populations are buffered (Barnes *et al.*, 2016). I also explored the inclusion of other species traits, but I did not find important effects (for details see Appendices).

I find that populations facing greater rates of climate warming are more likely to be declining at a faster rate. However, the analyses do not account for several additional factors, such as species exploitation, pollution and disease, which may help to further explain the degree of variability in population trends. Nevertheless, I provide evidence that populations facing high rates of climate warming tend to be in decline. Deepening our understanding of the processes that underlie the associations discussed here will be critical

for developing improved assessments of species' vulnerability to climate warming (e.g., Pacifici et al. 2015).

CHAPTER THREE:
PREDICTING POPULATION TRENDS FROM
HABITAT SUITABILITY MODELS

ABSTRACT

Habitat suitability models have been used to successfully estimate species ranges and predict shifts in these ranges driven by climate change. However, when habitat suitability models have been used to estimate spatial distributions of abundance the results have been mixed. Previous studies exploring the relationship between habitat suitability and abundance have used static snapshots of both these variables. However, habitat suitability and abundance are often dynamic and should not be expected to directly correlate, there may be lagged responses of abundance to changes in habitat suitability. I test this here by creating annual habitat suitability models for 16 mammal species (1950–2005) and explore the correlations between time-series of habitat suitability and the population growth rates of 177 populations, whilst accounting for lagged responses. I find that there is little evidence to support the idea that population growth rates are directly linked to habitat suitability. However, I find that when lagged responses are considered there is a stronger positive relationship between changes in habitat suitability and population growth rates. These findings suggest that lagged responses are important in understanding species responses to environmental change and where possible time-series, rather than static snapshots of data, should be used.

INTRODUCTION

Global vertebrate populations have declined on average 60% since 1970 (WWF 2018), and 25% of mammal species are threatened with extinction (IUCN 2018). Predicting the response of species distributions and population trends to anthropogenic threats, such as climate change and habitat loss, is key to effectively conserving biodiversity (Guisan et al., 2013). There are many methods available for modelling species distributions and populations which can be used to predict future states of biodiversity under a variety of

future scenarios. One of the most widely used approaches for predicting species distributions is habitat suitability modelling (Dawson *et al.*, 2011).

Habitat suitability models statistically associate species occurrence data with environmental data and use this to geographically map surfaces of habitat suitability. These models can then be projected onto climate change scenarios to predict future patterns of habitat suitability and also estimate the probability of species occurrence (Guisan & Thuiller, 2005; Pearson & Dawson, 2003; Peterson *et al.*, 2011). Habitat suitability modelling techniques have been used effectively multiple times. For example, climate envelope models were used to successfully identify a relationship between the climatic suitability trends and population trends of 42 species of British birds (Green *et al.*, 2008); and consensus bioclimatic models of the response of 116 British breeding birds to climate change performed well when compared to observed patterns (Araújo *et al.*, 2005). Successful examples of correlative habitat suitability modelling combined with the relative ease of use and low data requirements mean that this technique has become widely used and has been influential in policy making (Guisan *et al.*, 2013; Pearson, Dawson, & Liu, 2004).

Habitat suitability models are increasingly used to predict not only the probability of species occurrence but also more usable metrics such as species abundance; a more useful metric for species conservation. By its definition habitat suitability should be greatest in areas that support highest abundances (VanDerWal *et al.* 2009). However, when this assumption has been empirically tested there have been mixed results. A meta-analysis of the 'abundance-suitability' relationship found that there was an overall positive correlation between habitat suitability and abundance, although it should be noted that there were several examples of zero or negative correlations (Weber *et al.*, 2017).

Other multi-species studies have also struggled to identify a clear relationship between predicted habitat suitability and species abundance, finding similar numbers of positive and negative correlations for 246 mammal and 148 tree species (Dallas and Hastings, 2018). Attempts at predicting fine-scale occurrence and abundance for European butterfly species have been both successful (Gutiérrez *et al.*, 2013) and unsuccessful (Filz, Schmitt and Engler, 2013), although there are important differences between the two studies. The former includes species-specific environmental variables, such as the occurrence of the species host plant, whereas the latter use more general bioclimatic variables.

There is evidence for a wedge-shaped relationship between species abundance and predicted habitat suitability; with low species densities and abundances found across all levels of predicted habitat suitability, but with high densities and abundances restricted to areas of high predicted habitat suitability (Acevedo *et al.* 2017; Van Couwenberghe *et al.* 2013; VanDerWal *et al.* 2009). The range of abundances and densities found in areas of high predicted habitat suitability may be explained by processes such as human exploitation or ecological competition which can limit abundances (Tôrres *et al.* 2012). However, in contradiction to these findings, high densities of raptors in the Iberian peninsula have been found outside of areas of predicted habitat suitability (Estrada and Arroyo, 2012), suggesting that in this case the relationship between predicted habitat suitability and abundance is more complex.

The lack of a clear relationship between predicted habitat suitability and species abundance suggests that we are failing to consistently model the processes that drive species abundance. This may be because habitat suitability models do not account for important ecological mechanisms such as dispersal, population dynamics and species interactions. These processes have a fundamental impact on species abundance, however, integrating them into habitat suitability models is complicated and computationally intensive.

Additionally, previous studies which have attempted to quantify the nature of the relationship between predicted habitat suitability and abundance have used static estimates, from single points in time. These static snapshots of data do not provide any context about the state of the habitat, for example, whether it is in the process of becoming more or less suitable or if it has been in a stable equilibrium for several years. One should not expect predicted habitat suitability to be correlated with abundance if the habitat is in the process of change, as it is likely that the population dynamics are not in equilibrium with the environment (Weber *et al.*, 2017). If the habitat has changed recently or is in the process of changing, there may be a lag in the response of abundance of the species (Tilman *et al.*, 1994; Thuiller *et al.*, 2008; Hylander and Ehrlén, 2013). In particular, it is known that long-lived species often have a delayed response to habitat disturbance due to long generation times and low fecundity rates (Kuussaari *et al.*, 2009; Zarada and Drake, 2017). Lagged changes in abundance in response to habitat change are unlikely to be identified when single time points of data are used.

In this chapter I compare time-series of abundance estimates to time-series of habitat suitability estimates. I explore the correlation between these two trends over a series of lag-times in order to identify potential lagged responses of abundance to changes in habitat suitability. I compare trends in predicted habitat suitability with mammal abundance trends for 177 populations of 16 species in order to identify whether trends in predicted habitat suitability are correlated with observed abundance trends.

MATERIALS AND METHODS

HABITAT SUITABILITY MODELLING

To assess how well trends in habitat suitability explain animal population trends, I built time-series of annual habitat suitability maps (HSMs) for mammal 16 species (Table 4.1). For each species I generated a habitat suitability model based on average conditions for 2006-2016, as most species' occurrence data were available from this period (see below for details). To correct for sample selection bias, I also collated 10,000 target-group background points from species with similar distributions (Phillips et al. 2009; see below for details). Ecologically relevant average bioclimatic variables for 2006-2016 (Table S4.1) and HYDE land use data from 2005 were used to build the HSMs. Where species distributions covered more than one continent, I modelled each continent separately. The habitat suitability models created in this chapter provide the foundation for the computationally intensive coupled niche-demographic models in Chapter 4 which were only computationally tractable to run over single continents. Using the occurrence points, target-group background points and environmental data I built three types of habitat suitability models: a BIOCLIM envelope model, a generalised additive model (GAM) and a random forest (RF) model (see below for details on these models). For each species and model type, I split the data into a training dataset (75%) and a test dataset (25%). I used the training data set to build the models and then used the test data to evaluate the models using the Area Under the Curve (AUC) value. I used k-fold cross validation for each modelling technique, each time using different groups of data for training and testing to limit the effect of random partitioning on the AUC scores. The BIOCLIM, GAM and RF models were then run on the full data set (Figure 3.1) and combined into a weighted ensemble model based on their average AUC values (Figure 3.2; Araújo & New, 2007). The weighted habitat

suitability ensemble model was then used to predict maps of habitat suitability for each year from 1950 to 2005, based on the environmental conditions in those years.

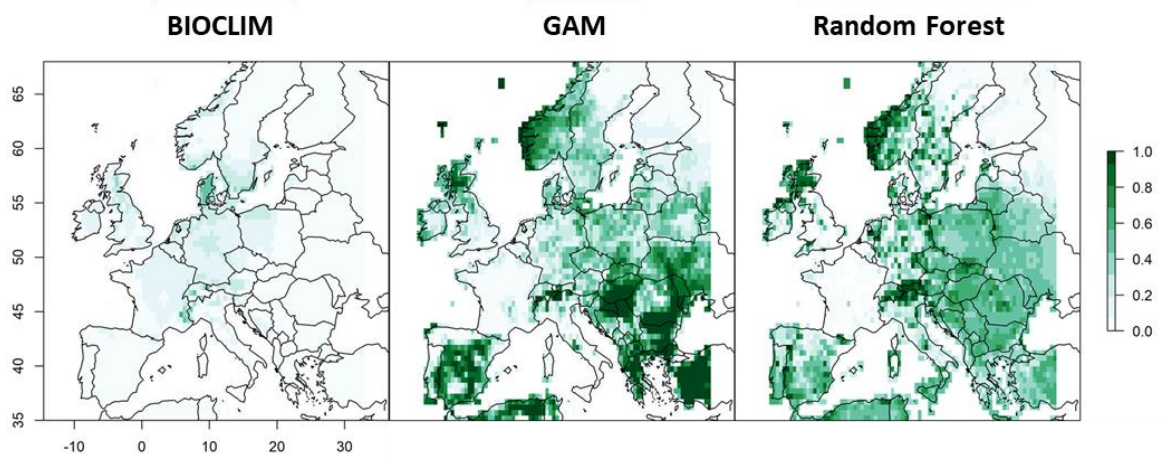


Figure 3.1 Example habitat suitability models for red deer (*Cervus elaphus*) in Europe. Each model had the same input data: occurrence data for 2006-2016; 10,000 target-group background points and average climate and land use variables (2006-2016). The predicted habitat suitability values range from zero to one with values of one representing predicted optimum habitat. The performance of the habitat suitability models was assessed with AUC scores from using k-fold cross validation (k=4). The average AUC value for each method (BIOCLIM = 0.71, GAM = 0.88, Random Forest = 0.91) was used to weight the ensemble model.

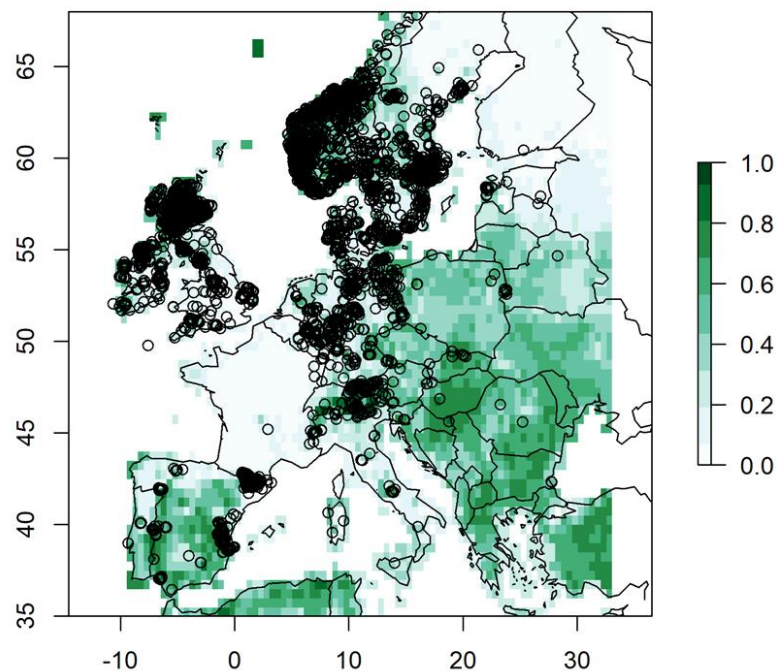


Figure 3.2 An ensemble model for red deer (*Cervus elaphus*). The ensemble was created through the weighted combination of three habitat suitability models (BIOCLIM, GAM and Random Forest) based on average AUC scores from k-fold cross validation (k = 4). Higher values correspond to higher predicted habitat suitability, the black circles denote the species occurrence data.

SPECIES OCCURRENCE DATA

I obtained species occurrence data for 16 species from the Global Biodiversity Information Facility (GBIF) (Flemons *et al.*, 2007; full list of citation DOIs in Table 4.1). This chapter provides the foundation for Chapter 4, which builds upon habitat suitability models by including mechanisms for dispersal, survival and fecundity. Thus, analysis for Chapter 4 is limited to species for which data to parameterize these mechanisms are available. In this chapter I focus on species which are sufficiently well studied to be included in Chapter 4 (Table 3.1), and species for which there are a large number of population trends available within the Living Planet database to compare with habitat suitability trends. I was also limited to species for which the specific location of population trends was available, this is necessary for identifying spatially specific trends in habitat suitability. The occurrence data were filtered so that only occurrence records for the 2006-2016 period were retained, as this was when a large number of GBIF data were available from (Figure S3.1). I excluded occurrence points outside the known extent of each species range (IUCN, 2018) as these were assumed to be erroneous. The remaining presence occurrence points were used to parameterise habitat suitability models (Table 3.1).

CORRECTING FOR SAMPLING BIAS

GBIF is a repository for opportunistic and surveyed species occurrence data. As a result, the data within GBIF are spatially biased towards areas of greater accessibility and available research effort (Beck *et al.*, 2014). In habitat suitability modelling background data are typically sampled randomly from the study region meaning that there is a potentially important difference in the environment that is being sampled by the occurrence points and the background points. Such bias in the occurrence points can lead to inferior habitat suitability model quality and poor model predictive ability (Beck *et al.*, 2014). To account for this, I gathered 10,000 occurrence points of mammal or bird species with

distributions that overlapped with at least 50% of the distribution of the species being modelled (Phillips et al. 2009; Table S3.2) and used these as target-group background points. I used species with 50% overlapping range as the target-group background points should ideally be subject to the same spatial bias as the subject species and thus occur over the same areas. The target-group background points have a similar spatial bias to the species occurrence points and therefore they should be more representative of the environment being sampled by the occurrence points. Using spatially biased background points rather than random background points has been shown to provide better habitat suitability models across multiple modelling methods (Phillips et al. 2009).

ENVIRONMENTAL DATA

I collated time-series of global climate and land use data to create annual maps of predicted habitat suitability. Monthly gridded climate time-series of minimum temperature, maximum temperature and precipitation were gathered from the global CRU TS v. 3.23 dataset (Harris *et al.*, 2014). These climate data were used to create global maps of nineteen bioclimatic variables (Table 3.1) (Hijmans *et al.*, 2017) at 0.5° spatial resolution, averaged over the 2006-2016 period. Additionally, I created annual maps of each of the bioclimatic variables for use in predicting annual maps of habitat suitability. Global land use data were gathered from the HYDE dataset (Klein Goldewijk *et al.*, 2011) for 2005, the most recent available date. HYDE provides gridded coverage of cropland and pasture at a spatial resolution of 0.083°. The percentage cover of cropland and pasture were summed to calculate percentage cover of anthropogenic land use in each cell. The HYDE data were bilinearly resampled to 0.5° to match the spatial resolution of the climate data. The HYDE dataset provides a global map of land use for each decade in this study. I linearly interpolated between these data points (see Chapter 2) to create annual maps of land use which I could use for creating annual time-series of predicted habitat suitability.

<i>Species</i>	No. occurrence points	No. observed population trends	Bioclimatic Layers	GBIF DOI
<i>Alpine Ibex</i>	172	10	1,5,6,13,15,18,19	https://doi.org/10.15468/dl.8aninz
<i>Blue Wildebeest</i>	577	19	8,9,12,13,14,15,16,17,18,19	https://doi.org/10.15468/dl.zdfk2
<i>Brown Bear (N. America)</i>	612	3	2,4,5,6,7,10,11	https://doi.org/10.15468/dl.x08j9g
<i>Common Warthog</i>	1,900	16	8,9,12,13,14,15,16,17,18,19	https://doi.org/10.15468/dl.jxhbdk
<i>European Roe Deer</i>	49,050	10	1,6,7,11,13,19	https://doi.org/10.15468/dl.h1wkdt
<i>Giraffe</i>	747	18	5,6,8,12,13,14,15,16,17,18,	https://doi.org/10.15468/dl.vnkjuk
<i>Hartebeest</i>	825	12	12,13,14,15,16,17,18,19	https://doi.org/10.15468/dl.0vmznd
<i>Plain's Zebra</i>	1,408	20	8,9,12,13,14,15,16,17,18,19	https://doi.org/10.15468/dl.3dkwvs
<i>Polar Bear (N. America)</i>	142	2	1,4,5,6,7,10,11	https://doi.org/10.15468/dl.zqwkfn
<i>Pyrenean Chamois</i>	1,239	10	1,6,7,11,13,19	https://doi.org/10.15468/dl.ftqumd
<i>Red Deer (Europe)</i>	8,566	5	2,4,5,6,7,10,11	https://doi.org/10.15468/dl.jaefxg
<i>Reindeer (Europe)</i>	2,600	2	6,8,10,11,13,16,19	https://doi.org/10.15468/dl.plw5dd
<i>Reindeer (N. America)</i>	230	9	6,8,10,11,13,16,19	https://doi.org/10.15468/dl.plw5dd
<i>Snowshoe Hare</i>	449	15	1,5,6,11,13	https://doi.org/10.15468/dl.0hcaxu
<i>Waterbuck</i>	829	19	8,9,12,13,14,15,16,17,18,19	https://doi.org/10.15468/dl.nemdcg
<i>White-tailed deer</i>	5,894	4	1,2,4,5,6,11,19	https://doi.org/10.15468/dl.md5glw
<i>Wolverine (Europe)</i>	11,040	2	1,5,6,8,11,13	https://doi.org/10.15468/dl.9umtlv
<i>Wolverine (N. America)</i>	11,502	1	1,5,6,8,11,13	https://doi.org/10.15468/dl.9umtlv

Table 3.1 Species for which habitat suitability models were built. The number of occurrence points shows for each species the number of occurrences downloaded from GBIF, these were filtered to occurrences collected between 2006 and 2016 and those within the known distribution of the species. The number of observed population trends shows the population trends available from the Living Planet database that I can compare the habitat suitability trends to. Bioclimatic layers show which bioclimatic layers were included in the habitat suitability model for each species (1 = annual mean temperature, 2 = mean diurnal range, 3 = isothermality, 4 = temperature seasonality, 5 = maximum temperature of the warmest month, 6 = minimum temperature of the coldest month, 7 = temperature annual range, 8 = mean temperature of the wettest quarter, 9 = mean temperature of the driest quarter, 10 = mean temperature of the warmest quarter, 11 = mean temperature of the coldest quarter, 12 = annual precipitation, 13 = precipitation of the wettest month, 14 = precipitation of the driest month, 15 = precipitation seasonality, 16 = precipitation of the wettest quarter, 17 = precipitation of the driest quarter, 18 = precipitation of the warmest quarter, 19 = precipitation of the coldest quarter). The GBIF DOI is a unique reference to the original occurrence data downloaded from GBIF.

HABITAT SUITABILITY MODELS

BIOCLIM (Nix, 1986; Booth *et al.*, 2014) is a climate-envelope-model which uses only presence occurrence data and the corresponding environmental variables. The percentile scores of environmental variables in each grid cell are compared to the percentile distribution of environmental variables at known presence locations. Locations are predicted to be more suitable the closer they are to the centre of the percentile distribution for each of the environmental variables included in the model. The advantage of using BIOCLIM is that the model is straightforward to implement, and it uses only presence data.

However, these presence data are often collected opportunistically and therefore are geographically biased towards more accessible areas (Kadmon, Farber and Danin, 2004; Schulman, Toivonen and Ruokolainen, 2007). The BIOCLIM model does not include background points, these are used in other models to characterise the range of environments in the study area and to correct for spatial bias in the occurrence points. Therefore the suitability predictions are limited to narrower range of environments meaning that BIOCLIM models are less reliable for predicting outside of this range, e.g. under climate change (Hijmans and Graham, 2006).

GAMs are a type of generalised linear model (GLM) which use a regression approach with smoothing functions (Hastie and Tibshirani, 1990). GAMs are more flexible than GLMs as they are “data-driven” meaning that the data determines the shape of the response curve, rather than fitting the data to a predetermined set of parameters (Yee and Mitchell, 1991). Thus, GAMs are better suited to modelling complex and often non-linear ecological responses than GLMs (Yee and Mitchell, 1991; Guisan, Edwards and Hastie, 2002).

RF models are a type of machine learning model (Breiman, 2001) which can be used for regression or classification. Here I use them for regression, to produce maps of predicted habitat suitability (Evans *et al.*, 2010). Both GAMs and random forest models require background locations to characterise the environment of study area. I used target-background locations to account for spatial bias in the species occurrence data.

OBSERVED POPULATION TRENDS

I gathered population trends from the Living Planet database (Collen *et al.*, 2009; McRae, Deinet & Freeman, 2017), which formed the basis of my analysis in Chapters 2 and 3. Some of the years in the population trends have missing data. In these cases I estimated missing data using the same method as in Chapter Two: for populations with six or more data points

I used GAMs (using a smoothing factor of half the number of data points) to estimate missing data, for populations with fewer than six data points I used linear interpolation (Collen *et al.*, 2009).

The average time-series length of populations included in the analysis was 17.6 (\pm 9.7) years. Most of the populations were from Africa (58.8%), there were also populations from Europe (20.9%), North America (18.6%) and Asia (1.7%). The majority of species in this analysis were ungulates (87.0%), there were also populations of lagomorphs (8.5%) and carnivores (4.5%).

HABITAT SUITABILITY TRENDS

I extracted spatiotemporally coincident predicted habitat suitability values at each location of the 177 observed population trends, to create a habitat suitability trend for each observed population. I averaged the predicted habitat suitability values over a 50 km buffer around the given coordinates for each observed population to account for environmental changes over a broader area which are likely to influence the population trends.

COMPARISON OF HABITAT SUITABILITY TRENDS AND POPULATION TRENDS

Within the Living Planet database each population trend can be recorded at a different spatial scale or using a different abundance metric, although to be included in the database this must be done consistently across years (Loh *et al.*, 2005). To account for this variation across population trends I calculate annual 'lambdas' which are the logged (base 10) rate of population change. To ensure that both observed population trends and predicted habitat suitability trends are on the same scale I also calculated the logged (base 10) rate of change in habitat suitability. This means that that I could compare the rate of change in predicted habitat suitability with the rate of observed population change.

It is possible that changes in habitat suitability will not cause immediate impacts on population trends but rather cause a lagged effect. To account for this, I calculated the cross-correlation function for each population trend with the corresponding predicted habitat suitability trend. This allowed me to calculate the correlation between two time-series trends over a series of six annual lag-times (0-5 years) and thus determine how well rates of change of predicted habitat suitability explains variation in rates of change of population trends. For each of the 177 populations I calculated maximum correlation coefficient value for each population. I limited the maximum lag time to five years as this was the minimum length of the population time-series.

All analyses were carried out using the statistical software R (R Core Team, 2018). The following packages were used to build habitat suitability models: raster (Hijmans, 2016), dismo (Hijmans *et al.*, 2017), sp (Pebesma and Bivand, 2005; Bivand, Pebesma and Gomez-Rubio, 2013), rgbif (Chamberlain and Boettinger, 2017; Chamberlain *et al.*, 2018a), mgcv (Wood, 2011) and randomForest (Liaw and Wiener, 2002). The dplyr (Wickham *et al.*, 2018), zoo (Zeileis and Grothendieck, 2005), taRifx (Friedman, 2014), mgcv (Wood, 2011), reshape2 (Wickham, 2007) and ggplot2 (Wickham, 2016) packages were used to process and visualise the trends in predicted habitat suitability and abundance.

RESULTS

The trained habitat suitability models were quite accurate across all species ($A\bar{U}C \pm SD = 0.83 \pm 0.14$; full list of AUC values in Appendices). For each species the RF models performed better than BIOCLIM and GAM (BIOCLIM = 0.71 ± 0.16 , GAM = 0.88 ± 0.08 , RF = 0.91 ± 0.07) and as a result, RF had the greatest weight in the resulting ensemble models.

There is no clear relationship across all the species between predicted habitat suitability and population growth rates (Figure 3.3). In 13 of the 16 species there was no significant relationship between predicted habitat suitability and annual population growth rates. For two species there was a significant negative relationship (Alpine ibex and Chamois) and for Reindeer there was a significant positive relationship.

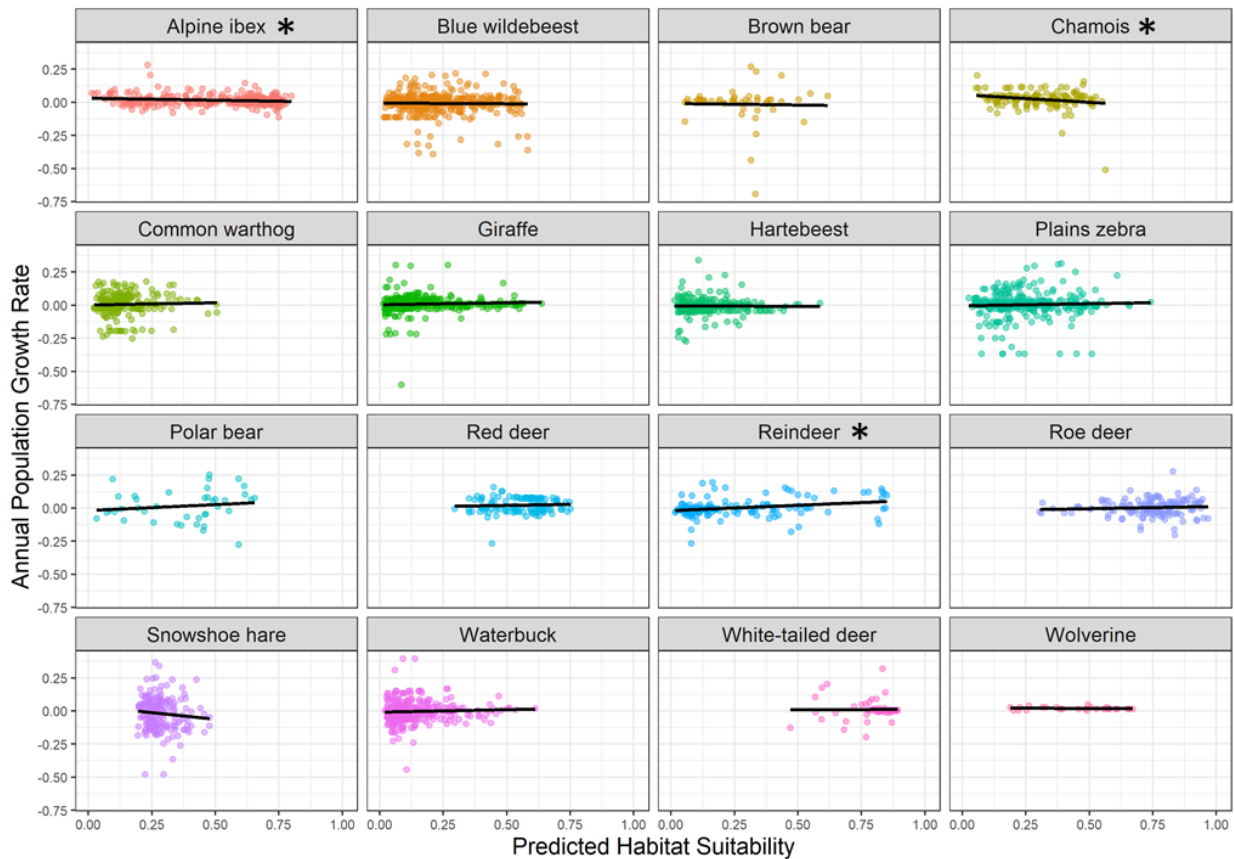


Figure 3.3 The relationship between predicted habitat suitability and annual population growth rates across each of the 16 mammal species. Each point shows the population growth rates for each year and their spatiotemporally corresponding predicted habitat suitability value. Population growth rate values above zero indicate a growing population and values below zero indicate a declining population trend. Panels marked with an asterisk indicate species for which there was a significant relationship between predicted habitat suitability and population growth rates.

I do not find any evidence for consistent correlations between trends in the rate of change of habitat suitability and population growth rates. There are almost equal numbers of correlation coefficients above (54.2%) and below (45.8%) zero (Figure 3.4A). The average correlation coefficient was -0.01 ± 0.20 (Figure 3.4A). None of the populations were found to have a statistically significant correlation.

However, when lagged responses of population growth rates to changes in habitat suitability are accounted for there is an overall positive relationship between the rate of change of predicted habitat suitability and population growth rates (Figure 3.4B). The average correlation coefficient across all populations is 0.18 ± 0.15 , which on average explains 3.1% of the variation in population growth rates. I find that 93.8% of these ‘maximum’ coefficients were positive and the average maximum coefficient size across all species was $0.18 (\pm 0.14)$ (Figure 3.4B). I note that none of the correlations were found to be significant. The mean lag time for the maximum coefficient across all populations was $2.2 (\pm 1.82)$ years, although the most frequent lag time for the maximum coefficient was at zero years 0 (23.2%), with each of other lag times having similar frequencies (11.8% – 19.2%; Table 3.2).

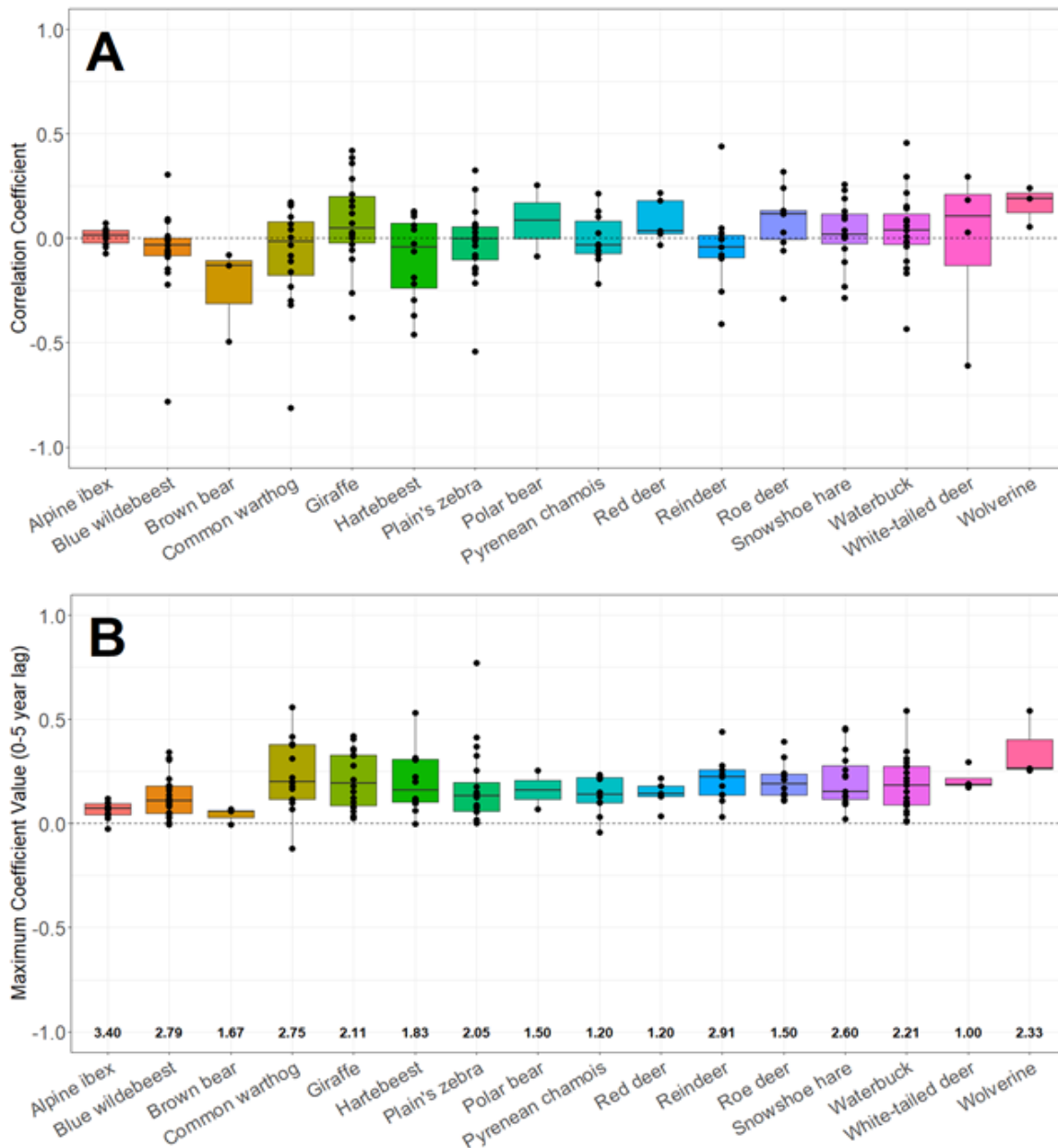


Figure 3.4 Panel A shows boxplots for each species showing the distribution of correlation coefficients between the rate of population change and the rate of change in predicted habitat suitability. Panel B shows boxplots for each species showing the distribution of the maximum correlation coefficients between the rate of population change and the rate of change in predicted habitat suitability at a series of lag times ($t = 0-5$). The numbers at the bottom of each column in panel B indicates the average lag time, in years, at which the maximum correlation was found for each species. In both panels the black dots represent each population with the box plots showing the spread of correlation coefficients for each species. Values closer to 1 or -1 indicate stronger positive or negative correlations, respectively.

<i>Species</i>	Mean correlation coefficient	Mean maximum correlation coefficient	Mean lag time for maximum coefficient
<i>Alpine ibex</i>	0.01 (± 0.05)	0.06 (± 0.04)	3.40 (± 1.96)
<i>Blue wildebeest</i>	-0.07 (± 0.21)	0.13 (± 0.11)	2.79 (± 1.90)
<i>Brown bear</i>	-0.24 (± 0.23)	0.04 (± 0.35)	1.67 (± 0.55)
<i>Common warthog</i>	-0.08 (± 0.25)	0.23 (± 0.17)	2.75 (± 1.77)
<i>Giraffe</i>	0.08 (± 0.21)	0.21 (± 0.14)	2.11 (± 1.84)
<i>Hartebeest</i>	-0.10 (± 0.21)	0.20 (± 0.15)	1.83 (± 1.59)
<i>Plain's zebra</i>	-0.02 (± 0.18)	0.17 (± 0.23)	2.05 (± 1.73)
<i>Polar bear</i>	0.08 (± 0.24)	0.16 (± 0.15)	1.50 (± 1.41)
<i>Pyrenean chamois</i>	0.00 (± 0.13)	0.14 (± 0.35)	1.20 (± 1.29)
<i>Red deer</i>	0.09 (± 0.11)	0.14 (± 0.28)	1.20 (± 2.00)
<i>Reindeer</i>	-0.04 (± 0.21)	0.21 (± 0.28)	2.91 (± 1.99)
<i>Roe deer</i>	0.07 (± 0.17)	0.21 (± 0.44)	1.50 (± 1.37)
<i>Snowshoe hare</i>	0.03 (± 0.16)	0.21 (± 0.13)	2.60 (± 2.10)
<i>Waterbuck</i>	0.04 (± 0.19)	0.19 (± 0.14)	2.21 (± 1.72)
<i>White-tailed deer</i>	-0.03 (± 0.41)	0.21 (± 0.50)	1.00 (± 1.06)
<i>Wolverine</i>	0.16 (± 0.10)	0.36 (± 0.16)	2.33 (± 2.31)

Table 3.2 The mean coefficient values for each species when lagged responses are not accounted for, contrasted with the species mean maximum coefficient across a series of annual lag times (0-5 years). The optimum lag time required to reach the maximum correlation coefficient.

DISCUSSION

My results show that there is evidence for a lagged response of abundance to changes in predicted habitat suitability. These findings help to explain the lack of consensus from previous studies, some of which have found a moderate and widely variable positive relationship between abundance and predicted habitat suitability (Weber *et al.*, 2017) and others which have not found any relationship (Nielsen *et al.*, 2005; Filz, Schmitt and Engler, 2013; Dallas and Hastings, 2018). These results are important as they suggest that there are lagged responses of species abundance to changes in predicted habitat suitability (Kuussaari *et al.*, 2009). This highlights the importance of using time series of abundance and predicted habitat suitability rather than static snapshots, which may not be representative of dynamic habitats (Doherty Jr., Boulinier and Nichols, 2003; Schurr *et al.*, 2012).

A drawback of using historic environmental data is the limited amount of global data which is available from 1950 onwards, the first year for which I have population trend data. Available data are often spatially coarse; for instance, the environmental data used in this analysis were 0.5° spatial resolution. This resolution may be an appropriate spatial scale for exploring macroecological biodiversity trends, but it is likely that the mechanisms which determine patterns of species abundance function at finer spatial scales (Pearson & Dawson, 2003) and that finer scale resolutions are more relevant to applied conservation (Seo *et al.*, 2009). Finer resolution data are available (e.g., ESA CCI) but with considerably less temporal coverage (1992 onwards), thus limiting the number of observed population trends available for analysis.

I note that the maximum correlation between predicted habitat suitability and species abundance is generally quite weak, on average 0.18 ± 0.15 across all populations. This low correlation may be because there are several factors that influence species abundance which are not included in the habitat suitability model. For example, the presence of an ecological competitor or human exploitation at a highly suitable site might mean that abundance is lower than at less environmentally suitable sites where competition and exploitation are absent (Johnson & VanDerWal, 2009; Suttle *et al.*, 2007). Furthermore, there are aspects of species behaviour which may mean they are not evenly distributed across their range. For example, it has been shown that it is more difficult to predict densities of species that exhibit colonial or semi-colonial behaviour than territorial species (Estrada and Arroyo, 2012). Therefore, it may be that habitat suitability is more strongly linked with the carrying capacity of a site (Thuiller *et al.*, 2014), rather than the realised abundance (VanDerWal *et al.*, 2009).

Another possible reason why I find relatively low correlation between predicted habitat suitability and abundance is that habitat suitability models do not account for important

ecological processes, such as dispersal, population dynamics (Acevedo et al., 2017; Boulangeat, Gravel, & Thuiller, 2012). These mechanisms directly influence species abundance and including them in the modelling process is likely to improve predictions of species abundance. Coupled niche-demographic models allow for the integration of mechanisms for dispersal and population dynamics (Buckley et al., 2010; Fordham, Akçakaya, Araújo, Keith, & Brook, 2013; Keith et al., 2008). Preliminary studies suggest that coupled niche-demographic models perform better than habitat suitability models at predicting range changes (Fordham et al., 2017), although the predictions have yet to be validated against observed population trends. However, the inclusion of these mechanisms is both data and computationally intensive and for most species there is not yet enough knowledge to parameterise these models (Keedwell, 2004).

I did not find a relationship when lagged responses were ignored; however, when I included them I found that predicted habitat suitability was more strongly correlated with species abundance. I therefore show, for the first time, that lagged responses are an important aspect of the relationship between predicted habitat suitability and abundance. Such lagged responses should be included in future studies that aim to estimate abundances from changing environmental conditions. The inclusion of ecological mechanisms such as dispersal and population dynamics into habitat suitability models may be an important step towards better understanding the relationship between habitat suitability and species abundance.

CHAPTER FOUR:
ASSESSING THE PREDICTIVE ABILITY OF COUPLED
NICHE-DEMOGRAPHIC MODELS

ABSTRACT

Habitat suitability models have been the method of choice for predicting species responses to environmental change, due to their simplicity of use and easily validated predictions. However, these models have been criticised for omitting ecological processes such as population dynamics and dispersal. Coupled niche-demographic models have been developed to incorporate such processes into habitat suitability models. Inclusion of these processes means that coupled niche-demographic models allow for the prediction of abundance, rather than habitat suitability. The superiority of coupled niche-demographic models over habitat suitability models in terms of predictive ability has been assumed and there has been limited validation of coupled niche-demographic models. To test the predictive accuracy of coupled niche-demographic models I used them to predict population trends for 17 populations of three mammal species (Alpine ibex, red deer and brown bear), and compared the predicted population trends to observed population trends from the Living Planet database. I find that coupled niche-demographic models are an improvement upon habitat suitability models for predicting population trends. However, I note that both perform quite poorly and that the linear mixed effects models (created in Chapter Two) outperform coupled niche-demographic models in predicting average population growth rates.

INTRODUCTION

Habitat suitability models have been the most widely used method for understanding broad scale impacts of environmental change on biodiversity. This is because they are relatively straightforward to produce and there are plentiful available data to validate their predictions, which are typically range shifts (Ehrlén and Morris, 2015). However, there are multiple limitations of habitat suitability models and their use in predicting the responses of biodiversity to environmental change. These limitations include: difficulties making

accurate predictions under novel climate conditions (Webber *et al.*, 2011); the often violated assumption that current species occupancy is in equilibrium with its environment (Varela, Rodríguez and Lobo, 2009); models are typically based on single species and do not consider biotic interactions which can play a key role in delimiting species distributions (Staniczenko *et al.*, 2017) and ecological processes such as population dynamics and dispersal, which lead directly to range contraction or expansion, are not accounted for (Elith, Kearney, & Phillips, 2010; Guisan & Thuiller, 2005). Despite these limitations, habitat suitability models have been shown to provide an effective starting point for predicting range shifts under climate change (Fordham *et al.*, 2017; Pearson & Dawson, 2003).

A number of more complex modelling strategies have been developed to tackle the aforementioned limitations of habitat suitability models. Coupled niche-demographic (CND) models are a leading example of these more complex models (Keith *et al.*, 2008). CND models link ecological niche models (synonymous with habitat suitability models) with stochastic demographic models and incorporate mechanisms for dispersal (Keith *et al.*, 2008). The output of CND models are maps of predicted abundance rather than habitat suitability. Population dynamics and dispersal have a fundamental influence on the responses of biodiversity to environmental change (Engler & Guisan, 2009; Keith *et al.*, 2008; Travis *et al.*, 2013) and it is therefore expected that explicitly accounting for these processes will result in improved predictions of both species occurrence and abundance. It has been shown that predictions of population trends from coupled niche-demographic models are often markedly different to predicted changes in range area, which is a metric that has typically been used to estimate extinction risk from climate change (Fordham *et al.*, 2012; Thomas *et al.*, 2004). This highlights the importance of accounting for complex processes that influence abundance. However, there has been relatively little validation of

these models as long-term records of abundance are much less plentiful than range maps (Urban *et al.*, 2016).

Virtual species data have also been used to compare habitat suitability models to a selection of more complex models, which to varying extents incorporated either population dynamics or dispersal, or both. In each case the more complex models outperformed the habitat suitability models (Zurell *et al.*, 2016), suggesting that the inclusion of population dynamics and dispersal into habitat suitability models can provide improved predictions. Thus far, the most significant effort to validate coupled niche-demographic models on observed, rather than simulated, data has been for 20 British bird species. A range of models with varying levels of complexity and environmental data were trained on data from 1970, with the predicted range shifts validated against data from 2010 (Fordham *et al.*, 2017). The more complex coupled niche-demographic models tended to outperform simpler habitat suitability models that accounted only for climatic variation. However, when static land use data were included into the simple habitat suitability models they performed similarly to the complex coupled niche-demographic models.

To my knowledge, predicted population trends from coupled niche-demographic have yet to be validated against observed population trends, and this is what I test here. Coupled niche-demographic models were built for three mammal species and were used to predict population trends from 1950-2005. I then assessed the accuracy of these predictions against observed time-series of abundance from the Living Planet database in order to gauge the ability of coupled niche-demographic models to predict population trends.

MATERIALS AND METHODS

To predict mammal population trends, I selected species with sufficient available data (red deer, brown bear and Alpine ibex; see below for details) and built two types of models: habitat suitability models and coupled niche-demographic models. With the habitat

suitability models, I used species occurrence data in conjunction with bioclimatic and land use data to create maps of estimated habitat suitability for each year of the study (1950 – 2005), these formed the basis of Chapter Three. With the coupled niche-demographic models, I coupled the habitat suitability models with a demographic model by scaling the carrying capacity of each cell by predicted habitat suitability (0-1) in order to produce spatial predictions of mammal population trends that vary with predicted habitat suitability. I then assessed the predictive accuracy of both models by comparing the predicted trends in both habitat suitability (HS models) and abundance (CND models) against observed population trends, which were taken from the Living Planet database.

HABITAT SUITABILITY MODELS

The CND models require time-series of annual maps of binary predicted presence or absence of suitable habitat. To create these, I used the habitat suitability models from Chapter Three and applied a threshold above which habitat is considered suitable (i.e., ‘present’) to create time series of presence/absence predictions. I calculated a threshold value from the weighted ensemble model to predict areas of species presence or absence (Figure 5.1). There are multiple possible methods for calculating the threshold; I used the true skill statistic, the threshold value at which the sum of the true positive rate and true negative rates is maximised, as it has been shown to outperform other methods (Allouche, Tsoar and Kadmon, 2006).

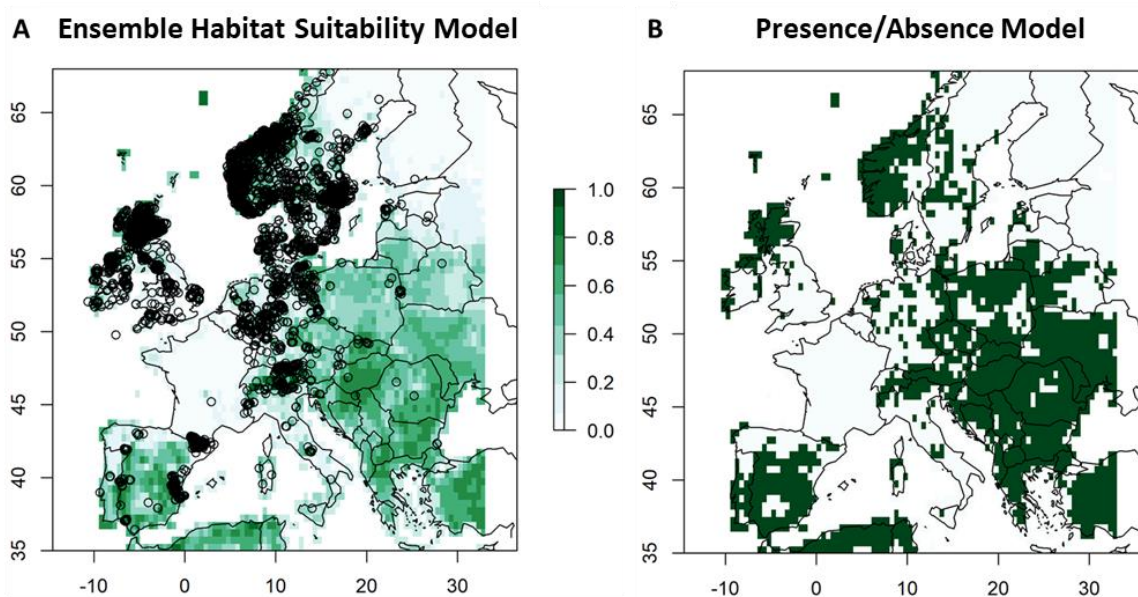


Figure 4.1 (A) Ensemble habitat suitability model for red deer. Higher values correspond to higher predicted habitat suitability and black circles denote the original species occurrence data. (B) A weighted threshold value was also calculated using the true skill statistic and this threshold value was applied to the ensemble model to create a predicted presence/absence map. Areas in green indicate predicted presence of red deer.

COUPLED NICHE-DEMOGRAPHIC MODELS

Coupled niche-demographic models require several ecologically based parameters and therefore could only be built for species for which the following data were available: (i) at least 100 occurrence data points available from GBIF (Table 3.1; Flemons *et al.*, 2007; Wisz *et al.*, 2008); (ii) a transition matrix containing survival and fecundity rates, available from the COMADRE database (Salguero-Gómez *et al.*, 2016); and in order to assess the predictive accuracy of the models, (iii) at least one observed population trend from the Living Planet database (Loh *et al.*, 2005).

The CND model used in this study is an extension of the model in the *demonic* R package (Nenzén *et al.* 2012), which provides a platform for simulating spatially-explicit population dynamics. The main changes made to the original *demonic* package were to the dispersal function. This function was previously configured for plants, so only individuals in the first age class (i.e. seeds) would disperse, I changed this so that all stages in the transition matrix would be able to disperse. I also changed the dispersal kernel to a half-Cauchy distribution,

which I could parameterise with median and maximum dispersal distances (full R code can be found in Appendices).

There are two possible techniques for coupling habitat suitability models with demographic models: through carrying capacity and/or species vital rates. There is little consensus in the literature on which is the best method. There is a positive relationship between carrying capacity and predicted habitat suitability (Thuiller *et al.*, 2014) and a link between high habitat suitability and greater densities and abundances has been established (Tôrres *et al.* 2012; VanDerWal *et al.* 2009). However, the relationship between predicted habitat suitability and the vital rates of the species is less well understood, with evidence for a negative relationship between population growth rate and predicted habitat suitability (Thuiller *et al.*, 2014), suggesting that linearly scaling vital rates to increase with predicted habitat suitability would not be appropriate. Here I couple the habitat suitability models with the population models through linearly scaling the carrying capacity of each cell, in each year, with predicted habitat suitability (Figure 4.2).

The models were initiated with uniform abundances in each cell, based on density estimates from the literature. This is done as the true abundance values for each cell are not known. I account for this by assessing the models in terms of relative abundance, comparing rates of population growth rather than absolute abundance. For each species, the CND models were run for a “burn-in” period of 10 years under initial habitat conditions (predicted habitat suitability for 1950). Population trends consistently stabilised after the first couple of years of the burn-in period (Figure S4.1). After the burn-in period the model was run for 56 years under predicted habitat suitability conditions for 1950-2005. The model output for each year is a predicted abundance in each cell over the species range.

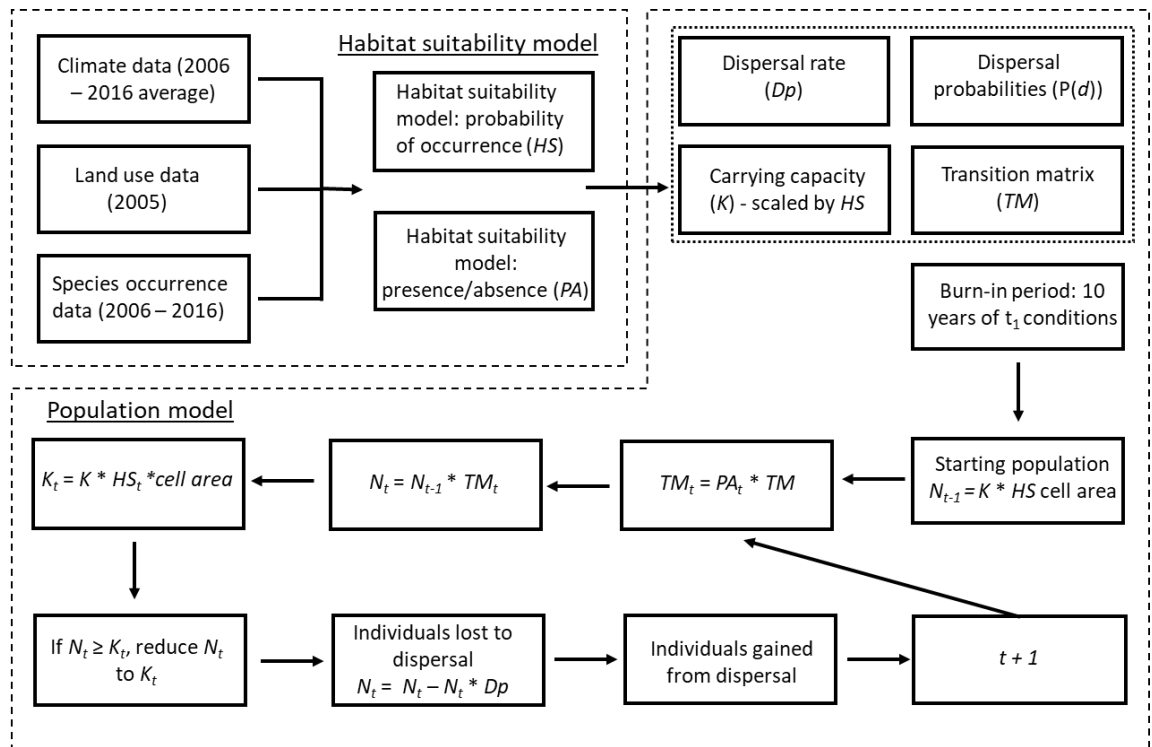


Figure 4.2 Schematic showing the coupled niche-demographic modelling process. The habitat suitability models directly impact the population models through the carrying capacity values, so that cells with higher predicted habitat suitability have higher carrying capacity.

TRANSITION MATRICES

For each species I gathered transition matrices from the COMADRE database (Salguero-Gómez *et al.*, 2016). Transition matrices provide survival and fecundity rates for each year or stage in a species life-cycle. Matrices were included in the analysis if they had values for both survival and fecundity and each stage in the matrix was a year, which is the temporal unit of the CND models. For each year in the CND model a transition matrix is drawn from a normal distribution where the mean is the transition matrix and the standard deviation is a value between 0 and 0.5, thereby building stochasticity into the model. I decided to limit the standard deviation around the transition matrix to 0.5 following a pilot study exploring how population growth rates vary with standard deviation across the three species (see Figure S4.2). When standard deviation was greater than 0.5 I found that more population growth rates tended to be less than one suggesting that the increased stochasticity would increase the likelihood of population declines.

DISPERSAL

Dispersal was incorporated into the CND model by creating species-specific dispersal kernels. Data on species' dispersal ability are not reliably available from the literature; instead, I estimated median and maximum dispersal distance using home range data, which are more readily available. The majority of mammal home range data are recorded in the PanTHERIA database (Jones *et al.*, 2009). If home range data were not available in PanTHERIA, estimates were gathered from the literature (Table 4.1). The square root of home range size is estimated to be linearly related to median dispersal distance by a constant of seven and maximum dispersal distance by a constant of 40 (Bowman *et al.*, 2012; Table 4.1). I used the estimated median dispersal distance as the scale parameter in a half-Cauchy distribution, meaning that 50% of dispersal events would be less than the median dispersal distance. The half-Cauchy distribution has been found to outperform exponential distributions (Paradis, Baillie and Sutherland, 2002) when used for creating dispersal kernels, as it allows for more frequent long-distance dispersal events which are an important component of population connectivity/metapopulation dynamics (Trakhtenbrot *et al.*, 2005). However, to ensure the model was computationally tractable I set the probability of dispersing further than the maximum dispersal distance to zero. I varied the dispersal rate of each cell between 0 and 0.5 so that no more than half of the individuals would disperse out of a given cell over a year.

<i>Species</i>	No. occurrences	Mean dispersal distance (km)	Max dispersal distance (km)	Carrying capacity (individuals per km ²)	Sources
<i>Alpine ibex</i>	172	19.8	113	1.4	(Gossow and Zeiler, 1997; Scillitani <i>et al.</i> , 2012)
<i>Red deer</i>	8566	53.3	305.7	25	(Coulson <i>et al.</i> , 2004; Jones <i>et al.</i> , 2009)
<i>Brown bear (North America)</i>	612	123.5	706.54	1.87	(Jones <i>et al.</i> , 2009; Santini, Isaac and Ficetola, 2018)

Table 4.1 List of all species for which the coupled niche-demographic models were built, the key parameters used to build the models and the sources of the key parameters.

CARRYING CAPACITY

Estimates of carrying capacity were gathered from the literature (Table 4.1). The carrying capacity of each cell was linearly scaled with predicted habitat suitability so that cells with high predicted habitat suitability had higher carrying capacity than cells with lower predicted habitat suitability values (Thuiller *et al.*, 2014). The carrying capacity of each cell can change on an annual basis with changes in predicted habitat suitability. Carrying capacity was implemented through a ceiling function meaning that the abundance of a cell cannot exceed its carrying capacity for a given year (Zurell *et al.*, 2016).

SAMPLING LIFE HISTORY CHARACTERISTICS

The parameters for annual dispersal rates and the standard deviation around the transition matrix (i.e. stochasticity of the demographic model) were difficult to quantify from the literature. For these two variables I estimated a reasonable range of both variables to be 0-0.5: the dispersal rate sets the proportion of individuals which emigrate out of a cell in a given year and it seemed reasonable to limit this to half the population of cell; for the Alpine ibex and brown bear transition matrices there was little different to population growth rates when stochasticity was above 0.5, in the red deer populations there was a high tendency of the populations to crash when stochasticity was greater than 0.5 (see Figure S4.2). Latin Hypercube Sampling (LHS) was used to ensure equal sampling across the variable space.

I set the number of LHS partitions to be 15.6 times the number of independent variables (Jia *et al.*, 2007). For each of the 31 partitions I ran the resulting model 100 times to capture the variation from the stochastic transition matrices.

MODEL ASSESSMENT

OBSERVED POPULATION TRENDS

To assess the predictive accuracy of the CND models I compared the predicted population trends to observed population trends from the Living Planet database (http://www.livingplanetindex.org/data_portal). The population trends vary in length and there are years within each population with missing data (Table 4.2). As in Chapters Two and Four, I estimate missing data in the observed population trends using either GAMs or LMs.

<i>Species</i>	ID	Start year	End year	Years with data	Country
<i>Alpine ibex</i>	a	1950	1980	31	Switzerland
	b	1950	1989	40	Switzerland
	c	1955	1964	10	Switzerland
	d	1950	1964	14	Switzerland
	e	1955	2000	45	Italy
	f	1950	1984	35	Switzerland
	g	1950	1985	35	Switzerland
	h	1989	2005	9	France
	i	1950	2002	51	Switzerland
	j	1950	1984	35	Switzerland
<i>Brown bear</i>	k	1982	1993	12	United States
	l	1973	1982	20	United States
	m	1973	1994	10	United States
<i>Red deer</i>	n	1952	1984	5	Spain
	o	1986	2005	12	Spain
	p	1979	1998	20	France
	q	1979	2001	23	France

Table 4.2 The ID, temporal coverage, years with abundance data available and location of each observed population trend.

COMPARISON OF PREDICTED POPULATION TRENDS AND OBSERVED POPULATION TRENDS

To assess the predictive accuracy of the CND models I compared them to observed population trends. The output of the CND models are annual maps of predicted abundance.

At the location of each observed population I extracted the annual predicted abundance averaged over a 50km radius buffer, to create a time-series of predicted abundance. For each population I excluded predictions from before the first population estimate and after the last one. The spatial resolution of the model predictions is relatively coarse (0.5° by 0.5°). The resolution at which the observed populations are made is likely to be more local, meaning that the predicted abundance values are likely to be much higher than the observed values simply due to the difference in scale. To allow for this I converted both the predicted and observed population trends to population growth rates, thereby comparing relative rates of abundance change rather than absolute abundance values.

To compare the predicted trends to the observed trends I use the same method as in Chapter Three: at the location of each population I compare each of the 3,100 predicted population trends to the observed population trends using the cross-correlation function with series of lag times (0-5 years). I compared the correlations between the observed population trends and both the abundance trends predicted by the CND models, and the predicted habitat suitability trends calculated in Chapter Three.

I calculated the average population growth rate for each CND model run and used the top performing linear mixed effects (LME) model from Chapter Two to predict average population growth rates for each population. The top performing LME model for mammals from Chapter Two had the following explanatory variables: rate of conversion to anthropogenic land use (RCA); rate of climate warming (RCW); the interaction between RCA and RCW; and body mass). I compared both the CND and LME predicted population growth rates to the observed population growth rates as a means of assessing the predictive accuracy of two contrasting modelling approaches.

All analyses were carried out using the statistical software R). The raster (Hijmans, 2016), dismo (Hijmans *et al.*, 2017), sp (Pebesma and Bivand, 2005; Bivand, Pebesma and

Gomez-Rubio, 2013), `rgbif` (Chamberlain and Boettinger, 2017; Chamberlain *et al.*, 2018b), `mgcv` (Wood, 2011) and `randomForest` (Liaw and Wiener, 2002), `demoniche` (Nenzén *et al.*, 2012), `LaplacesDemon` (Statisticat, 2018), `popbio` (Stubben and Milligan, 2007), `snow` (Tierney), `lhs` (Carnell, 2018) and `doParallel` packages were used to build the coupled niche-demographic suitability models. The `dplyr` (Wickham *et al.*, 2018), `zoo`, `taRifx` (Friedman, 2014), `reshape2` and `ggplot2` (Wickham, 2016) packages were used to process and visualise the trends habitat suitability and abundance.

RESULTS

The output from the coupled niche-demographic models closely follow the predicted habitat suitability trends (Figure 4.3), with extreme values becoming exaggerated in the CND models. The closeness of the two trends is expected as the habitat suitability models form the basis of the coupled niche-demographic model and is directly linked to the demographic models by scaling carrying capacity. The spatial patterns in habitat suitability dynamics are also echoed in the outputs of the CND models (Figure 4.4). However, there are key differences, such as high levels net increase in abundance in areas in and beyond cells which have seen a high net increase in predicted habitat suitability (Figure 4.4). This demonstrates the influence of the population dynamics and dispersal mechanisms in the CND models.

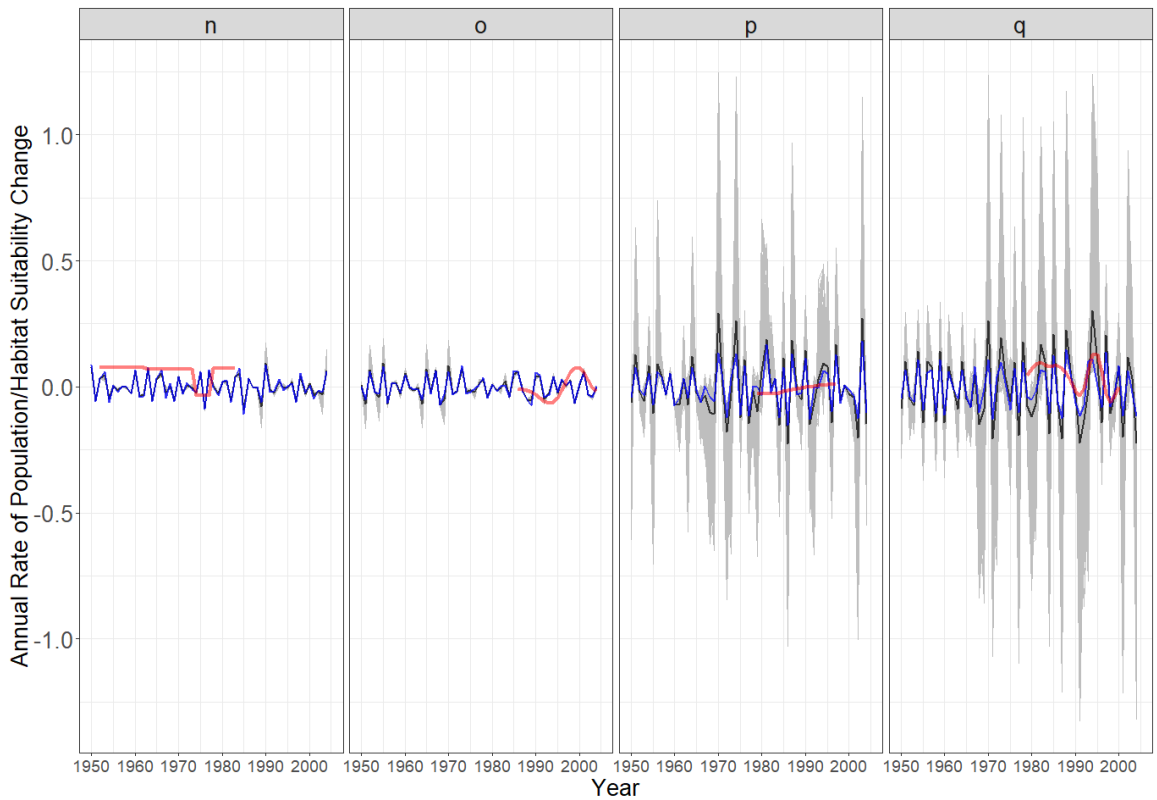


Figure 4.3 For each of the red deer populations the predicted trends in population growth rates are shown (grey) alongside the trends in the rates of change in habitat suitability (blue) and the observed population growth rates (red).

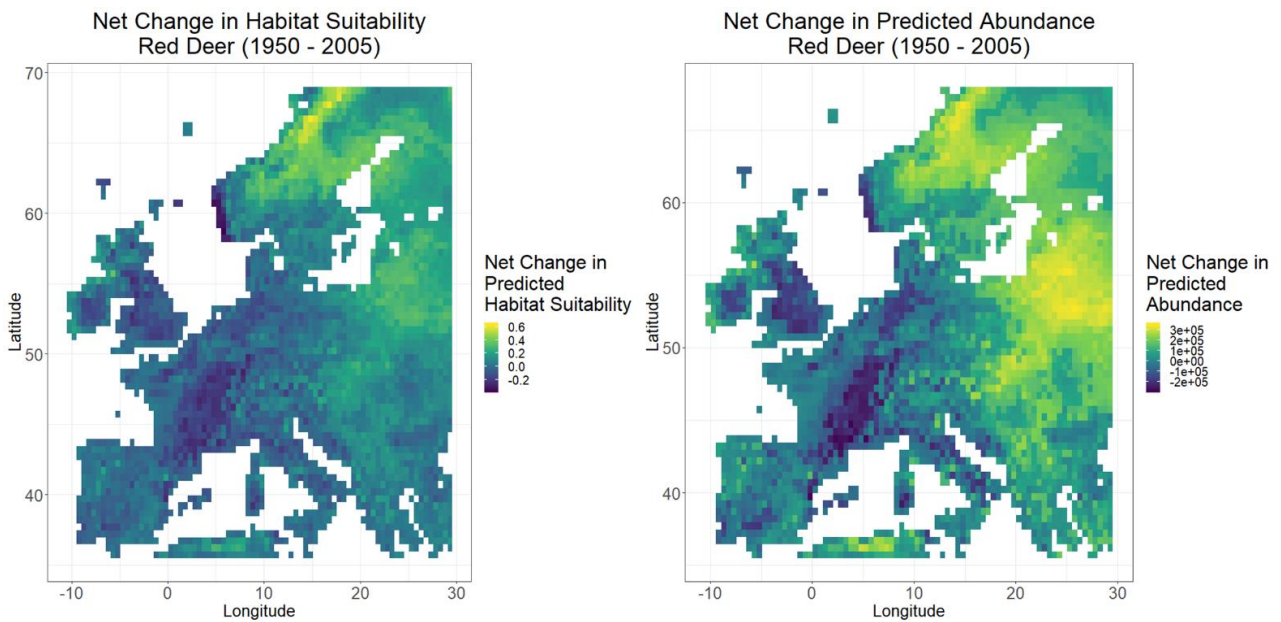


Figure 4.4 Maps of the net change in predicted habitat suitability and average net change in predicted abundance for red deer between 1950-2005. Corresponding maps for the Alpine ibex and brown bear are available in the Appendices.

In order to assess the ability of the CND models to predict population trends I correlated trends in predicted population growth rates with observed population growth rates, for each of the 3,100 model runs of each of the 17 study populations. Here I assume that higher correlations between the predicted population growth rates and the observed population growth rates, suggest better performance of the CND models. I found that correlations between predicted population growth rates and observed population growth rates varied markedly within and across populations and species (Figure 4.5). Notably I found that the median correlation between the output from the CND models and the observed population trends (0.019 ± 0.155) were on average higher than the correlations between the predicted habitat suitability (HS) trends and observed population trends (-0.005 ± 0.153 ; Table 4.3), produced in Chapter Three. This suggests that although the CND and HS models both perform quite poorly; the CND models, on average, were slightly better predictors of population growth rates than HS models.

There is considerable variation in the correlations between the predicted abundance trends from the CND models and observed abundance trends of the Alpine ibex. This is likely to be because the predicted habitat suitability trends for the alpine ibex are highly variable over time (Alpine ibex, $\overline{HS} = 0.473 \pm 0.222$; brown bear, $\overline{HS} = 0.307 \pm 0.163$; red deer, $\overline{HS} = 0.502 \pm 0.097$). Conversely, the predicted habitat suitability trends of the red deer are relatively high and stable, this is reflected in the low variation of the predicted population growth rates (Figure 4.6) and correlation coefficients (Figure 4.5). The median values of the correlations between the predicted and observed red deer abundance trends are 0.008 higher on average than the correlations between the predicted habitat suitability trends and observed abundance trends.

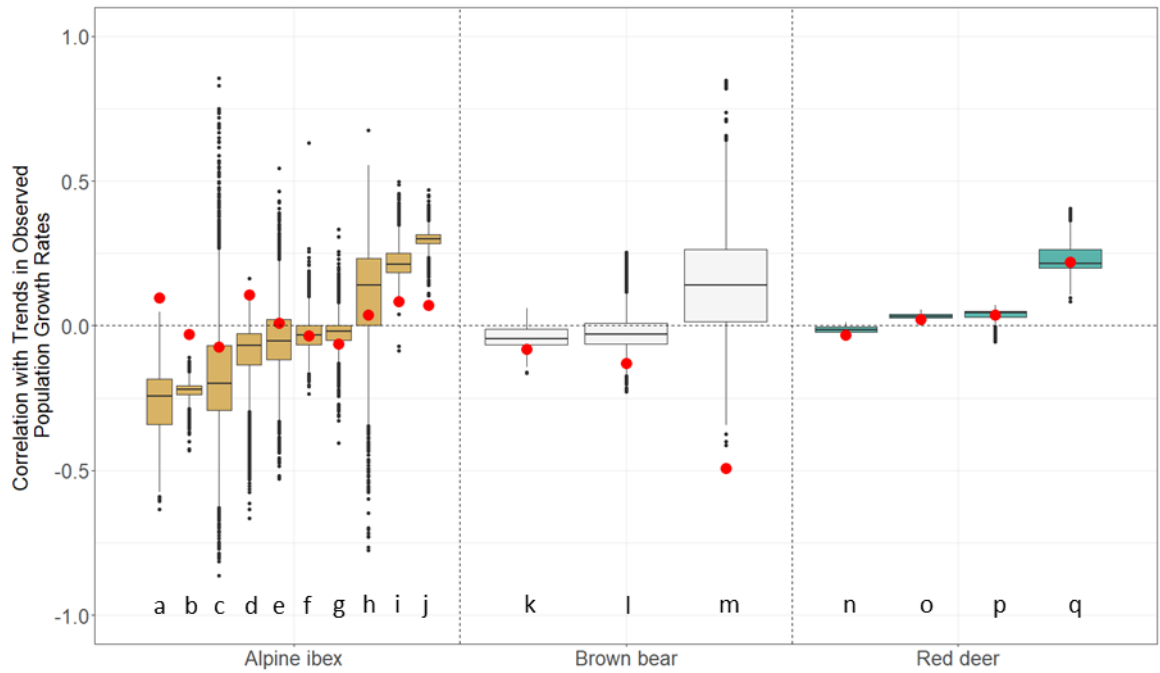


Figure 4.5 Boxplots for each population showing the distribution of correlation coefficients between the observed rate of population change and the predicted rates of population change from the coupled niche-demographic models. For each boxplot there is a corresponding red dot showing the correlation coefficient between the observed population growth rates and the rate of change in predicted habitat suitability. Values closer to 1 or -1 indicate stronger positive or negative correlations, respectively. The small black dots indicate outlier values from the boxplots and the letters a-q are for identification of individual populations.

In the Alpine ibex populations there are mixed results when comparing the performance of the CND models to the HS models. In half the populations the predicted population trends from the CND models tend to have stronger correlations than the predictions from the HS models. In the other half of the Alpine ibex populations the opposite is true. Within the brown bear populations the median correlations between the predicted abundance trends from the CND models and the observed trends are, on average, 0.257 higher, than the correlations between the predicted habitat suitability trends and observed abundance trends. For the red deer populations the correlations are similar with both modelling strategies, this is likely to be because varying the dispersal rate and stochasticity around the transition matrix had little effect on red deer population growth rates Figure S4.5.

<i>Species</i>	ID	Correlation coefficient (HS vs observed)	Mean correlation coefficient (CND vs observed)
<i>Alpine ibex</i>	a	0.096	-0.265 (± 0.04)
	b	-0.030	-0.225 (± 0.03)
	c	-0.074	-0.173 (± 0.23)
	d	0.107	-0.096 (± 0.10)
	e	0.008	-0.045 (± 0.13)
	f	-0.034	-0.026 (± 0.06)
	g	-0.064	-0.025 (± 0.06)
	h	0.036	0.089 (± 0.21)
	i	0.082	0.218 (± 0.05)
	j	0.071	0.299 (± 0.03)
<i>Brown bear</i>	k	-0.080	-0.039 (± 0.04)
	l	-0.130	-0.023 (± 0.06)
	m	-0.494	0.161 (± 0.23)
<i>Red deer</i>	n	-0.031	-0.013 (± 0.01)
	o	0.020	0.033 (± 0.01)
	p	0.036	0.039 (± 0.02)
	q	0.218	0.234 (± 0.05)

Table 4.3 The correlation coefficients between the HS models and observed population trends for each population contrasted with the mean correlation coefficients between each of the CND model runs and the observed population trends.

Another method I used to assess the performance of the CND models was to compare the predicted average population growth from each of the CND predictions to the observed average population growth rate for each population (Figure 4.6). Using the average population growth rate as a metric for comparison also allowed me to compare the performance of the CND models to the simple linear mixed effects models built in Chapter 2. Here the closer predicted average population growth rates are to the observed population growth rates the better we consider the performance of the models to be (Figure 4.6). Overall, I find that the simple linear mixed effects models provide better predictions of the average population growth rate than the CND models.

The median predicted population growth rates ($-4.94\% \pm 2.57\%$) for the Alpine ibex are considerably lower than the observed values ($6.17\% \pm 7.65\%$; Figure 4.6). Each of the Alpine ibex observed population growth rates are higher than the entire range of predicted population growth rates from the CND model. Most of the observed populations show on average little change or increasing population trends. Whereas, the CND model predicts that

in most cases (99.4%) each of the recorded populations of this species would have faced declines in abundance.

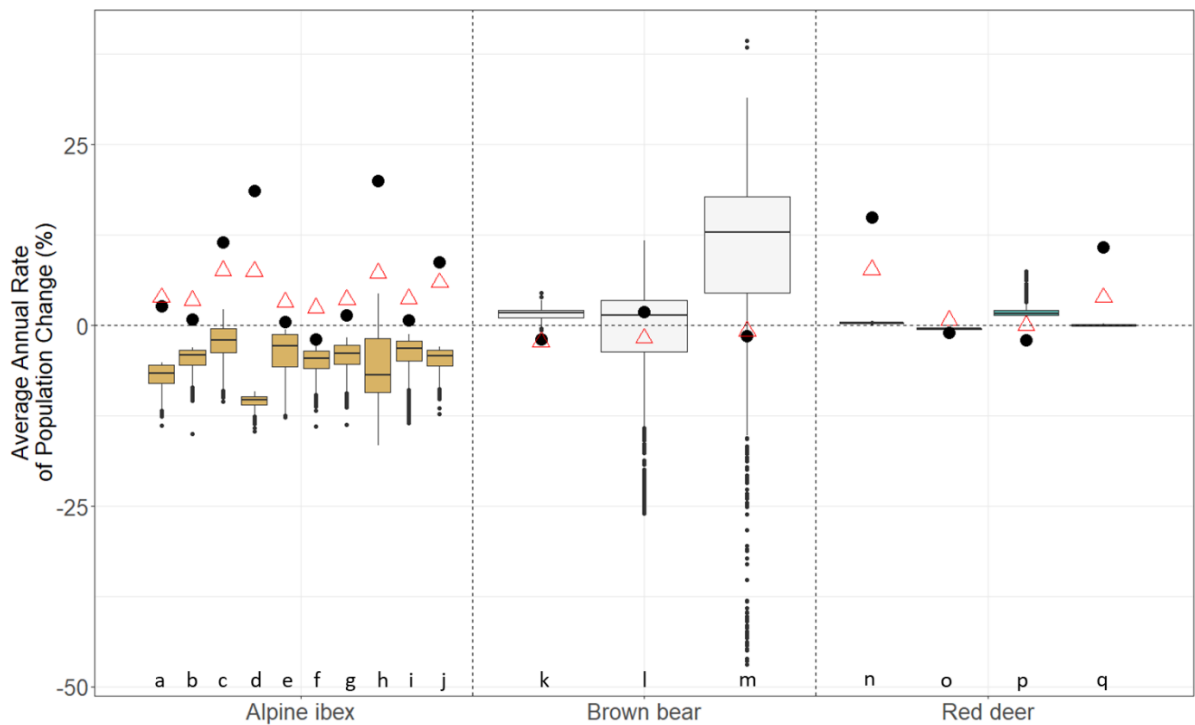


Figure 4.6 Each boxplot shows the distribution of the predicted average annual rate of change for each population. The black dots show the observed average annual rate of population change for each population. The red triangles show the fitted values for the top performing model for mammals from Chapter Two. The explanatory variables of this model are: rate of conversion to anthropogenic land use (RCA); rate of climate warming (RCW); the interaction between RCA and RCW; and species body mass. The closer the boxplots or red triangles are to the black dot the better their respective models have performed at predicting the average population growth rate for that population. Values below zero indicate population decline and values above zero indicate growing populations. The letters a-q are for the identification of individual populations.

Within the brown bear populations, the observed population growth rates are within the range of predicted growth rates, suggesting the CND models are useful for this species.

There is very little variation in the predicted population growth rates of the red deer, with the population trends predicted to be relatively stable. Two of the red deer populations (“n” and “q”) have high population growth rates which are not captured by the CND models.

In 82.4% of the populations the estimated population growth rates from the LME models are closer to the observed values than the median estimates from the CND models (Figure 4.6). Furthermore, in 64.7% of the populations the estimated population growth rates from

the LME models are closer to the observed values than any of the estimates from the CND models (Figure 4.6). In 70.6% of cases the predicted growth rates from the LME models are in the same direction as the observed trends (i.e. increasing or decreasing). However, only 23.5% of the median predicted growth rates from the CND models correctly estimate the correct direction of the population trend, this rises to 41.2% when I take the “best” estimate from the CND models. It is not possible to estimate population growth rates directly from predicted habitat suitability trends, so I am therefore unable to compare them directly to the LME and CND models using this metric.

DISCUSSION

My results suggest that both CND and HS models perform quite poorly at predicting mammal population trends, although the CND models do provide a slight improvement on the HS models. I also find that within the study populations presented here simple linear mixed effects models provide more accurate predictions of population growth rates than complex CND models.

Within the brown bear and red deer populations the CND models consistently outperform the HS models, in terms of correlation coefficients (Figure 4.5). The disparity between the CND and HS models, for these populations, is even greater when lagged responses are considered (Figure 4.5). These findings suggest that CND models can provide an improvement upon HS models and provide support to the findings that the inclusion of population dynamics and dispersal is important for predicting population trends (Keith *et al.*, 2008). However, it is important to highlight that the CND models performed poorly when predicting average population growth rates. In most cases (82.4%) the median CND predictions were in the opposite direction to the observed population growth rates This

suggests that in their current form, the usefulness of CND models to applied conservation is limited.

The CND models performed especially poorly on the Alpine ibex populations. The correlation coefficients between predicted and observed trends in population growth rates were highly variable (Figure 4.5). Additionally, the CND models consistently underestimated the Alpine ibex population growth rates (Figure 4.6). The wide range in CND correlation coefficients is likely to be because of the high levels of variability in the predicted habitat suitability for the Alpine ibex populations.

These populations have also experienced high levels of management which could be a contributing factor to the poor performance of the models. For example, the discrepancy between the observed population growth rates and the predicted growth rates might be due to the highly successful reintroduction efforts throughout this species' range, which have not been incorporated into the models. The reintroductions increased the abundance of Alpine ibex from a remnant population of <100 individuals in the early 1800s to estimates of >20,000 individuals in the late twentieth century (Stüwe and Nievergelt, 1991). This species was first successfully captive bred in the early twentieth century, with reintroductions of ten populations taking place between 1911 and 1976 across the Alps Switzerland. By 1976 many populations were beginning to overlap (Stüwe and Nievergelt, 1991) and populations were high enough for hunting to begin in 1977, with 6-10% of the population being culled annually.

There is a similar pattern of the CND models underestimating population growth rates for the “n” and “q” red deer populations. Both of these populations were reintroduced in the mid-20th century and hunting was later initiated to control both populations (Escós and Alados, 1992). In both the reintroduced Alpine ibex and red deer populations there are very high levels of observed population growth rates. This rapid population growth is typical of

colonizing ungulates in areas where predation is rare, as is the case in the study sites of these populations (Breitenmoser, 1998; Larkin *et al.*, 2003). This irruptive growth is typically followed by population crashes (Riney, 1964; Caughley, 1970); however, this might have been avoided through the introduction of hunting to each of the reintroduced populations (Bouquier, 2003). The CND models over-estimated the population growth rates for the red deer population “p”. This population underwent a cull over the study period, which ensured the average population growth rate was lower than it might otherwise be (Bonenfant *et al.*, 2002).

There is considerable variation in the CND model predicted population trends of the “l” and “m” brown bear populations, which are highly variable both in terms of correlation coefficients (Figure 4.5) and predicted population growth rates (Figure 4.6). Both populations are from Yellowstone National Park but cover different periods of time (Knight, 1994). These brown bear populations are likely to be highly variable because they are located on an isolated patch of suitable habitat at the edge of the species range, >2,400km from the centre of the species’ extant North American distribution (IUCN, 2017). These highly variable negative predicted population growth rates of the brown bear populations are associated with low dispersal rates and low stochasticity (Figure S4.5). This suggests that within the model these populations are dependent on immigration or stochastically occurring high population growth rates to survive.

Although I vary each of the CND models in the same way for each species, by sampling dispersal rate and transition matrix stochasticity from the same sample space, there are considerable differences in the variation of the predicted population trends. For populations at sites which have great variation in predicted habitat suitability (e.g. Alpine ibex populations), there is a corresponding high level of variability in predicted population trends. Conversely, for populations at sites with stable trends in predicted habitat suitability,

there is very little variation in the resulting population trends. This suggests that within this modelling framework, the variation in predicted habitat suitability is the key driving force and the variables of dispersal rate and the stochasticity of the transition matrix are more influential when predicted habitat suitability is less stable. In stochastic environments dispersal is thought to be of high importance in maintaining populations (Kuno, 1981). However, here Alpine ibex population growth rates were lower in the simulations with high dispersal rates and population stochasticity (Figure S4.5). This may be because there were not enough patches of suitable habitat to maintain the populations under highly variable conditions (Bascompte, Possingham and Roughgarden, 2002).

CND models are an improvement on HS models for predicting mammal abundance trends. However, there are still a number of improvements that could be made to CND models that should lead to accurate predictions. The effect of species interactions on trends in species abundance is likely to be of fundamental importance. Species interactions can have multiple impacts on species distribution and abundance (Van Der Putten, Macel and Visser, 2010), such as: influencing the rate at which species' ranges shift (Svenning *et al.*, 2014); significantly altering the response of species to climate change (Suttle, Thomsen and Power, 2007); and causing abrupt and non-linear responses under climate change (Walther, 2010). The impact of species interactions on species distributions can be somewhat addressed through the use of joint species distribution models (Pollock *et al.*, 2014). However, there is not yet a method for incorporating species interactions into CND models (but see Fordham *et al.*, 2013).

Within the CND models I vary the dispersal rate across model runs and I find it to be an important factor in predicting population trends, particularly in habitats of fluctuating stability (Figure S4.5). Although I vary dispersal rate across model runs, I do not allow it to vary spatially or temporally or across age groups within each model run. The dispersal

process is likely to be much more complicated, particularly across dynamic heterogeneous environments (Bocedi *et al.*, 2014). Dispersal is likely to vary across species range, being greater at range margins (Travis *et al.*, 2013). Methods for incorporating density dependence and habitat suitability into probabilities of emigration and settlement may increase the predictive ability of CND models (Bocedi *et al.*, 2014).

The CND models worked best for the least managed populations (“l”, “m” and “o”), as the observed population growth rates are within the range of predicted growth rates for these populations. However, the relatively simple LME models provide more accurate estimates of average annual population growth rates than CND models. The superior performance of the LME models is partly due to the large amount of variation in population growth rates that is explained by the random effects, site and species (Figure S4.6). The random effects in the LME capture site- and species-specific processes that influence the population growth rates but are not explicitly accounted for in either model, such as; reintroduction, exploitation, species interactions and disease. However, it should be noted that LME models still perform well when only fixed effects are used for predictions (Figure S4.6).

Despite the LME models providing more accurate estimates of average population growth rate, there are multiple benefits of using CND models. For example, CND models produce much richer outputs, such as, time-series of abundance maps which can be used to extract annual abundance estimates across the entire species range, as opposed to the average rate of population growth produced by the LME models. Time series maps of predicted abundance can be used to predict spatial patterns of extinction risk, which could be used for estimating time to extinction.

Despite the increased complexity of CND models, I do not find that this results in a substantially improved performance. The relatively simple linear mixed effects models (Chapter Two) are not only faster and more straightforward to implement than the CND

models, but they also provide superior predictions of average population growth rates for the species in question. Although the CND models here account for dispersal and population dynamics which are important ecological processes, there are still a few ways in which they could be improved. Firstly, higher resolution spatiotemporal environmental data for smaller areas could help to capture important processes which occur at fine spatiotemporal scales. Secondly, species interactions are important for delimiting species ranges and for mediating species responses to climate change, methods of incorporating species interactions into CND models (e.g. Fordham *et al.*, 2013) are likely to provide improved predictions. Lastly, the relationship between both vital rates and dispersal with predicted habitat suitability and range position are likely to have been oversimplified here. Increased understanding of these relationships and the inclusion of these into the CND models is likely to provide more accurate predictions.

CHAPTER FIVE: DISCUSSION

OVERVIEW

In recent decades global biodiversity has faced multiple human-driven threats, leading to extinction rates being 1,000 times higher than expected (De Vos *et al.*, 2015). Two of the most significant threats to biodiversity are climate change and loss of habitat to anthropogenic land use (Travis, 2003). Both processes are anticipated to continue to threaten biodiversity for the foreseeable future (Sala, 2000). Understanding the patterns and processes of these threats on biodiversity is crucial to the effective conservation of populations and the consequent maintenance of ecosystem function. In this thesis I examined a range of approaches for predicting the impacts of recent climate change and land use change on observed animal population trends. I focussed on population trends of terrestrial birds and mammals, as these species tend to be well studied, and there is sufficient information available on them to build models across a spectrum of complexity. This thesis is made up of two main parts: firstly, I explored the associations between recent climate and land use change and observed animal population trends at a global scale, to identify generalisable patterns; secondly, I used species occurrence points and environmental data to predict both habitat suitability and species abundance trends, and then assessed the usefulness of these predictions for predicting population trends by comparing them to observed trends.

In Chapter Two I analysed the recent impacts of climate change and land use change on observed bird and mammal population trends (1950-2005), providing the first global study of the impacts of recent environmental change on vertebrate population trends. I performed an analysis of 987 population trends (571 mammals, 416 birds) of 481 species from 76 countries, in each continent except Antarctica. For each population trend I calculated the average population growth rate. For the area surrounding each population I calculated a

spatiotemporally coincident annual rate of climate warming (RCW) and rate of conversion to anthropogenic land use (RCA). I also gathered species body mass data and data on protected area coverage for each population. Using these data, I built a series of linear mixed effects models to quantify the amount of variation in population growth rates which could be explained by the following variables: RCW, RCA, the interaction between RCW and RCA, species body mass and protected area coverage. I modelled the bird and mammal population trends separately. I found that both bird and mammal population trends have declined fastest in locations where mean temperature has increased most rapidly, this effect is more noticeable in birds. I did not find a strong effect of conversion to anthropogenic land use, body mass or protected area coverage in either bird or mammal populations. Further understanding of the processes that drive the association between rapid climate warming and population declines is crucial for developing improved assessments of species vulnerability to climate warming.

Within the Appendices I further explored the findings of Chapter Two: I used alternative methods of model averaging; a wider range of population trends; additional species trait data; higher spatial and temporal resolution land use data; and extrapolated 2005-2100 bird and mammal population indices under contrasting climate change scenarios. I found the results did not vary when I used an alternative method of model averaging; nor did they change when I used a wider set of population trends. I did not find diet to be an important variable in explaining bird or mammal population trends. When the models were extrapolated forward under climate change scenarios the mean predicted decline of bird populations by 2100 was 67.6% under RCP 2.6 and 99.2% under RCP 8.5; for mammal populations there were predicted increases of 43.8% under RCP 2.6 and 70.3% declines under RCP 8.5. When I used higher resolution land use data for a smaller set of population trends, over a shorter time-period I found that rate of conversion to anthropogenic land use

was an important predictor for bird population trends. Bird populations tended to decline faster in areas where conversion to anthropogenic land use has been more rapid.

I then explored the relationship between predicted habitat suitability and population abundance. I created BIOCLIM, GAM and random forest habitat suitability models which I combined into weighted ensemble models based on their AUC value (Chapter Three). I used weighted ensemble models to predict annual habitat suitability for each species annually 1950-2005. From these maps I extracted time-series in predicted habitat suitability at the location of 177 populations from the Living Planet database and for each population I calculated a time-series in population growth rates. I explored the correlations between time-series of rates of change in predicted habitat suitability and the corresponding time-series of population growth rates. I found that there is little evidence to support the idea that population growth rates are directly linked to predicted habitat suitability. However, when lagged responses are considered there is a stronger positive relationship between changes in predicted habitat suitability and population growth rates. This suggests that lagged responses are important in understanding population responses to environmental change and where possible time-series data, rather than single time-points of abundance and predicted habitat suitability, should be used.

In Chapter Four I built coupled niche-demographic models. These are habitat suitability models which are linked with population models and also allow dispersal. These additional processes mean that the coupled models can be used to predict species abundance trends rather than simply estimating habitat suitability. Coupled niche-demographic models have been assumed have greater predictive accuracy than habitat suitability models, but there has been limited validation of coupled niche-demographic model predictions against observed data. I built coupled niche-demographic models for three species: Alpine ibex, brown bear and red deer. I used these species as they are sufficiently well studied, this

means that there are data available in the literature to parameterise the population model and the dispersal mechanism. I used these models to predict population trends and validated them for the first time by comparing them to 17 observed population trends from Living Planet database. I found that outputs of coupled niche-demographic models are more correlated with observed population trends than the outputs of habitat suitability models. This suggests that coupled niche-demographic models are an improvement on habitat suitability models. However, both sets of models perform relatively poorly, with linear mixed effects models (Chapter Two) providing more accurate estimates of average population growth rates than the coupled niche-demographic models. Further development of coupled niche-demographic models is required for them to be a useful tool in applied species conservation. My results suggest that the high data requirements and computational resources needed to run coupled niche-demographic models may be excessive, as currently more parsimonious models provide better predictions of population growth rates.

COMPARISONS TO THE LITERATURE

DRIVERS OF BIODIVERSITY LOSS

Human impacts have resulted in global animal population declines and widespread defaunation (Dirzo *et al.*, 2014; WWF, 2018) and this in turn degrades ecosystem function, which could lead to ecosystem collapse (Chapin *et al.*, 2000). Understanding the responses of animal populations to anthropogenic environmental change lies at the crux of ecology and is critical for implementing effective conservation. In this thesis I present a range of techniques for predicting the impacts of environmental change on animal population trends. In Chapter Two I highlighted the association between bird and mammal population declines and the rate of climate warming, with bird and mammal population declines being greater where climate warming had been most rapid. This supports previous findings which have found shifts in species phenology and latitude to be greatest where climate warming has

been greatest (Rosenzweig *et al.*, 2008; Chen *et al.*, 2011). When using the HYDE dataset to quantify the rate of conversion to anthropogenic land use (RCA) I do not find RCA to be an important predictor of bird or mammal population trends, which contradicts the findings of previous studies (Newbold *et al.*, 2015). However, when using the ESA CCI land cover data set, which has higher spatial and temporal resolution but is available for a shorter time-period, I do find rate of conversion to anthropogenic land use to be an important predictor of bird population trends (Appendices). This suggests that perhaps high spatial and temporal resolution data are required to identify impacts of land use change (Pearson and Dawson, 2003; Heikkinen *et al.*, 2007).

PREDICTING SPECIES RESPONSES TO ENVIRONMENTAL CHANGE

In Chapter Three I explored the correlations between time-series of predicted habitat suitability and abundance, specifically time-series of rates of change in predicted habitat suitability and time-series of population growth rates. There are mixed results in the literature exploring the correlations between predicted habitat suitability and abundance. Some studies have found a positive correlation between climatic suitability and bird population trends (Green *et al.*, 2008), whereas other studies have found equal numbers of positive and negative correlations between predicted habitat suitability and species abundance (Dallas and Hastings, 2018). Most studies correlate predicted habitat suitability and abundance at single points in time. However, both can be dynamic, if they are not in equilibrium there is unlikely to be a clear correlation between them. To account for this, I explored correlations between predicted habitat suitability and lagged population growth rates over a series of years (0-5). I found that when lagged responses are not accounted for there is no clear relationship between the rate of change in predicted habitat suitability and population growth rates. This aligns with some previous findings that have not found any clear correlations between predicted habitat suitability and abundance (Nielsen *et al.*, 2005;

Filz, Schmitt and Engler, 2013; Dallas and Hastings, 2018). Importantly, I found that correlations between population growth rates and predicted habitat suitability were higher when lagged responses were accounted for. This suggests that changes in predicted habitat suitability do not immediately impact abundance. This may be because declines in predicted habitat suitability impact species birth rates, rather than survival rates, so that changes in abundance are not detectable until a generation has passed (Gaillard, Festa-Bianchet and Yoccoz, 1998; Thompson and Ollason, 2001).

Coupled niche-demographic models have been shown to produce more accurate estimates of range shifts of both observed British bird species and virtual species, when compared to habitat suitability models (Zurell *et al.*, 2016; Fordham *et al.*, 2017). When built with the *demonic* package, coupled niche-demographic models perform well at predicting the relative abundance of virtual species (Zurell *et al.*, 2016). However, there are not yet any examples of coupled niche-demographic models being validated against observed population trends and this is what I presented in Chapter Four. My results are congruent with the literature in that they show that coupled niche-demographic models are an improvement upon habitat suitability models (Zurell *et al.*, 2016; Fordham *et al.*, 2017), for predicting population trends.

CAVEATS AND LIMITATIONS

Building upon an existing body of literature on the responses of biodiversity to environmental change, this thesis contributes to our knowledge of how animal populations are influenced by habitat loss and climate change. It has also tested novel methods for modelling the impacts of environmental change on spatial distributions of species abundance trends. There are, however, several limitations to the findings in this thesis, which I explore below. There is much still to learn about the impacts of climate change and

habitat loss on animal population trends and I suggest improvements to how these impacts might be modelled.

DATA LIMITATIONS AND SCALE

Each of the chapters in this thesis are based on either quantifying or predicting the impacts of changes in land use and climate on population trends since 1950. One of the key limitations of this thesis is that freely available data on land use and climate, which have data from 1950 onwards, are often both spatially and temporally coarse. This was especially the case for the land use data (HYDE), which were only available on a decadal basis from 1950 onwards. I required annual data for the analysis, so I linearly interpolated the decadal data to annual data. This assumes that any changes in land use between decades is constant and monotonic. Another limitation of this dataset is that it only provides coverage of arable and pastoral land use cover in each cell and it does not provide information on other land use types, which is commonly available in more recent land use datasets (e.g. ESA CCI). These combined limitations may mean that the impacts of land use change have been underestimated within this thesis. This is supported by one of the findings in the Appendices in which I used the fine scale (300m, annual) ESA CCI land use dataset to quantify the rate of conversion to anthropogenic land use for each population. When used as an explanatory variable in linear mixed effects models to explain variation in population growth rates I found it was an important predictor for bird populations, the same metric calculated with the HYDE data had not been found to be important. However, it is important to note that the models built with the ESA CCI data were run on a smaller set of populations for which at least 5 years of abundance data were available from 1992 onwards. The spatial resolution of available data was also a limiting factor for the coupled niche-demographic models. The habitat suitability models were built at 0.5° resolution as this was the highest resolution at which historical global climate data were available. A consequence

of this was that dispersal distances between cells were high (>18km). Therefore, coupled niche-demographic models could only be run for species with sufficiently high dispersal ability so that individuals to move between cells.

In this thesis I only considered the impacts of land use change and climate change on animal population trends. Historical data for these threats are relatively straightforward to access and to process. However, there are a multiple other drivers of animal population trends such as invasive species, pollution, direct exploitation and conservation interventions (WWF, 2018). For these drivers there are scant global data available and historical data are even rarer. The lack of information on these processes within the modelling process limits both the amount of variation in population trends I can explain and our ability to predict population trends.

I used observed population trends from the Living Planet database, both as a response variable when exploring the environmental correlates of population declines and to validate predictions of population trends made with coupled niche-demographic models. The Living Planet database is the foremost repository of freely available population trend data. However, there are some limitations to this dataset. For example, there are often years with missing population estimates. These are typically dealt with by fitting a generalised additive model, or linear model to the existing data to estimate abundance values for years with missing data. This is a potential source of error in each of the models used in this thesis. However, uninterrupted annual records of species abundance are rare and limiting analysis to these trends would severely restrict the amount of data which could be used.

The coupled niche-demographic models predicted annual abundance trends across the entire species range (1950 – 2005). However, I was only able to assess the models at locations and for years which observed population data were available. This means that

there are predictions for large tracts of the species' ranges and long periods of time which I was unable to validate.

COUPLE NICHE-DEMOGRAPHIC MODEL LIMITATIONS

The development of coupled niche-demographic models was driven by the idea that habitat suitability models should include ecological processes. However, there remain important functions which have been omitted from coupled niche-demographic models, most notably species interactions. Species interactions are known to play a key role in shaping species distributions (Wiszniewski *et al.*, 2013) and in mediating the impacts of climate change (Suttle, Thomsen and Power, 2007). Joint species distribution models (JSDMs) are a method for accommodating species interactions into habitat suitability models. JSDMs model patterns of species co-occurrence and shared environmental responses, they also allow predictions of abundance (Clark *et al.*, 2014; Pollock *et al.*, 2014). However, unlike coupled niche-demographic models, they do not incorporate processes for dispersal or population dynamics.

A key limitation of the coupled niche-demographic model framework I used (demoniche; Nenzén *et al.*, 2012) is that it only allows relatively simple manipulation of how predicted habitat suitability influences population dynamics and dispersal functions. For example, dispersal probability varies only with distance and is not influenced by predicted habitat suitability, the age/stage of individuals or the location of a cell within a species range. RAMAS (Akçakaya, 2012) is a similar, but more established, tool which allows for the inclusion of more detailed information about species and environmental drivers (Lurgi *et al.*, 2014). However, the cost of this software is prohibitive, as is the lack of availability of the detailed data required to parameterise these models.

FUTURE DIRECTIONS

This thesis focussed on the application of data that are available historically at a global scale and thus choice was limited to a handful of datasets. However, there are several countries which have higher resolution historical datasets available, such as the CORINE land use data set which covers the UK at 25 metre resolution; the UKCP09 climate data set which has historical climate data for the UK at 5km resolution; the Land Cover Trends Dataset which covers the USA at 60m resolution; and the PRISM climate data which is available at 800m resolution across the USA. These countries also have a long record of natural history recording and thus there are several long-term abundance datasets available to validate coupled niche-demographic models. Future work should focus on building and validating high spatiotemporal resolution coupled niche-demographic models at country level scales. This may help elucidate the impacts of climate and land use processes which happen at finer scales.

Coupled niche-demographic models could also be improved by allowing vital rates and dispersal to vary geographically and in relation to habitat suitability. This requires further work in understanding the relationships between both survival and fecundity rates, and habitat suitability. Additionally, further research is needed on how these relationships varies across species age classes. Furthermore, knowledge of how dispersal varies across species ranges and with habitat suitability may improve the predictive performance of these models (Travis *et al.*, 2013; Bocedi *et al.*, 2014).

Species interactions are increasingly incorporated into habitat suitability models and have been shown to improve predictive accuracy. For example, adding in predator pressure and prey availability into habitat suitability models of Arctic fox enhanced the predictive accuracy (Hof, Jansson and Nilsson, 2012). Additionally, experimental studies in the Swiss Alps have shown that climate change is likely to lead to novel species interactions and that

these interactions may outweigh the direct impacts of climate change (Alexander, Diez and Levine, 2015). Further work modelling Californian grassland species shows that including biotic interaction networks improves habitat suitability models (Staniczenko *et al.*, 2017). However, inclusion of species interactions into coupled niche-demographic models has so far been limited. The sole example involves predator-prey interactions between Iberian lynx and European rabbit, which was also used to explore management options (Fordham *et al.*, 2013). Future work incorporating species interactions into coupled niche-demographic models and exploring how these interactions might vary under climate change (Kissling and Schleuning, 2014), will likely yield improved predictions.

CONCLUSIONS

In this thesis I have presented the first global assessment of the impacts of recent climate warming and anthropogenic land use conversion on animal population trends. I have identified rapid climate warming to be strongly associated with bird and mammal population declines since 1950, at a global scale. I explored the relationship between changes in predicted habitat suitability and population growth rates. I found that this relationship is stronger when lagged responses of population growth rates to changes in predicted habitat suitability are considered. I built coupled niche-demographic models for three species: red deer, brown bear and Alpine ibex. I assessed the ability of these coupled niche-demographic models to predict animal population trends. I showed coupled niche-demographic models were an improvement upon habitat suitability models for predicting population trends. Despite this, I found that the increased complexity of the coupled niche-demographic models did not lead to increased accuracy in predicting mammal population growth rates. The linear mixed effects models (Chapter Two) outperformed the coupled niche-demographic models (Chapter Four) in predicting animal population growth rates. In this instance, following the principle of Occam's Razor is justified. The simple models are

not only easier and faster to implement but also produce more accurate predictions for the species in question. The relatively poor performance of coupled niche-demographic models may be due to the following reasons: the environmental data were only available at coarse spatiotemporal resolutions for the required time-period; I make potentially overly simplistic assumptions regarding the relationship between dispersal and vital rates with predicted habitat suitability and range position; and I do not incorporate species interactions into the models. If these deficits are addressed coupled niche-demographic models may yet become a useful tool for understanding species vulnerability to climate change and land use change.

REFERENCES

- Acevedo, P., Ferreres, J., Escudero, M. A., Jimenez, J., Boadella, M. and Marco, J. (2017) 'Population dynamics affect the capacity of species distribution models to predict species abundance on a local scale', *Diversity and Distributions*, 23(9), pp. 1008–1017. doi: 10.1111/ddi.12589.
- Akçakaya, H. R. (2012) 'RAMAS GIS: Linking Landscape Data with Population Viability Analysis'. Setauket, NY: Applied Biomathematics.
- Alexander, J. M., Diez, J. M. and Levine, J. M. (2015) 'Novel competitors shape species' responses to climate change', *Nature*, 525(7570), pp. 515–518. doi: 10.1038/nature14952.
- Allouche, O., Tsoar, A. and Kadmon, R. (2006) 'Assessing the accuracy of species distribution models: Prevalence, kappa and the true skill statistic (TSS)', *Journal of Applied Ecology*, 43(6), pp. 1223–1232. doi: 10.1111/j.1365-2664.2006.01214.x.
- AMAP (2017) 'Snow, Water, Ice and Permafrost in the Arctic - Summary for Policy-makers'.
- Araújo, M. B. and New, M. (2007) 'Ensemble forecasting of species distributions', *Trends in Ecology and Evolution*, 22(1), pp. 42–47. doi: 10.1016/j.tree.2006.09.010.
- Araújo, M. B. and Peterson, A. T. (2012) 'Uses and misuses of bioclimatic envelope modeling', *Ecology*, 93(7), pp. 1527–1539. doi: 10.1890/11-1930.1.
- Araújo, M. B., Whittaker, R. J., Ladle, R. J. and Erhard, M. (2005) 'Reducing uncertainty in projections of extinction risk from climate change', *Global Ecology and Biogeography*, 14(6), pp. 529–538. doi: 10.1111/j.1466-822X.2005.00182.x.
- Bagley, J. E., Desai, A. R., Harding, K. J., Snyder, P. K. and Foley, J. A. (2014) 'Drought and deforestation: Has land cover change influenced recent precipitation extremes in the Amazon?', *Journal of Climate*, 27(1), pp. 345–361. doi: 10.1175/JCLI-D-12-00369.1.
- Barnes, M. D., Craigie, I. D., Harrison, L. B., Geldmann, J., Collen, B., Whitmee, S., Balmford, A., Burgess, N. D., Brooks, T., Hockings, M. and Woodley, S. (2016) 'Wildlife population trends in protected areas predicted by national socio-economic metrics and body size', *Nature Communications*. Nature Publishing Group, 7, pp. 1–9. doi: 10.1038/ncomms12747.
- Barnosky, A. D., Matzke, N., Tomiya, S., Wogan, G. O. U., Swartz, B., Quental, T. B., Marshall, C., McGuire, J. L., Lindsey, E. L., Maguire, K. C., Mersey, B. and Ferrer, E. A. (2011) 'Has the Earth's sixth mass extinction already arrived?', *Nature*. Nature Publishing Group, 471(7336), pp. 51–57. doi: 10.1038/nature09678.
- Barton, K. (2016) 'MuMIn: Multi-Model Inference'. Available at: <https://cran.r-project.org/package=MuMIn>.
- Bascompte, J., Possingham, H. and Roughgarden, J. (2002) 'Patchy Populations in Stochastic Environments: Critical Number of Patches for Persistence', *The American Naturalist*, 159(2), pp. 128–137. doi: 10.1086/324793.
- Bates, D., Maechler, M., Bolker, B. and Walker, S. (2015) 'Fitting Linear Mixed-Effects Models Using lme4', *Journal of Statistical Software*, 1(67), pp. 1–48.

- Beck, J., Böller, M., Erhardt, A. and Schwanghart, W. (2014) 'Spatial bias in the GBIF database and its effect on modeling species' geographic distributions', *Ecological Informatics*. Elsevier B.V., 19, pp. 10–15. doi: 10.1016/j.ecoinf.2013.11.002.
- Bellard, C., Bertelsmeier, C., Leadley, P., Thuiller, W. and Courchamp, F. (2012) 'Impacts of climate change on the future of biodiversity', *Ecology Letters*, 15(4), pp. 365–377. doi: 10.1111/j.1461-0248.2011.01736.x.
- Benning, T. L., LaPointe, D., Atkinson, C. T. and Vitousek, P. M. (2002) 'Interactions of climate change with biological invasions and land use in the Hawaiian Islands: Modeling the fate of endemic birds using a geographic information system', *Proceedings of the National Academy of Sciences*, 99(22), pp. 14246–14249. doi: 10.1073/pnas.162372399.
- Bivand, R., Pebesma, E. and Gomez-Rubio, V. (2013) *Applied spatial data analysis with R, Second edition*. New York, NY: Springer.
- Bocedi, G., Zurell, D., Reineking, B. and Travis, J. M. J. (2014) 'Mechanistic modelling of animal dispersal offers new insights into range expansion dynamics across fragmented landscapes', *Ecography*, 37(12), pp. 1240–1253. doi: 10.1111/ecog.01041.
- Bonenfant, C., Gaillard, J. M., Klein, F. and Loison, A. (2002) 'Sex- and age-dependent effects of population density on life history traits of red deer *Cervus elaphus* in a temperate forest', *Ecography*, 25(4), pp. 446–458. doi: 10.1034/j.1600-0587.2002.250407.x.
- Bontemps, S., Defourny, P., Radoux, J., Van Bogaert, E., Lamarche, C., Achard, F., Mayaux, P., Boettcher, M., Brockmann, C. and Kirches, G. (2013) 'Consistent Global Land Cover Maps for Climate Modelling Communities: Current Achievements of the ESA's Land Cover CCI.', in *Proceedings of the ESA Living Planet Symposium, Edinburgh*.
- Booth, T. H., Nix, H. A., Busby, J. R. and Hutchinson, M. F. (2014) 'Bioclim: The first species distribution modelling package, its early applications and relevance to most current MaxEnt studies', *Diversity and Distributions*, 20(1), pp. 1–9. doi: 10.1111/ddi.12144.
- Boulangéat, I., Gravel, D. and Thuiller, W. (2012) 'Accounting for dispersal and biotic interactions to disentangle the drivers of species distributions and their abundances', *Ecology Letters*, 15(6), pp. 584–593. doi: 10.1111/j.1461-0248.2012.01772.x.
- Bouquier, G. (2003) *Contribution à l'étude de la gestion de la population de cerfs (*Cervus elaphus*) de la Pinatelle d'Allanche (Cantal, France)*. Université de Toulouse.
- Boutin, S. and Lane, J. E. (2014) 'Climate change and mammals: Evolutionary versus plastic responses', *Evolutionary Applications*, 7(1), pp. 29–41. doi: 10.1111/eva.12121.
- Bowler, D. E., Haase, P., Krüger, I., Tackenberg, O., Bauer, H. G., Brendel, C., Brooker, R. W., Gerisch, M., Henle, K., Hickler, T., Hof, C., Klotz, S., Kühn, I., Matesanz, S., O'Hara, R., Russell, D., Schweiger, O., Valladares, F., Welk, E., Wiemers, M. and Böhning-Gaese, K. (2015) 'A cross-taxon analysis of the impact of climate change on abundance trends in central Europe', *Biological Conservation*. Elsevier Ltd, 187, pp. 41–50. doi: 10.1016/j.biocon.2015.03.034.
- Bowman, J., Jaeger, J. a G., Fahrig, L., Ecology, S. and Jul, N. (2012) 'Dispersal Distance of Mammals Is Proportional to Home Range Size', 83(7), pp. 2049–2055.
- Breiman, L. (2001) 'Random forests', *Machine Learning*, 45(1), pp. 5–32. doi: 10.1023/A:1010933404324.

- Breitenmoser, U. (1998) 'Large predators in the Alps: The fall and rise of man's competitors', *Biological Conservation*, 83(3), pp. 279–289. doi: 10.1016/S0006-3207(97)00084-0.
- Brook, B. W., Akçakaya, H. R., Keith, D. A., Mace, G. M., Pearson, R. G. and Araújo, M. B. (2009) 'Integrating bioclimate with population models to improve forecasts of species extinctions under climate change.', *Biology letters*, 5(June), pp. 723–725. doi: 10.1098/rsbl.2009.0480.
- Brook, B. W., Sodhi, N. S. and Bradshaw, C. J. . (2008) 'Synergies among extinction drivers under global change', *Trends in Ecology and Evolution*, 23(June), pp. 453–460. doi: 10.1016/j.tree.2008.03.011.
- Buckley, L. B., Urban, M. C., Angilletta, M. J., Crozier, L. G., Rissler, L. J. and Sears, M. W. (2010) 'Can mechanism inform species' distribution models?', *Ecology Letters*, 13(8), pp. 1041–1054. doi: 10.1111/j.1461-0248.2010.01479.x.
- Burnham, K. P. and Anderson, D. R. (2002) *Model Selection and Multimodel Inference: A Practical Information-Theoretic Approach (2nd ed)*, *Ecological Modelling*. doi: 10.1016/j.ecolmodel.2003.11.004.
- Cardinale, B. J., Duffy, J. E., Gonzalez, A., Hooper, D. U., Perrings, C., Venail, P., Narwani, A., MacE, G. M., Tilman, D., Wardle, D. A., Kinzig, A. P., Daily, G. C., Loreau, M., Grace, J. B., Larigauderie, A., Srivastava, D. S. and Naeem, S. (2012) 'Biodiversity loss and its impact on humanity', *Nature*, 486(7401), pp. 59–67. doi: 10.1038/nature11148.
- Carnell, R. (2018) 'lhs: Latin Hypercube Samples'. Available at: <https://cran.r-project.org/package=lhs>.
- Caughley, G. (1970) 'Eruptions of ungulate populations, with emphasis on Himalayan thar in New Zealand', *Ecology*, 51, pp. 53–72.
- Ceballos, G. and Ehrlich, P. R. (2002) 'Mammal population losses and the extinction crisis.', *Science*, 296(5569), pp. 904–907. doi: 10.1126/science.1069349.
- Chamberlain, S. A. and Boettinger, C. (2017) 'R Python, and Ruby clients for GBIF species occurrence data. 5:e3304v', *PeerJ Preprints* 5:e3304v, (5:e3304v). doi: 10.7287/peerj.preprints.3304v1.
- Chamberlain, S., Barve, V., Mcglinn, D. and Oldoni, D. (2018a) 'rgbif: Interface to the Global Biodiversity Information Facility API'. Available at: <https://cran.r-project.org/package=rgbif>.
- Chamberlain, S., Barve, V., Mcglinn, D. and Oldoni, D. (2018b) 'rgbif: Interface to the Global Biodiversity Information Facility API'.
- Chapin, F. S., Zavaleta, E. S., Eviner, V. T., Naylor, R. L., Vitousek, P. M., Reynolds, H. L., Hooper, D. U., Lavorel, S., Sala, O. E., Hobbie, S. E., C., M. M. and Diaz, S. (2000) 'Consequences of changing biodiversity', *Nature*, 405, pp. 234–242. doi: 10.1093/asj/sjx227.
- Chen, I., Hill, J. K., Ohlemüller, R., Roy, D. B. and Thomas, C. D. (2011) 'Rapid range shifts of species of climate warming', *Science*, 333, pp. 1024–1026. doi: 10.1126/science.1206432.

- Clark, J. S., Gelfand, A. E., Woodall, C. W. and Zhu, K. (2014) 'More than the sum of the parts: Forest climate response from joint species distribution models', *Ecological Applications*, 24(5), pp. 990–999. doi: 10.1890/13-1015.1.
- Collen, B., Loh, J., Whitmee, S., McRae, L., Amin, R. and Baillie, J. E. M. (2009) 'Monitoring Change in Vertebrate Abundance: the Living Planet Index', *Conservation Biology*, 23(2), pp. 317–327. doi: 10.1111/j.1523-1739.2008.01117.x.
- Corlett, R. T. (2011) 'Impacts of warming on tropical lowland rainforests', *Trends in Ecology and Evolution*. Elsevier Ltd, 26(11), pp. 606–613. doi: 10.1016/j.tree.2011.06.015.
- Coulson, T., Guinness, F., Pemberton, J. and Clutton-Brock, T. (2004) 'a-The demographic consequences of releasing a deer population from culling', *Ecology*, 85(2), pp. 411–422. doi: 10.1890/03-0009.
- Van Couwenberghe, R., Collet, C., Pierrat, J. C., Verheyen, K. and Gégout, J. C. (2013) 'Can species distribution models be used to describe plant abundance patterns?', *Ecography*, 36(6), pp. 665–674. doi: 10.1111/j.1600-0587.2012.07362.x.
- Craigie, I. D., Baillie, J. E. M., Balmford, A., Carbone, C., Collen, B., Green, R. E. and Hutton, J. M. (2010) 'Large mammal population declines in Africa's protected areas', *Biological Conservation*. Elsevier Ltd, 143(9), pp. 2221–2228. doi: 10.1016/j.biocon.2010.06.007.
- Dallas, T. A. and Hastings, A. (2018) 'Habitat suitability estimated by niche models is largely unrelated to species abundance', *Global Ecology and Biogeography*, (December 2017), pp. 1–9. doi: 10.1111/geb.12820.
- Daskin, J. H. and Pringle, R. M. (2018) 'Warfare and wildlife declines in Africa's protected areas', *Nature*. Nature Publishing Group, 553(7688), pp. 328–332. doi: 10.1038/nature25194.
- Dawson, T. P., Jackson, S. T., House, J. I., Prentice, I. C. and Mace, G. M. (2011) 'Beyond predictions: biodiversity conservation in a changing climate.', *Science (New York, N.Y.)*, 332(6025), pp. 53–8. doi: 10.1126/science.1200303.
- Dirzo, R., Young, H. S., Galetti, M., Ceballos, G., Isaac, N. J. B. and Collen, B. (2014) 'Defaunation in the Anthropocene', *Science*, 345(6195), pp. 401–406. doi: 10.1126/science.1251817.
- Doherty Jr., P. F., Boulinier, T. and Nichols, J. D. (2003) 'Local extinction and turnover rates at the edge and interior of species' ranges', *Annales Zoologici Fennici*, 40(April), pp. 145–153. doi: 10.1073/pnas.1419563112.
- Dornelas, M., Gotelli, N. J., McGill, B., Shimadzu, H., Moyes, F., Sievers, C. and Magurran, A. E. (2014) 'Assemblage Time Series Reveal Biodiversity Change but Not Systematic Loss', *Science*, 344(6181). doi: 10.1126/science.1248484.
- Ecosystem, A. M. (2005) *Ecosystems and Human Well-being: Synthesis*. Island Press, Washington D.C.
- Eglington, S. M. and Pearce-Higgins, J. W. (2012) 'Disentangling the relative importance of changes in climate and land-use intensity in driving recent bird population trends', *PLoS ONE*, 7(3), pp. 1–8. doi: 10.1371/journal.pone.0030407.

- Ehrlén, J. and Morris, W. F. (2015) 'Predicting changes in the distribution and abundance of species under environmental change', *Ecology Letters*, 18, pp. 303–314. doi: 10.1111/ele.12410.
- Ehrlich, P. R. and Daily, G. C. (1993) 'Population Extinction and Saving Biodiversity', *AMBIO: A Journal of the Human Environment*, 22(2), pp. 64–68.
- Elith, J., Kearney, M. and Phillips, S. (2010) 'The art of modelling range-shifting species', *Methods in Ecology and Evolution*, 1(4), pp. 330–342. doi: 10.1111/j.2041-210X.2010.00036.x.
- Engler, R. and Guisan, A. (2009) 'MigClim: Predicting plant distribution and dispersal in a changing climate', *Diversity and Distributions*, 15(4), pp. 590–601. doi: 10.1111/j.1472-4642.2009.00566.x.
- Escós, J. and Alados, C. L. (1992) 'Habitat preference of Spanish ibex and other ungulates in Sierras de Cazorla y Segura (Spain)', *Mammalia*, 56(3), pp. 393–406. doi: 10.1515/mamm.1992.56.3.393.
- Estrada, A. and Arroyo, B. (2012) 'Occurrence vs abundance models: Differences between species with varying aggregation patterns', *Biological Conservation*. Elsevier Ltd, 152, pp. 37–45. doi: 10.1016/j.biocon.2012.03.031.
- Evans, J., Murphy, M., Holden, Z. and Cushman, S. (2010) 'Modelling Species Distribution and Change Using Random Forest', in Drew, C. A., Wiersma, Y., and Huettmann, F. (eds) *Predictive Species and Habitat Modeling in Landscape Ecology*. New York, NY: Springer, pp. 139–159.
- Filz, K. J., Schmitt, T. and Engler, J. O. (2013) 'How fine is fine-scale? Questioning the use of fine-scale bioclimatic data in species distribution models used for forecasting abundance patterns in butterflies', *European Journal of Entomology*, 110(2), pp. 311–317. doi: 10.14411/eje.2013.044.
- Flemons, P., Guralnick, R., Krieger, J., Ranipeta, A. and Neufeld, D. (2007) 'A web-based GIS tool for exploring the world's biodiversity: The Global Biodiversity Information Facility Mapping and Analysis Portal Application (GBIF-MAPA)', *Ecological Informatics*, 2(1), pp. 49–60. doi: 10.1016/j.ecoinf.2007.03.004.
- Fordham, D. A., Akçakaya, H. R., Araújo, M. B., Elith, J., Keith, D. A., Pearson, R., Auld, T. D., Mellin, C., Morgan, J. W., Regan, T. J., Tozer, M., Watts, M. J., White, M., Wintle, B. A., Yates, C. and Brook, B. W. (2012) 'Plant extinction risk under climate change: Are forecast range shifts alone a good indicator of species vulnerability to global warming?', *Global Change Biology*, 18(4), pp. 1357–1371. doi: 10.1111/j.1365-2486.2011.02614.x.
- Fordham, D. A., Akçakaya, H. R., Araújo, M. B., Keith, D. A. and Brook, B. W. (2013) 'Tools for integrating range change, extinction risk and climate change information into conservation management', *Ecography*, 36(9), pp. 956–964. doi: 10.1111/j.1600-0587.2013.00147.x.
- Fordham, D. A., Akçakaya, H. R., Araújo, M. B., Keith, D. A., Brook, B. W., Akçakaya, H. R., Thuiller, W., Midgley, G. F., Pearson, R. G., Phillips, S. J., Regan, H. M., Araújo, M. B. and Rebelo, T. G. (2013) 'Predicting extinction risks under climate', *Biology letters*, 4(5), pp. 956–964. doi: 10.1111/j.1600-0587.2013.00147.x.

Fordham, D. A., Akçakaya, H. R., Brook, B. W., Rodríguez, A., Alves, P. C., Civantos, E., Triviño, M., Watts, M. J. and Araújo, M. B. (2013) 'Adapted conservation measures are required to save the Iberian lynx in a changing climate', *Nature Climate Change*, 3(10), pp. 899–903. doi: 10.1038/nclimate1954.

Fordham, D. A., Bertelsmeier, C., Brook, B. W., Early, R., Neto, D., Brown, S. C., Ollier, S. and Araújo, M. B. (2017) 'How complex should models be? Comparing correlative and mechanistic range dynamics models', *Global Change Biology*, (November). doi: 10.1111/gcb.13935.

Freeman, B. G. and Class Freeman, A. M. (2014) 'Rapid upslope shifts in New Guinean birds illustrate strong distributional responses of tropical montane species to global warming.', *Proceedings of the National Academy of Sciences of the United States of America*, 111(12), pp. 4490–4. doi: 10.1073/pnas.1318190111.

Freeman, B. G., Scholer, M. N., Ruiz-Gutierrez, V. and Fitzpatrick, J. W. (2018) 'Climate change causes upslope shifts and mountaintop extirpations in a tropical bird community', *Proceedings of the National Academy of Sciences*, p. 201804224. doi: 10.1073/pnas.1804224115.

Friedman, A. (2014) 'taRifx: Collection of utility and convenience functions'. Available at: <https://cran.r-project.org/package=taRifx>.

Frishkoff, L., Karp, D., Flanders, J., Zook, J., Hadly, E., Daily, G. and M'Gonigle, L. (2016) 'Climate change and habitat conversion favour the same species', 19, pp. 1081–1090. doi: 10.1111/ele.12645.

Gaillard, J. M., Festa-Bianchet, M. and Yoccoz, N. G. (1998) 'Population dynamics of large herbivores: Variable recruitment with constant adult survival', *Trends in Ecology and Evolution*, 13(2), pp. 58–63. doi: 10.1016/S0169-5347(97)01237-8.

Geldmann, J., Barnes, M., Coad, L., Craigie, I. D., Hockings, M. and Burgess, N. D. (2013) 'Effectiveness of terrestrial protected areas in reducing habitat loss and population declines', *Biological Conservation*. Elsevier Ltd, 161, pp. 230–238. doi: 10.1016/j.biocon.2013.02.018.

Gossow, H. and Zeiler, H. (1997) *Status Survey and Conservation Action Plan for Caprinae - Wild Sheep and Goats and their Relatives*. Edited by S. DM. Gland, Switzerland: IUCN.

Gottfried, M., Pauli, H., Futschik, A., Akhalkatsi, M., Barančok, P., Benito Alonso, J. L., Coldea, G., Dick, J., Erschbamer, B., Fernández Calzado, M. R., Kazakis, G., Krajčič, J., Larsson, P., Mallaun, M., Michelsen, O., Moiseev, D., Moiseev, P., Molau, U., Merzouki, A., Nagy, L., Nakhutsrishvili, G., Pedersen, B., Pelino, G., Puscas, M., Rossi, G., Stanisci, A., Theurillat, J. P., Tomaselli, M., Villar, L., Vittoz, P., Vogiatzakis, I. and Grabherr, G. (2012) 'Continent-wide response of mountain vegetation to climate change', *Nature Climate Change*, 2(2), pp. 111–115. doi: 10.1038/nclimate1329.

Green, R. E., Collingham, Y. C., Willis, S. G., Gregory, R. D., Smith, K. W. and Huntley, B. (2008) 'Performance of climate envelope models in retrodicting recent changes in bird population size from observed climatic change', *Biology Letters*, 4(5), pp. 599–602. doi: 10.1098/rsbl.2008.0052.

Gregory, R. D., Willis, S. G., Jiguet, F., Voříšek, P., Klvaňová, A., van Strien, A., Huntley, B., Collingham, Y. C., Couvet, D. and Green, R. E. (2009) 'An indicator of the impact of

- climatic change on European bird populations', *PLoS ONE*, 4(3). doi: 10.1371/journal.pone.0004678.
- Guisan, A., Edwards, T. C. and Hastie, T. (2002) 'Generalized linear and generalized additive models in studies of species distributions: setting the scene', *Ecological Modelling*, 157(2–3), pp. 89–100. doi: 10.1016/S0304-3800(02)00204-1.
- Guisan, A. and Thuiller, W. (2005) 'Predicting species distribution: Offering more than simple habitat models', *Ecology Letters*, 8(9), pp. 993–1009. doi: 10.1111/j.1461-0248.2005.00792.x.
- Guisan, A., Tingley, R., Baumgartner, J. B., Naujokaitis-Lewis, I., Sutcliffe, P. R., Tulloch, A. I. T., Regan, T. J., Brotons, L., McDonald-Madden, E., Mantyka-Pringle, C., Martin, T. G., Rhodes, J. R., Maggini, R., Setterfield, S. A., Elith, J., Schwartz, M. W., Wintle, B. A., Broennimann, O., Austin, M., Ferrier, S., Kearney, M. R., Possingham, H. P. and Buckley, Y. M. (2013) 'Predicting species distributions for conservation decisions', *Ecology Letters*, 16(12), pp. 1424–1435. doi: 10.1111/ele.12189.
- Gutiérrez, D., Harcourt, J., Díez, S. B., Gutiérrez Illán, J. and Wilson, R. J. (2013) 'Models of presence-absence estimate abundance as well as (or even better than) models of abundance: The case of the butterfly *Parnassius apollo*', *Landscape Ecology*, 28(3), pp. 401–413. doi: 10.1007/s10980-013-9847-3.
- Harris, I., Jones, P. D., Osborn, T. J. and Lister, D. H. (2014) 'Updated high-resolution grids of monthly climatic observations - the CRU TS3.10 Dataset', *International Journal of Climatology*, 34(May 2013), pp. 623–642. doi: 10.1002/joc.3711.
- Harrison, X. A., Donaldson, L., Correa-Cano, M. E., Evans, J., Fisher, D. N., Goodwin, C. E. D., Robinson, B. S., Hodgson, D. J. and Inger, R. (2018) 'A brief introduction to mixed effects modelling and multi-model inference in ecology', *PeerJ*, 6, p. e4794. doi: 10.7717/peerj.4794.
- Hastie, T. and Tibshirani, R. J. (1990) *Generalized Additive Models*. Chapman & Hall.
- He, F. and Gaston, K. J. (2000) 'Estimating Species Abundance from Occurrence', *The American Naturalist*, 156(5), pp. 553–559. doi: 10.1086/303403.
- Heikkinen, R. K., Luoto, M., Virkkala, R., Pearson, R. G. and Körber, J. H. (2007) 'Biotic interactions improve prediction of boreal bird distributions at macro-scales', *Global Ecology and Biogeography*, 16, pp. 754–763. doi: 10.1111/j.1466-8238.2007.00345.x.
- Hijmans, R. J. (2016) 'raster: Geographic Data Analysis and Modeling'. Available at: <https://cran.r-project.org/package=raster>.
- Hijmans, R. J. and Elith, J. (2013) '[R Manual] Species distribution modeling with R Introduction', *R Manual*, p. 71. doi: 10.1016/S0550-3213(02)00216-X.
- Hijmans, R. J. and Graham, C. H. (2006) 'The ability of climate envelope models to predict the effect of climate change on species distributions', *Global Change Biology*, 12(12), pp. 2272–2281. doi: 10.1111/j.1365-2486.2006.01256.x.
- Hijmans, R. J., Phillips, S., Leathwick, J. R. and Elith, J. (2017) 'dismo: Species Distribution Modelin', *R CRAN Project*, p. 55. doi: 10.1016/j.jhydrol.2011.07.022.
- Hilbers, J. P., Schipper, A. M., Hendriks, A. J., Verones, F., Pereira, H. M. and Huijbregts,

M. A. J. (2016) 'An allometric approach to quantify the extinction vulnerability of birds and mammals', *Ecology*, 97(3), pp. 615–626. doi: 10.1890/14-2019.1.

Hof, A. R., Jansson, R. and Nilsson, C. (2012) 'How biotic interactions may alter future predictions of species distributions: Future threats to the persistence of the arctic fox in Fennoscandia', *Diversity and Distributions*, 18(6), pp. 554–562. doi: 10.1111/j.1472-4642.2011.00876.x.

Hooper, D. U., Adair, E. C., Cardinale, B. J., Byrnes, J. E. K., Hungate, B. A., Matulich, K. L., Gonzalez, A., Duffy, J. E., Gamfeldt, L. and Connor, M. I. (2012) 'A global synthesis reveals biodiversity loss as a major driver of ecosystem change', *Nature*. Nature Publishing Group, 486(7401), pp. 105–108. doi: 10.1038/nature11118.

Hylander, K. and Ehrlén, J. (2013) 'The mechanisms causing extinction debts', *Trends in Ecology and Evolution*, 28(6), pp. 341–346. doi: 10.1016/j.tree.2013.01.010.

Inger, R., Gregory, R., Duffy, J. P., Stott, I., Voříšek, P. and Gaston, K. J. (2015) 'Common European birds are declining rapidly while less abundant species' numbers are rising', *Ecology Letters*, 18(1), pp. 28–36. doi: 10.1111/ele.12387.

IPBES (2018) *Summary for policymakers of the assessment report on land degradation and restoration of the Intergovernmental Science-Policy Platform on Biodiversity and Ecosystem Services*. Edited by M. ; Scholes, R. ; Montanarella, L. ; Brainich, A. ; Barger, N. ; Brink, B. ; Cantele, M. ; Erasmus, B. ; Fisher, J. ; Gardner, T. ; G. Holland, T. ; Kohler, F. ; Kotiaho, J. ; Von Maltitz, G. ; Nangendo, G. ; Pandit, R. ; Prince, R. ; Parrotta, J. ; Potts and L. Willemsen, S. ; Sankaran. Bonn Germany: IPBES secretariat. doi: 10.1016/0025-326x(95)90325-6.

IPCC (2014) 'Summary for Policy Makers', in *Climate Change 2014: Impacts, Adaptation and Vulnerability - Contributions of the Working Group II to the Fifth Assessment Report*, pp. 1–32. doi: 10.1016/j.renene.2009.11.012.

Isbell, F., Calcagno, V., Hector, A., Connolly, J., Harpole, W. S., Reich, P. B., Scherer-Lorenzen, M., Schmid, B., Tilman, D., Van Ruijven, J., Weigelt, A., Wilsey, B. J., Zavaleta, E. S. and Loreau, M. (2011) 'High plant diversity is needed to maintain ecosystem services', *Nature*. Nature Publishing Group, 477(7363), pp. 199–202. doi: 10.1038/nature10282.

IUCN (2017) *The IUCN red list of threatened species. Version 2016.3*. Available at: www.iucnRedList.org (Accessed: 26 September 2017).

Jantz, S. M., Barker, B., Brooks, T. M., Chini, L. P., Huang, Q., Moore, R. M., Noel, J. and Hurr, G. C. (2015) 'Future habitat loss and extinctions driven by land-use change in biodiversity hotspots under four scenarios of climate-change mitigation', *Conservation Biology*, 29(4), pp. 1122–1131. doi: 10.1111/cobi.12549.

Jenouvrier, S., Holland, M., Stroeve, J., Barbraud, C., Weimerskirch, H., Serreze, M. and Caswell, H. (2012) 'Effects of climate change on an emperor penguin population: analysis of coupled demographic and climate models', *Global Change Biology*, 18(9), pp. 2756–2770. doi: 10.1111/j.1365-2486.2012.02744.x.

Jetz, W., Wilcove, D. S. and Dobson, A. P. (2007) 'Projected impacts of climate and land-use change on the global diversity of birds', *PLoS Biology*, 5(6), pp. 1211–1219. doi: 10.1371/journal.pbio.0050157.

- Jia, J., Yue, H., Liu, T. and Wang, H. (2007) 'Global Sensitivity Analysis of Cell Signalling Transduction Networks Based on Latin Hypercube Sampling Method', *2007 1st International Conference on Bioinformatics and Biomedical Engineering*, pp. 434–437. doi: 10.1109/ICBBE.2007.114.
- Jiguet, F., Gregory, R. D., Devictor, V., Green, R. E., Vořšek, P., Van Strien, A. and Couvet, D. (2010) 'Population trends of European common birds are predicted by characteristics of their climatic niche', *Global Change Biology*, 16(2), pp. 497–505. doi: 10.1111/j.1365-2486.2009.01963.x.
- Johnson, C. N. and VanDerWal, J. (2009) 'Evidence that dingoes limit abundance of a mesopredator in eastern Australian forests', *Journal of Applied Ecology*, 46, pp. 641–646. doi: 10.1111/j.1365-2664.2007.0.
- Jones, C. D., Hughes, J. K., Bellouin, N., Hardiman, S. C., Jones, G. S., Knight, J., Liddicoat, S., O'Connor, F. M., Andres, R. J., Bell, C., Boo, K. O., Bozzo, A., Butchart, N., Cadule, P., Corbin, K. D., Doutriaux-Boucher, M., Friedlingstein, P., Gornall, J., Gray, L., Halloran, P. R., Hurtt, G., Ingram, W. J., Lamarque, J. F., Law, R. M., Meinshausen, M., Osprey, S., Palin, E. J., Parsons Chini, L., Raddatz, T., Sanderson, M. G., Sellar, A. A., Schurer, A., Valdes, P., Wood, N., Woodward, S., Yoshioka, M. and Zerroukat, M. (2011) 'The HadGEM2-ES implementation of CMIP5 centennial simulations', *Geoscientific Model Development*, 4(3), pp. 543–570. doi: 10.5194/gmd-4-543-2011.
- Jones, K. E., Bielby, J., Cardillo, M., Fritz, S. A., O'Dell, J., Orme, C. D. L., Safi, K., Sechrest, W., Boakes, E. H., Carbone, C., Connolly, C., Cutts, M. J., Foster, J. K., Grenyer, R., Habib, M., Plaster, C. A., Price, S. A., Rigby, E. A., Rist, J., Teacher, A., Bininda-Emonds, O. R. P., Gittleman, J. L., Mace, G. M. and Purvis, A. (2009) 'PanTHERIA: a species-level database of life history, ecology, and geography of extant and recently extinct mammals.', *Ecology*, 90, p. 2648.
- Jones, K. R., Venter, O., Fuller, R. A., Allan, J. R., Maxwell, S. L., Negret, P. J. and Watson, J. E. M. (2018) 'One-third of global protected land is under intense human pressure', *Science*, 360(6390), pp. 788–791. doi: 10.1126/science.aap9565.
- Kadmon, R., Farber, O. and Danin, A. (2004) 'Effect of Roadside Bias on the Accuracy of Predictive Maps Produced by Bioclimatic Models Author (s): Ronen Kadmon , Oren Farber and Avinoam Danin Published by : Wiley on behalf of the Ecological Society of America Stable URL : <http://www.jstor.org/stab>', 14(2), pp. 401–413.
- Kampichler, C., van Turnhout, C. A. M., Devictor, V. and van der Jeugd, H. P. (2012) 'Large-scale changes in community composition: Determining land use and climate change signals', *PLoS ONE*, 7(4), pp. 1–9. doi: 10.1371/journal.pone.0035272.
- Karp, D. S., Frishkoff, L. O., Echeverri, A., Zook, J., Juárez, P. and Chan, K. M. A. (2018) 'Agriculture erases climate-driven β -diversity in Neotropical bird communities', *Global Change Biology*, 24(1), pp. 338–349. doi: 10.1111/gcb.13821.
- Kearney, M. and Porter, W. P. (2004) 'Mapping the Fundamental Niche: Physiology, Climate, and the Distribution of a Nocturnal Lizard', 85(11), pp. 3119–3131.
- Keedwell, R. (2004) 'Use of population viability analysis n conservation management in New Zealand', *Science for Conservation*, 243. doi: 10.1177/1352458516663086.
- Keith, D. A., Akçakaya, H. R., Thuiller, W., Midgley, G. F., Pearson, R. G., Phillips, S. J.,

Regan, H. M., Araújo, M. B. and Rebelo, T. G. (2008) 'Predicting extinction risks under climate change: coupling stochastic population models with dynamic bioclimatic habitat models.', *Biology letters*, 4(5), pp. 560–563. doi: 10.1098/rsbl.2008.0049.

Keogan, K., Daunt, F., Wanless, S., Phillips, R. A., Walling, C. A., Agnew, P., Ainley, D. G., Anker-Nilssen, T., Ballard, G., Barrett, R. T., Barton, K. J., Bech, C., Becker, P., Berglund, P.-A., Bollache, L., Bond, A. L., Bouwhuis, S., Bradley, R. W., Burr, Z. M., Camphuysen, K., Catry, P., Chiaradia, A., Christensen-Dalsgaard, S., Cuthbert, R., Dehnhard, N., Descamps, S., Diamond, T., Divoky, G., Drummond, H., Dugger, K. M., Dunn, M. J., Emmerson, L., Erikstad, K. E., Fort, J., Fraser, W., Genovart, M., Gilg, O., González-Solís, J., Granadeiro, J. P., Grémillet, D., Hansen, J., Hanssen, S. A., Harris, M., Hedd, A., Hinke, J., Igual, J. M., Jahncke, J., Jones, I., Kappes, P. J., Lang, J., Langset, M., Lescroël, A., Lorentsen, S.-H., Lyver, P. O., Mallory, M., Moe, B., Montevecchi, W. A., Monticelli, D., Mostello, C., Newell, M., Nicholson, L., Nisbet, I., Olsson, O., Oro, D., Pattison, V., Poisbleau, M., Pyk, T., Quintana, F., Ramos, J. A., Ramos, R., Reiertsen, T. K., Rodríguez, C., Ryan, P., Sanz-Aguilar, A., Schmidt, N. M., Shannon, P., Sittler, B., Southwell, C., Surman, C., Svagelj, W. S., Trivelpiece, W., Warzybok, P., Watanuki, Y., Weimerskirch, H., Wilson, P. R., Wood, A. G., Phillimore, A. B. and Lewis, S. (2018) 'Global phenological insensitivity to shifting ocean temperatures among seabirds', *Nature Climate Change*. Springer US, 8(4), pp. 313–318. doi: 10.1038/s41558-018-0115-z.

Kissling, W. D. and Schleuning, M. (2014) 'Multispecies interactions across trophic levels at macroscales: Retrospective and future directions', *Ecography*, (March), pp. 1–12. doi: 10.1111/ecog.00819.

Klein Goldewijk, K., Beusen, A., Van Drecht, G. and De Vos, M. (2011) 'The HYDE 3.1 spatially explicit database of human-induced global land-use change over the past 12,000 years', *Global Ecology and Biogeography*, 20(1), pp. 73–86. doi: 10.1111/j.1466-8238.2010.00587.x.

Knight, R. (1994) *Yellowstone grizzly bear investigations: annual report of the Interagency Study Team, 1994*. Bozeman, Montana.

Kuno, E. (1981) 'Dispersal and persistence of populations in unstable habitats: a theoretical note', *Oecologia*, 49, pp. 123–126.

Kuussaari, M., Bommarco, R., Heikkinen, R. K., Helm, A., Krauss, J., Lindborg, R., Öckinger, E., Pärtel, M., Pino, J., Rodà, F., Stefanescu, C., Teder, T., Zobel, M. and Steffan-Dewenter, I. (2009) 'Extinction debt: a challenge for biodiversity conservation', *Trends in Ecology and Evolution*, 24(10), pp. 564–571. doi: 10.1016/j.tree.2009.04.011.

Larkin, J., Maehr, D. S., Cox, J. T., Bolin, D. C. and Wichrowski, M. W. (2003) 'Demographic Characteristics of a Reintroduced Elk Population in Kentucky', *The Journal of Wildlife Management*, 67(3), pp. 467–476.

Lee, T. M. and Jetz, W. (2010) 'Unravelling the structure of species extinction risk for predictive conservation science', *Proceedings of the Royal Society B: Biological Sciences*, pp. 1–10. doi: 10.1098/rspb.2010.1877.

Lemoine, N., Bauer, H.-G., Peintinger, M. and Böhning-Gaese, K. (2007) 'Effects of climate and land-use change on species abundance in a Central European bird community.', *Conservation biology: the journal of the Society for Conservation Biology*, 21(2), pp. 495–503. doi: 10.1111/j.1523-1739.2006.00633.x.

- Liaw, A. and Wiener, M. (2002) ‘Classification and Regression by randomForest’. *R News* 2(3), pp. 18–22.
- Loh, J., Green, R. E., Ricketts, T., Lamoreux, J., Jenkins, M., Kapos, V. and Randers, J. (2005) ‘The Living Planet Index: using species population time series to track trends in biodiversity.’, *Philosophical transactions of the Royal Society of London. Series B, Biological sciences*, 360(February), pp. 289–295. doi: 10.1098/rstb.2004.1584.
- Lurgi, M., Brook, B. W., Saltré, F. and Fordham, D. a. (2014) ‘Modelling range dynamics under global change: which framework and why?’, *Methods in Ecology and Evolution*, p. n/a-n/a. doi: 10.1111/2041-210X.12315.
- Malhi, Y., Roberts, J. T., Betts, R. A., Killeen, T. J., Li, W. and Nobre, C. A. (2008) ‘Climate Change, Deforestation, and the Fate of the Amazon’, *Science*, 319(January), pp. 169–172. doi: 10.1126/science.1146961.
- Mantyka-Pringle, C. S., Martin, T. G. and Rhodes, J. R. (2012) ‘Interactions between climate and habitat loss effects on biodiversity: a systematic review and meta-analysis’, *Global Change Biology*, 18(4), pp. 1239–1252. doi: 10.1111/j.1365-2486.2011.02593.x.
- La Marca, E., Lips, K. R., Lötters, S., Puschendorf, R., Ibáñez, R., Rueda-Almonacid, J. V., Schulte, R., Marty, C., Castro, F., Manzanilla-Puppo, J., Garcia-Pérez, J. E., Bolaños, F., Chaves, G., Pounds, J. A., Toral, E. and Young, B. E. (2005) ‘Catastrophic population declines and extinctions in neotropical harlequin frogs (Bufonidae: Atelopus)’, *Biotropica*, 37(December 2004), pp. 190–201. doi: 10.1111/j.1744-7429.2005.00026.x.
- Di Marco, M., Venter, O., Possingham, H. P. and Watson, J. E. M. (2018) ‘Changes in human footprint drive changes in species extinction risk’, *Nature Communications*. Springer US, 9, pp. 1–9. doi: 10.1038/s41467-018-07049-5.
- Martay, B., Brewer, M. J., Elston, D. A., Bell, J. R., Harrington, R., Brereton, T. M., Barlow, K. E., Botham, M. S. and Pearce-Higgins, J. W. (2017) ‘Impacts of climate change on national biodiversity population trends’, *Ecography*, 40(10), pp. 1139–1151. doi: 10.1111/ecog.02411.
- McKinney, M. L. and Lockwood, J. L. (1999) ‘Biotic homogenization: A few winners replacing many losers in the next mass extinction’, *Trends in Ecology and Evolution*, 14(11), pp. 450–453. doi: 10.1016/S0169-5347(99)01679-1.
- McRae, L., Deinet, S. and Freeman, R. (2017) ‘The diversity-weighted living planet index: Controlling for taxonomic bias in a global biodiversity indicator’, *PLoS ONE*, 12(1), pp. 1–20. doi: 10.1371/journal.pone.0169156.
- Microsoft, C. and Weston, S. (2015) ‘doParallel: Foreach Parallel Adaptor for the “parallel” Package’. Available at: <https://cran.r-project.org/package=doParallel>.
- Millenium, E. A. (2005) *Ecosystems and Human Well-being: Synthesis*. Island Press, Washington D.C.
- Myhrvold, N., Baldrige, E., Chan, B., Freeman, D. L. and Ernest, S. K. M. (2015) ‘An amniote life-history database to perform comparative analyses with birds, mammals, and reptiles’, *Ecology*, 96(11), p. 3109. doi: 10.5061/dryad.t6m96.
- Nenzén, H. K., Swab, R. M., Keith, D. a. and Araújo, M. B. (2012) ‘demoniche - an R-package for simulating spatially-explicit population dynamics’, *Ecography*, 35(February),

pp. 577–580. doi: 10.1111/j.1600-0587.2012.07378.x.

Newbold, T., Hudson, L. N., Arnell, A., Contu, S., De Palma, A., Ferrier, S., Hill, S., Hoskins, A., Lysenko, I., Phillips, H., Burton, V., Chng, C., Emerson, S., Gao, D., Pask-Hale, G., Hutton, J., Jung, M., Sanchez-Ortiz, K., Simmons, B., Whitmee, S., Zhang, H., Scharlemann, J. and Purvis, A. (2016) ‘Has land use pushed terrestrial biodiversity beyond the planetary boundary? A global assessment’, *Science*, 353(6296), pp. 288–291.

Newbold, T., Hudson, L. N., Hill, S. L., Contu, S., Lysenko, I., Senior, R. A., Börger, L., Bennett, D. J., Choimes, A., Collen, B., Day, J., De Palma, A., Díaz, S., Echeverria-Londoño, S., Edgar, M. J., Feldman, A., Garon, M., Harrison, M. L. K., Alhousseini, T., Ingram, D. J., Itescu, Y., Kattge, J., Kemp, V., Kirkpatrick, L., Kleyer, M., Laginha Pinto Correia, D., Martin, C. D., Meiri, S., Novosolov, M., Pan, Y., Phillips, H. R. P., Purves, D. W., Robinson, A., Simpson, J., Tuck, S. L., Weiher, E., White, H. J., Ewers, R. M., Mace, G. M., Scharlemann, J. P. W. and Purvis, A. (2015) ‘Global effects of land use on local terrestrial biodiversity’, *Nature*, 520, p. 45-. doi: 10.1038/nature14324.

Nielsen, S. E., Johnson, C. J., Heard, D. C. and Boyce, M. S. (2005) ‘Can models of presence-absence be used to scale abundance? Two case studies considering extremes in life history’, *Ecography*, 28(2), pp. 197–208. doi: 10.1111/j.0906-7590.2005.04002.x.

Nix, H. A. (1986) ‘A biogeographic analysis of Australian elapid snakes.’, in Longmore, R. (ed.) *Australian Flora and Fauna Series Number 7*. Canberra: Australian Government Publishing Service, pp. 4–15.

Oliver, T. H. and Morecroft, M. D. (2014) ‘Interactions between climate change and land use change on biodiversity: attribution problems, risks, and opportunities’, *Wiley Interdisciplinary Reviews: Climate Change*, 5(3), pp. 317–335. doi: 10.1002/wcc.271.

Pacifici, M., Foden, W. B., Visconti, P., Watson, J. E. M., Butchart, S. H. M., Kovacs, K. M., Scheffers, B. R., Hole, D. G., Martin, T. G., Akçakaya, H. R., Corlett, R. T., Huntley, B., Bickford, D., Carr, J. A., Hoffmann, A. A., Midgley, G. F., Pearce-Kelly, P., Pearson, R. G., Williams, S. E., Willis, S. G., Young, B. and Rondinini, C. (2015) ‘Assessing species vulnerability to climate change’, 5, pp. 215–225. doi: 10.1038/nclimate2448.

Paradis, E., Baillie, S. R. and Sutherland, W. J. (2002) ‘Modeling large-scale dispersal distances’, *Ecological Modelling*, 151(2–3), pp. 279–292. doi: 10.1016/S0304-3800(01)00487-2.

Parmesan, C. (2006) ‘Ecological and evolutionary responses to recent climate change’, *Annual Review of Ecology, Evolution, and Systematics*, 37, pp. 637–669. doi: 10.2307/annurev.ecolsys.37.091305.30000024.

Parmesan, C. and Yohe, G. (2003) ‘A globally coherent fingerprint of climate change impacts across natural systems.’, *Nature*, 421, pp. 37–42. doi: 10.1038/nature01286.

Pearce-Higgins, J. W., Eglington, S. M., Martay, B. and Chamberlain, D. E. (2015) ‘Drivers of climate change impacts on bird communities’, *Journal of Animal Ecology*, 84(4), pp. 943–954. doi: 10.1111/1365-2656.12364.

Pearson, R. G. and Dawson, T. P. (2003) ‘Predicting the impacts of climate change on the distribution of species: are bioclimate envelope models useful?’, *Global Ecology and Biogeography*, 12, pp. 361–371.

- Pearson, R. G., Dawson, T. P. and Liu, C. (2004) 'Modelling species distributions in Britain: A hierarchical integration of climate and land-cover data', *Ecography*, 27(3), pp. 285–298. doi: 10.1111/j.0906-7590.2004.03740.x.
- Pebesma, E. and Bivand, R. (2005) 'Classes and methods for spatial data in R'. *R News* 5 (2).
- Peterson, A. T., Soberon, J., Pearson, R., Anderson, R., Martinez-Meyer, E., Nakamura, M. and Araújo, M. (2011) *Ecological Niches and Geographic Distributions*. Princeton: Princeton University Press.
- Phillips, S., Dudík, M. and Schapire, R. (2004) 'A maximum entropy approach to species distribution modeling', *Proceedings of the twenty-first ...*. Available at: <http://dl.acm.org/citation.cfm?id=1015412> (Accessed: 3 May 2013).
- Phillips, S. J., Dudík, M., Elith, J., Graham, C. H., Lehmann, A., Leathwick, J. and Ferrier, S. (2009) 'Sample selection bias and presence-only distribution models: implications for background and pseudo-absence data.', *Ecological applications: a publication of the Ecological Society of America*, 19(1), pp. 181–97. Available at: <http://www.ncbi.nlm.nih.gov/pubmed/19323182>.
- Pollock, L. J., Tingley, R., Morris, W. K., Golding, N., O'Hara, R. B., Parris, K. M., Vesk, P. A. and McCarthy, M. A. (2014) 'Understanding co-occurrence by modelling species simultaneously with a Joint Species Distribution Model (JSDM)', *Methods in Ecology and Evolution*, 5(5), pp. 397–406. doi: 10.1111/2041-210X.12180.
- Purvis, A., Gittleman, J. L., Cowlishaw, G. and Mace, G. M. (2000) 'Predicting extinction risk in declining species.', *Proceedings. Biological sciences / The Royal Society*, 267(1456), pp. 1947–52. doi: 10.1098/rspb.2000.1234.
- Van Der Putten, W. H., Macel, M. and Visser, M. E. (2010) 'Predicting species distribution and abundance responses to climate change: Why it is essential to include biotic interactions across trophic levels', *Philosophical Transactions of the Royal Society B: Biological Sciences*, 365(1549), pp. 2025–2034. doi: 10.1098/rstb.2010.0037.
- R Core Team (2018) 'R: A language and environment for statistical computing'. Vienna, Austria. Available at: <https://www.r-project.org/>.
- Riahi, K., Rao, S., Krey, V., Cho, C., Chirkov, V., Fischer, G., Kindermann, G., Nakicenovic, N. and Rafaj, P. (2011) 'RCP 8.5-A scenario of comparatively high greenhouse gas emissions', *Climatic Change*, 109(1), pp. 33–57. doi: 10.1007/s10584-011-0149-y.
- Riney, T. (1964) 'The impact of introductions of large herbivores on the tropical environment', *International Union for the Conservation of Nature and Natural Resources Publication*, 4, pp. 261–273.
- Ripple, W. J., Estes, J. A., Beschta, R. L., Wilmers, C. C., Ritchie, E. G., Hebblewhite, M., Berger, J., Elmhagen, B., Letnic, M., Nelson, M. P., Schmitz, O. J., Smith, D. W., Wallach, A. D. and Wirsing, A. J. (2014) 'Status and ecological effects of the world's largest carnivores', *Science*, 343(6167). doi: 10.1126/science.1241484.
- Ripple, W. J., Wolf, C., Newsome, T. M., Hoffmann, M., Wirsing, A. J. and McCauley, D. J. (2017) 'Extinction risk is most acute for the world's largest and smallest vertebrates',

Proceedings of the National Academy of Sciences, p. 201702078. doi: 10.1073/pnas.1702078114.

Rodríguez, J. P. (2002) 'Range contraction in declining North American Bird populations', *Ecological Applications*, 12(1), pp. 238–248. doi: 10.1890/1051-0761(2002)012[0238:RCIDNA]2.0.CO;2.

Root, T., Price, J., Hall, K. and Schneider, S. (2003) 'Fingerprints of global warming on wild animals and plants', *Nature*, 421(tier 2), pp. 57–60. doi: 10.1038/nature01309.1.

Rosenzweig, C., Karoly, D., Vicarelli, M., Neofotis, P., Wu, Q., Casassa, G., Menzel, A., Root, T. L., Estrella, N., Seguin, B., Tryjanowski, P., Liu, C., Rawlins, S. and Imeson, A. (2008) 'Attributing physical and biological impacts to anthropogenic climate change.', *Nature*, 453(7193), pp. 353–7. doi: 10.1038/nature06937.

Sagarin, R. D. and Gaines, S. D. (2002) 'The “abundant centre” distribution: To what extent is it a biogeographical rule?', *Ecology Letters*, 5(1), pp. 137–147. doi: 10.1046/j.1461-0248.2002.00297.x.

Sala, O. E. (2000) 'Global Biodiversity Scenarios for the Year 2100 ', *Science*, 287(5459), pp. 1770–1774. doi: 10.1126/science.287.5459.1770.

Salguero-Gómez, R., Jones, O. R., Archer, C. R., Bein, C., de Buhr, H., Farack, C., Gottschalk, F., Hartmann, A., Henning, A., Hoppe, G., Römer, G., Ruoff, T., Sommer, V., Wille, J., Voigt, J., Zeh, S., Vieregg, D., Buckley, Y. M., Che-Castaldo, J., Hodgson, D., Scheuerlein, A., Caswell, H. and Vaupel, J. W. (2016) 'COMADRE: A global data base of animal demography', *Journal of Animal Ecology*, 85(2), pp. 371–384. doi: 10.1111/1365-2656.12482.

Santini, L., Isaac, N. J. B. and Ficetola, G. F. (2018) 'TetraDENSITY: A database of population density estimates in terrestrial vertebrates', *Global Ecology and Biogeography*, pp. 1–5. doi: 10.1111/geb.12756.

Santini, L., Isaac, N. J. B., Maiorano, L., Ficetola, G. F., Huijbregts, M. A. J., Carbone, C. and Thuiller, W. (2018) 'Global drivers of population density in terrestrial vertebrates', *Global Ecology and Biogeography*, 27(8), pp. 968–979. doi: 10.1111/geb.12758.

Santini, L., Pironon, S., Maiorano, L. and Thuiller, W. (2018) 'Addressing common pitfalls does not provide more support to geographical and ecological abundant-centre hypotheses', *Ecography*, pp. 1–10. doi: 10.1111/ecog.04027.

Säterberg, T., Sellman, S. and Ebenman, B. (2013) 'High frequency of functional extinctions in ecological networks', *Nature*, 499(7459), pp. 468–470. doi: 10.1038/nature12277.

Schulman, L., Toivonen, T. and Ruokolainen, K. (2007) 'Analysing botanical collecting effort in Amazonia and correcting for it in species range estimation', *Journal of Biogeography*, 34(8), pp. 1388–1399. doi: 10.1111/j.1365-2699.2007.01716.x.

Schurr, F. M., Pagel, J., Cabral, J. S., Groeneveld, J., Bykova, O., O'Hara, R. B., Hartig, F., Kissling, W. D., Linder, H. P., Midgley, G. F., Schröder, B., Singer, A. and Zimmermann, N. E. (2012) 'How to understand species' niches and range dynamics: A demographic research agenda for biogeography', *Journal of Biogeography*, 39, pp. 2146–2162. doi: 10.1111/j.1365-2699.2012.02737.x.

- Scillitani, L., Sturaro, E., Menzano, A., Rossi, L., Viale, C. and Ramanzin, M. (2012) 'Post-release spatial and social behaviour of translocated male Alpine ibexes (*Capra ibex ibex*) in the eastern Italian Alps', *European Journal of Wildlife Research*, 58(2), pp. 461–472. doi: 10.1007/s10344-011-0596-9.
- Selwood, K. E., Mcgeoch, M. A. and Mac Nally, R. (2015) 'The effects of climate change and land-use change on demographic rates and population viability', *Biological Reviews*, 90(3), pp. 837–853. doi: 10.1111/brv.12136.
- Seo, C., Thorne, J. H., Hannah, L. and Thuiller, W. (2009) 'Scale effects in species distribution models: Implications for conservation planning under climate change', *Biology Letters*, 5(1), pp. 39–43. doi: 10.1098/rsbl.2008.0476.
- Staniczenko, P. P. A., Sivasubramaniam, P., Suttle, K. B. and Pearson, R. G. (2017) 'Linking macroecology and community ecology: refining predictions of species distributions using biotic interaction networks', *Ecology Letters*, 20(6), pp. 693–707. doi: 10.1111/ele.12770.
- Statisticat, L. (2018) 'LaplaceDemon: Complete Environment for Bayesian Inference'. Available at: <http://www.bayesian-inference.com/software>.
- Stephens, P. A., Mason, L. R., Green, R. E., Gregory, R. D., Sauer, J. R., Alison, J., Aunins, A. and Brotons, L. (2016) 'Consistent response of bird populations to climate change on two continents', 352(6281).
- Stevenson, I. R. and Bryant, D. M. (2000) 'Avian phenology: Climate change and constraints on breeding', *Nature*, 406(6794), pp. 366–367. doi: 10.1038/35019151.
- Stuart, S. N., Chanson, J. S., Cox, N. A., Young, B. E., Rodrigues, A. S. L., Fischman, D. L. and Waller, R. W. (2004) 'Status and Trends of Amphibian Declines and Extinctions Worldwide', *Science*, 309(September), pp. 1783–1786. doi: 10.1126/science.1112996.
- Stubben, C. and Milligan, B. (2007) 'Estimating and Analyzing Demographic Models Using the popbio Package in R', *Journal of Statistical Software*, 22(11).
- Stüwe, M. and Nievergelt, B. (1991) 'Recovery of alpine ibex from near extinction: the result of effective protection, captive breeding, and reintroductions', *Applied Animal Behaviour Science*, 29(1–4), pp. 379–387. doi: 10.1016/0168-1591(91)90262-V.
- Suttle, K. B., Thomsen, M. and Power, M. E. (2007) 'Species interactions reverse grassland responses to changing climate.', *Science (New York, N.Y.)*, 315, pp. 640–642. doi: 10.1126/science.1136401.
- Svenning, J. C., Gravel, D., Holt, R. D., Schurr, F. M., Thuiller, W., Münkemüller, T., Schiffers, K. H., Dullinger, S., Edwards, T. C., Hickler, T., Higgins, S. I., Nabel, J. E. M. S., Pagel, J. and Normand, S. (2014) 'The influence of interspecific interactions on species range expansion rates', *Ecography*, 37(12), pp. 1198–1209. doi: 10.1111/j.1600-0587.2013.00574.x.
- Thomas, C. D., Cameron, A., Green, R. E., Bakkenes, M., Beaumont, L. J., Collingham, Y. C., Erasmus, B. F. N., De Siqueira, M. F., Grainger, A., Hannah, L., Hughes, L., Huntley, B., Van Jaarsveld, A. S., Midgley, G. F., Miles, L., Ortega-Huerta, M. A., Peterson, A. T., Phillips, O. L. and Williams, S. E. (2004) 'Extinction risk from climate change.', *Nature*, 427(6970), pp. 145–8. doi: 10.1038/nature02121.

Thomas, C., Franco, a and Hill, J. (2006) 'Range retractions and extinction in the face of climate warming', *Trends in Ecology & Evolution*, 21(8), pp. 415–416. doi: 10.1016/j.tree.2006.05.012.

Thomas, J. A. (2004) 'Comparative Losses of British Butterflies, Birds, and Plants and the Global Extinction Crisis', *Science*, 303(March), pp. 1879–1881. doi: 10.1126/science.1095046.

Thompson, P. M. and Ollason, J. C. (2001) 'Lagged effects of ocean climate change on fulmar population dynamics', *Nature*, 413(6854), pp. 417–420. doi: 10.1038/35096558.

Thuiller, W., Albert, C., Araújo, M. B., Berry, P. M., Cabeza, M., Guisan, A., Hickler, T., Midgley, G. F., Paterson, J., Schurr, F. M., Sykes, M. T. and Zimmermann, N. E. (2008) 'Predicting global change impacts on plant species' distributions: Future challenges', *Perspectives in Plant Ecology, Evolution and Systematics*, 9(3–4), pp. 137–152. doi: 10.1016/j.ppees.2007.09.004.

Thuiller, W., Münkemüller, T., Schiffrers, K. H., Georges, D., Dullinger, S., Eckhart, V. M., Edwards, T. C., Gravel, D., Kunstler, G., Merow, C., Moore, K., Piedallu, C., Vissault, S., Zimmermann, N. E., Zurell, D. and Schurr, F. M. (2014) 'Does probability of occurrence relate to population dynamics?', *Ecography*, 37(12), pp. 1155–1166. doi: 10.1111/ecog.00836.

Tierney, L., Rossini, A., Li, N. and Sevcikova, H. (2018) 'snow: Simple Network of Workstations'. Available at: <https://cran.r-project.org/package=snow>.

Tilman, D., May, R., Lehman, C. and Nowak, M. (1994) 'Habitat destruction and the extinction debt', *Mathematical Biosciences*, 371, pp. 65–66. doi: 10.1016/j.mbs.2009.06.003.

Tôrres, N. M., De Marco, P., Santos, T., Silveira, L., de Almeida Jácomo, A. T. and Diniz-Filho, J. A. F. (2012) 'Can species distribution modelling provide estimates of population densities? A case study with jaguars in the Neotropics', *Diversity and Distributions*, 18(6), pp. 615–627. doi: 10.1111/j.1472-4642.2012.00892.x.

Trakhtenbrot, A., Nathan, R., Perry, G. and Richardson, D. M. (2005) 'The importance of long-distance dispersal in biodiversity conservation', *Diversity and Distributions*, 11(2), pp. 173–181. doi: 10.1111/j.1366-9516.2005.00156.x.

Travis, J. M. J. (2003) 'Climate change and habitat destruction: a deadly anthropogenic cocktail.', *Proceedings. Biological sciences / The Royal Society*, 270(1514), pp. 467–73. doi: 10.1098/rspb.2002.2246.

Travis, J. M. J., Delgado, M., Bocedi, G., Baguette, M., Bartoń, K., Bonte, D., Boulangeat, I., Hodgson, J. A., Kubisch, A., Penteriani, V., Saastamoinen, M., Stevens, V. M. and Bullock, J. M. (2013) 'Dispersal and species' responses to climate change', *Oikos*, 122(11), pp. 1532–1540. doi: 10.1111/j.1600-0706.2013.00399.x.

Urban, M. C. (2015) 'Accelerating extinction risk from climate change', *Science*, 248(6234), pp. 571–573.

Urban, M. C., Bocedi, G., Hendry, A. P., Mihoub, J. B., Pe'er, G., Singer, A., Bridle, J. R., Crozier, L. G., De Meester, L., Godsoe, W., Gonzalez, A., Hellmann, J. J., Holt, R. D., Huth, A., Johst, K., Krug, C. B., Leadley, P. W., Palmer, S. C. F., Pantel, J. H., Schmitz,

- A., Zollner, P. A. and Travis, J. M. J. (2016) 'Improving the forecast for biodiversity under climate change', *Science*, 353(6304). doi: 10.1126/science.aad8466.
- VanDerWal, J., Shoo, L. P., Johnson, C. N. and Williams, S. E. (2009) 'Abundance and the Environmental Niche: Environmental Suitability Estimated from Niche Models Predicts the Upper Limit of Local Abundance', *The American Naturalist*, 174(2), pp. 282–291. doi: 10.1086/600087.
- Varela, S., Rodríguez, J. and Lobo, J. M. (2009) 'Is current climatic equilibrium a guarantee for the transferability of distribution model predictions? A case study of the spotted hyena', *Journal of Biogeography*, 36(9), pp. 1645–1655. doi: 10.1111/j.1365-2699.2009.02125.x.
- Vié, J. C., Hilton-Taylor, C. and Stuart, S. N. (2009) *Wildlife in a Changing World—An Analysis of the 2008 IUCN Red List of Threatened Species*. Gland, Switzerland. doi: 10.2305/IUCN.CH.2009.17.en.
- Visconti, P., Bakkenes, M., Baisero, D., Brooks, T., Butchart, S. H. M., Joppa, L., Alkemade, R., Di Marco, M., Santini, L., Hoffmann, M., Maiorano, L., Pressey, R. L., Arponen, A., Boitani, L., Reside, A. E., van Vuuren, D. P. and Rondinini, C. (2015) 'Projecting Global Biodiversity Indicators under Future Development Scenarios', *Conservation Letters*, (January). doi: 10.1111/conl.12159.
- Visconti, P., Pressey, R. L., Giorgini, D., Maiorano, L., Bakkenes, M., Boitani, L., Alkemade, R., Falcucci, A., Chiozza, F. and Rondinini, C. (2011) *Future hotspots of terrestrial mammal loss*, *Philosophical Transactions of the Royal Society B: Biological Sciences*. doi: 10.1098/rstb.2011.0105.
- Visser, M. E., Both, C. and Lambrechts, M. M. (2004) 'Global Climate Change Leads to Mismatched Avian Reproduction', *Advances in Ecological Research*, 35(04), pp. 89–110. doi: 10.1016/S0065-2504(04)35005-1.
- De Vos, J. M., Joppa, L. N., Gittleman, J. L., Stephens, P. R. and Pimm, S. L. (2015) 'Estimating the normal background rate of species extinction', *Conservation Biology*, 29(2), pp. 452–462. doi: 10.1111/cobi.12380.
- Walther, G.-R., Post, E., Convey, P., Menzel, A., Parmesan, C., Beebee, T. J. C., Fromentin, J.-M., Hoegh-Guldberg, O. and Bairlein, F. (2002) 'Ecological responses to recent climate change.', *Nature*, 416, pp. 389–395. doi: 10.1038/416389a.
- Walther, G. R. (2010) 'Community and ecosystem responses to recent climate change', *Philosophical Transactions of the Royal Society B: Biological Sciences*, 365(1549), pp. 2019–2024. doi: 10.1098/rstb.2010.0021.
- Webber, B. L., Yates, C. J., Le Maitre, D. C., Scott, J. K., Kriticos, D. J., Ota, N., McNeill, A., Le Roux, J. J. and Midgley, G. F. (2011) 'Modelling horses for novel climate courses: Insights from projecting potential distributions of native and alien Australian acacias with correlative and mechanistic models', *Diversity and Distributions*, 17(5), pp. 978–1000. doi: 10.1111/j.1472-4642.2011.00811.x.
- Weber, M. M., Stevens, R. D., Diniz-Filho, J. A. F. and Grelle, C. E. V. (2017) 'Is there a correlation between abundance and environmental suitability derived from ecological niche modelling? A meta-analysis', *Ecography*, 40(7), pp. 817–828. doi: 10.1111/ecog.02125.
- Wickham, H. (2007) 'Reshaping Data with the reshape Package', *Journal of Statistical*

Software, 21(12), pp. 1–20. doi: 10.1016/S0142-1123(99)00007-9.

Wickham, H. (2011) ‘The Split-Apply-Combine Strategy for Data’, *Journal of Statistical Software*, 40(1), pp. 1–29. doi: 10.1.1.182.5667.

Wickham, H. (2016) *ggplot2: Elegant Graphics for Data Analysis*. New York: Springer-Verlag.

Wickham, H., François, R., Henry, L. and Müller, K. (2018) ‘dplyr: A Grammar of Data Manipulation.’ Available at: <https://cran.r-project.org/package=dplyr>.

Wilman, H., Belmaker, J., Simpson, J., de la Rosa, C., Rivadeneira, M. M. and Jetz, W. (2014) ‘EltonTraits 1.0: Species-level foraging attributes of the world’s birds and mammals.’, *Ecology*, 95(2027).

Winfree, R., Fox, J. W., Williams, N. M., Reilly, J. R. and Cariveau, D. P. (2015) ‘Abundance of common species, not species richness, drives delivery of a real-world ecosystem service’, *Ecology Letters*, 18(7), pp. 626–635. doi: 10.1111/ele.12424.

Winfree, R., Reilly, J. R., Bartomeus, I., Cariveau, D. P., Williams, N. M. and Gibbs, J. (2018) ‘Species turnover promotes the importance of bee diversity for crop pollination at regional scales’, *Science*, 359(6377), pp. 791–793. doi: 10.1126/science.aao2117.

Wisz, M. S., Hijmans, R. J., Li, J., Peterson, A. T., Graham, C. H., Guisan, A., Elith, J., Dudík, M., Ferrier, S., Huettmann, F., Leathwick, J. R., Lehmann, A., Lohmann, L., Loiselle, B. A., Manion, G., Moritz, C., Nakamura, M., Nakazawa, Y., Overton, J. M. C., Phillips, S. J., Richardson, K. S., Scachetti-Pereira, R., Schapire, R. E., Soberón, J., Williams, S. E. and Zimmermann, N. E. (2008) ‘Effects of sample size on the performance of species distribution models’, *Diversity and Distributions*, 14(5), pp. 763–773. doi: 10.1111/j.1472-4642.2008.00482.x.

Wisz, M. S., Pottier, J., Kissling, W. D., Pellissier, L., Lenoir, J., Damgaard, C. F., Dormann, C. F., Forchhammer, M. C., Grytnes, J. A., Guisan, A., Heikkinen, R. K., Høye, T. T., Kühn, I., Luoto, M., Maiorano, L., Nilsson, M. C., Normand, S., Öckinger, E., Schmidt, N. M., Termansen, M., Timmermann, A., Wardle, D. A., Aastrup, P. and Svenning, J. C. (2013) ‘The role of biotic interactions in shaping distributions and realised assemblages of species: Implications for species distribution modelling’, *Biological Reviews*, 88(1), pp. 15–30. doi: 10.1111/j.1469-185X.2012.00235.x.

Wood, S. N. (2011) ‘Fast stable restricted maximum likelihood and marginal likelihood estimation of semiparametric generalized linear models’, *Journal of the Royal Statistical Society: Series B (Statistical Methodology)*, 73(1), pp. 3–36. doi: 10.1111/j.1467-9868.2010.00749.x.

Worm, B., Barbier, E. B., Beaumont, N., Duffy, J. E., Folke, C., Halpern, B. S., Jackson, J. B., Lotze, H. K., Micheli, F., Palumbi, S. R., Sala, E., Selkoe, K. A., Stachowicz, J. J. and Watson, R. (2006) ‘Impacts of Biodiversity Loss on Ocean Ecosystem Services’, *Science*, 314(5829), pp. 787–790. doi: 10.1126/science.1139114.

Wright, S. J. (2005) ‘Tropical forests in a changing environment’, *Trends in Ecology and Evolution*, 20(10), pp. 553–560. doi: 10.1016/j.tree.2005.07.009.

WWF (2016) *Living Planet Report 2016. Risk and resilience in a new era*. WWF International, Gland, Switzerland.

WWF (2018) *Living Planet Report - 2018: Aiming Higher*. Edited by M. Grooten and R. E. A. Almond. WWF, Gland, Switzerland. Available at: <http://scholar.google.com/scholar?hl=en&btnG=Search&q=intitle:LIVING+PLANET+REPORT+2004#0>.

Yee, T. W. and Mitchell, N. D. (1991) 'Generalized Additive Models in Plant Ecology Author', *Journal of Vegetation Science*, 2(5), pp. 587–602.

Young, R. P., Hudson, M. A., Terry, A. M. R., Jones, C. G., Lewis, R. E., Tatayah, V., Zuël, N. and Butchart, S. H. M. (2014) 'Accounting for conservation: Using the IUCN Red List Index to evaluate the impact of a conservation organization', *Biological Conservation*. Elsevier Ltd, 180, pp. 84–96. doi: 10.1016/j.biocon.2014.09.039.

Zarada, K. and Drake, J. M. (2017) 'Time to extinction in deteriorating environments', *Theoretical Ecology*. *Theoretical Ecology*, 10(1), pp. 65–71. doi: 10.1007/s12080-016-0311-2.

Zeileis, A. and Grothendieck, G. (2005) 'zoo: S3 Infrastructure for Regular and Irregular Time Series', *Journal of Statistical Software*, 30(6), pp. 1--27. doi: 10.1017/CBO9781107415324.004.

Zurell, D., Thuiller, W., Pagel, J., Cabral, J. S., Münkemüller, T., Gravel, D., Dullinger, S., Normand, S., Schiffers, K. H., Moore, K. A. and Zimmermann, N. E. (2016) 'Benchmarking novel approaches for modelling species range dynamics', *Global Change Biology*, 22(8), pp. 2651–2664. doi: 10.1111/gcb.13251.

APPENDICES

MODEL AVERAGING

Model averaging provides a way of combining multiple models into a single weighted model which can be used to make predictions. In Chapter Two it also meant that each variable was included in the average model. This was advantageous in this study as I expected each of the explanatory variables to influence bird and mammal population trends. A criterion is required for selecting models to be combined into an average model, to avoid the inclusion of poorly performing models. There are two principle criteria that are commonly used: firstly, the selection of models based on the ΔAIC , i.e. the difference in AIC points between each model and the model with the lowest AIC score; secondly, the minimum number of models needed for the cumulative sum of the Akaike weights to meet a threshold value, commonly 0.95. In Chapter Two, I selected models to be used to create the average model using the latter method. I feel that this is a more conservative approach and, given the variability in potential effects within my analysis, was more appropriate. Here I explore the effect of using the former criterion, with models $\Delta AIC < 6$ (as recommended in Harrison et al., 2018) included in the average model.

The results of the averaged models under $\Delta AIC < 6$ (Figure S2.1) are very similar to the results under Akaike weights ≥ 0.95 , with the differences between each of the values being very small (<6.5%). Both methods are conservative approaches, in that they include a relatively wide set of models. I believe a conservative approach is appropriate here as I am attempting to capture complex processes where I expect each of the explanatory variables to have an important influence on the model.

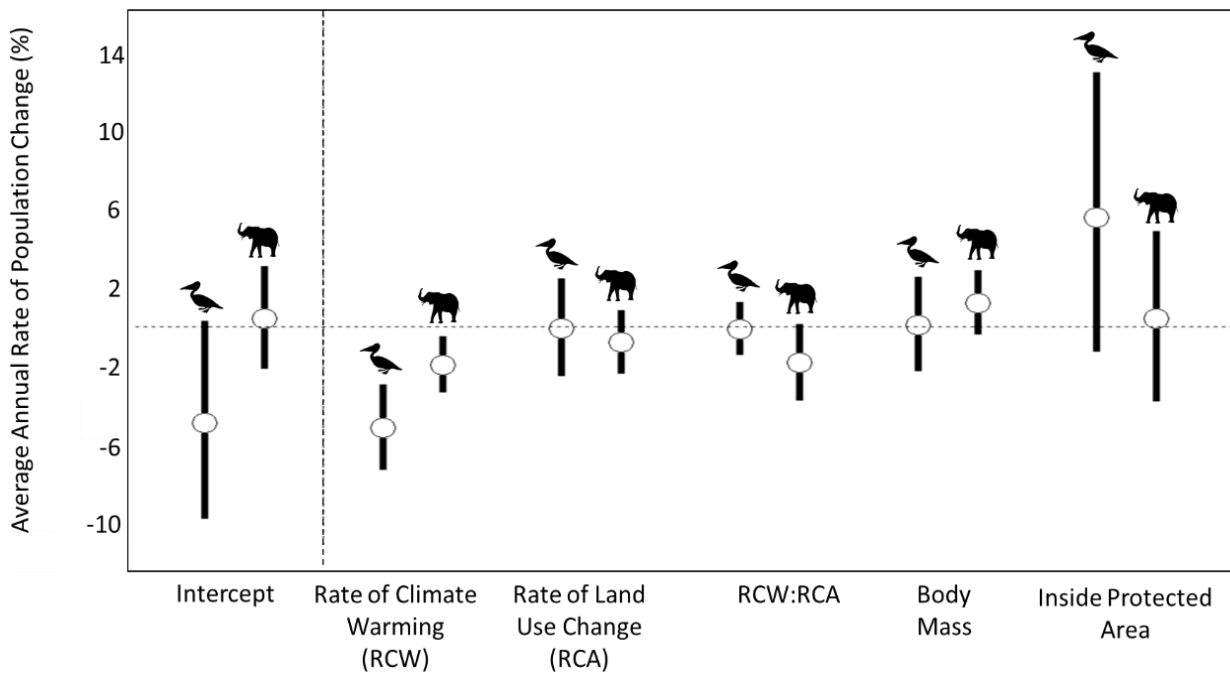


Figure S2.1 The distribution of the coefficients of the average models ($\Delta AIC < 6$) for both bird and mammal populations. The circles show the estimated coefficient values for each variable and the solid lines show the 2.5 - 97.5% confidence intervals. The intercept shows the distribution of the annual population growth rates in the absence of the effects of explanatory variables. The explanatory variables were scaled and centred, therefore the coefficients show the change in annual population growth rate given a one standard deviation increase in each explanatory variable. When the confidence intervals do not overlap with zero this shows a clear signal of either a positive or negative effect of a variable. Confidence intervals that overlap with zero show that within the averaged model an increase in a given variable has a mixture both positive and negative effect sizes on the rate of population change across different populations.

CHAPTER TWO APPENDIX

Results from bird population trends

<i>Model</i>	Δ AIC	Akaike Weight	Marg. R ²	Cond. R ²	Intercept	Rate of Climate Warming (RCW)	Rate of Conversion to Anthropogenic Land Use (RCA)	RCW:RCA	Body Mass	Inside Protected Area
RCW+PA	0.00	0.28	0.08	0.79	-6.12 (± 2.63)	-5.09 (± 1.17)				5.60 (± 3.50)
RCW	0.42	0.22	0.06	0.79	-3.38 (± 1.88)	-5.29 (± 1.17)				
RCW+BM+PA	2.06	0.10	0.08	0.79	-6.18 (± 2.69)	-5.10 (± 1.17)			0.12 (± 1.24)	5.62 (± 3.51)
RCA+RCW+PA	2.06	0.10	0.08	0.79	-6.13 (± 2.63)	-5.08 (± 1.17)	-0.11 (± 1.28)			5.62 (± 3.50)
RCW+BM	2.48	0.08	0.06	0.79	-3.40 (± 1.94)	-5.30 (± 1.17)			0.04 (± 1.25)	
RCA+RCW	2.48	0.08	0.06	0.79	-3.39 (± 1.88)	-5.29 (± 1.17)	-0.02 (± 1.29)			
RCW*RCA+PA	4.12	0.04	0.08	0.79	-6.12 (± 2.63)	-5.13 (± 1.22)	-0.11 (± 1.28)	-0.11 (± 0.69)		5.60 (± 3.51)
RCA+RCW+BM+PA	4.13	0.04	0.08	0.79	-6.19 (± 2.69)	-5.08 (± 1.17)	-0.12 (± 1.28)		0.13 (± 1.25)	5.64 (± 3.51)
RCA*RCW	4.51	0.03	0.06	0.79	-3.38 (± 1.88)	-5.35 (± 1.22)	-0.02 (± 1.29)	-0.14 (± 0.70)		
RCA+RCW+BM	4.55	0.03	0.06	0.79	-3.40 (± 1.94)	-5.29 (± 1.17)	-0.02 (± 1.30)		0.05 (± 1.25)	
RCA*RCW+BM+PA	6.20	0.01	0.08	0.79	-6.17 (± 2.70)	-5.13 (± 1.22)	-0.12 (± 1.28)	-0.10 (± 0.69)	0.12 (± 1.25)	5.62 (± 3.51)
RCA*RCW+BM	6.59	0.01	0.06	0.79	-3.39 (± 1.94)	-5.35 (± 1.22)	-0.03 (± 1.30)	-0.14 (± 0.70)	0.03 (± 1.25)	
RCA+PA	18.89	<0.01	0.03	0.76	-6.00 (± 2.62)		-0.71 (± 1.26)			7.33 (± 3.46)
BM+PA	19.21	<0.01	0.02	0.76	-5.91 (± 2.69)				-0.08	7.25 (± 3.46)
NULL	19.27	<0.01	0.00	0.77	-2.34 (± 1.88)					
RCA+BM+PA	20.96	<0.01	0.03	0.76	-5.98 (± 2.69)		-0.71 (± 1.26)		-0.04	7.32 (± 3.46)
RCA	21.06	<0.01	<0.01	0.77	-2.36 (± 1.88)		-0.65 (± 1.28)			
BM	21.30	<0.01	<0.01	0.77	-2.27 (± 1.94)				-0.19	
RCA+BM	23.11	<0.01	<0.01	0.77	-2.31 (± 1.94)		-0.64 (± 1.29)		-0.15	
					RVI	1.00	0.33	0.09	0.26	0.55

Table S2.2 All competing models used to explain the growth rate of bird populations. The models are ranked in order of performance based on AIC, with higher ranking models listed towards the top of each table. Models within $< 2 \Delta$ AIC of the highest ranked model are highlighted with bold text and a grey background. A null model is included for comparison. RCW = annual rate of climate warming, RCA = annual rate of conversion to anthropogenic land use, BM = body mass, PA = population inside a protected area. The coefficient values have been transformed into percentage population change. According to the top ranked model for birds, an increase in RCW to rates expected under climate scenario RCP 8.5 (5-6°C, 2006-2100) would lead to an annual population decline of 3.85 - 4.65% in bird populations and 1.46 - 1.76% for mammal populations. RVI (relative variable importance) is the sum of Akaike weights over all models including the explanatory variable. P values show the results of an ANOVA comparing each model to the null model, and therefore give the probability that for a given model it is purely chance that it explains more of the variation in population trends than the null model.

Results from mammal population trends

<i>Model</i>	Δ AIC	Akaike Weight	Marg. R ²	Cond. R ²	Intercept	Rate of Climate Warming (RCW)	Rate of Conversion to Anthropogenic Land Use (RCA)	RCW:RCA	Body Mass	Inside Protected Area
<i>RCA*RCW+BM</i>	0.00	0.17	0.03	0.44	0.68 (±0.94)	-2.20 (±0.73)	-0.75 (±0.82)	-1.82 (±1.02)	1.24 (±0.82)	
<i>RCA*RCW</i>	0.12	0.16	0.02	0.45	0.38 (±0.95)	-2.22 (±0.73)	-0.55 (±0.81)	-1.88 (±1.02)		
<i>RCW</i>	1.05	0.10	0.01	0.42	0.38 (±0.93)	-1.72 (±0.68)				
<i>RCA+RCW+BM</i>	1.18	0.09	0.02	0.42	0.56 (±0.93)	-1.71 (±0.68)	-1.17 (±0.78)		1.28 (±0.81)	
<i>RCW+BM</i>	1.41	0.08	0.02	0.42	0.64 (±0.93)	-1.71 (±0.68)			1.06 (±0.80)	
<i>RCA+RCW</i>	1.50	0.08	0.02	0.43	0.26 (±0.93)	-1.73 (±0.68)	-0.97 (±0.78)			
<i>RCA*RCW+PA</i>	1.97	0.06	0.02	0.45	-0.36 (±1.91)	-2.24 (±0.73)	-0.58 (±0.82)	-1.86 (±1.02)		0.95 (±2.10)
<i>RCA*RCW+BM+PA</i>	2.06	0.06	0.03	0.44	0.82 (±2.08)	-2.20 (±0.73)	-0.74 (±0.82)	-1.83 (±1.02)	1.27 (±0.88)	-0.17 (±2.25)
<i>RCW+PA</i>	2.93	0.04	0.01	0.42	-0.27 (±1.88)	-1.74 (±0.69)				
<i>RCA+RCW+BM+PA</i>	3.24	0.03	0.02	0.42	0.62 (±2.06)	-1.71 (±0.68)	-1.17 (±0.79)		1.29 (±0.87)	0.83 (±2.11)
<i>RCA+RCW+PA</i>	3.28	0.03	0.02	0.45	-0.59 (±1.90)	-1.75 (±0.68)	-1.01 (±0.78)			1.09 (±2.09)
<i>RCW+BM+PA</i>	3.45	0.03	0.02	0.42	0.80 (±2.07)	-1.70 (±0.68)			1.09 (±0.89)	-0.19 (±2.25)
<i>NULL</i>	5.36	0.01	0.00	0.41	0.41 (±0.92)					
<i>RCA+BM</i>	5.48	0.01	0.01	0.41	0.60 (±0.91)		-1.18 (±0.79)		1.28 (±0.80)	
<i>BM</i>	5.69	0.01	0.01	0.41	0.66 (±0.92)				1.06 (±0.79)	
<i>RCA</i>	5.87	0.01	<0.0	0.41	0.31 (±0.92)		-0.96 (±0.78)			
<i>RCA+BM+PA</i>	7.46	<0.01	0.01	0.41	1.07 (±2.06)		-1.17 (±0.79)		1.37 (±0.86)	-0.57 (±2.25)
<i>BM+PA</i>	7.64	<0.01	0.01	0.41	1.23 (±2.06)				1.16 (±0.86)	
<i>RCA+PA</i>	7.81	<0.01	<0.01	0.41	-0.23 (±1.90)		-0.98 (±0.78)			0.69 (±2.09)
					RVI	0.95	0.72	0.45	0.50	0.27

Table S2.3 All competing models used to explain the growth rate of mammal populations. The models are ranked in order of performance based on AIC, with higher ranking models listed towards the top of each table. Models within < 2 Δ AIC of the highest ranked model are highlighted with bold text and a grey background. A null model is included for comparison. RCW = annual rate of climate warming, RCA = annual rate of conversion to anthropogenic land use, BM = body mass, PA = population inside a protected area. The coefficient values have been transformed into percentage population change. According to the top ranked model for birds, an increase in RCW to rates expected under climate scenario RCP 8.5 (5-6°C, 2006-2100) would lead to an annual population decline of 3.85 - 4.65% in bird populations and 1.46 - 1.76% for mammal populations. RVI (relative variable importance) is the sum of Akaike weights over all models including the explanatory variable. P values show the results of an ANOVA comparing each model to the null model, and therefore give the probability that for a given model it is purely chance that it explains more of the variation in population trends than the null model.

FUTURE PROJECTIONS

In Chapter Two I showed the rate of climate warming (RCW) to be an important predictor of both bird and mammal population growth rates. Climate change is expected to be a major threat to biodiversity in the coming century. There are four Representative Concentration Pathways (RCPs) provided by the IPCC which outline a range of potential climate change pathways. Here I project models with RCW as an explanatory variable forward under two contrasting climate change scenarios (RCP 2.6 and RCP 8.5, both under the HadGEM2-ES model; Jones et al., 2011). I expect that population declines will be considerably more severe under RCP 8.5 than RCP 2.6. Extrapolating forward models from Chapter Two allows for comparison against other published predictions of climate change impacts on biodiversity.

RCP 2.6 is the “best case” scenario under which emissions peak between 2010-2020 and decline in the following years meaning that warming plateaus after 2050; RCP 8.5 is the “worst case” scenario, where emissions continue to rise at a steady rate throughout the twenty-first century (Figure S2.2). For each scenario I calculated the predicted annual rate of change in mean temperature and used these values to model a population index of both bird and mammal population trends from 2005 – 2100, under both scenarios (Figure S2.3).

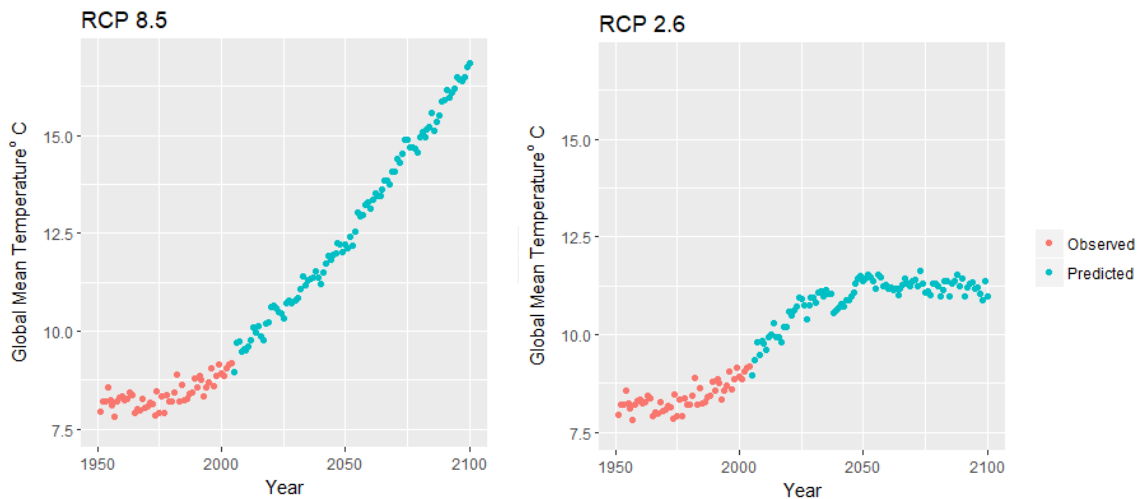


Figure S2.2 Annual global mean temperature 1950 – 2100, observed temperatures from the period 1950-2005 are shown in red and predicted temperatures under scenarios HadGEM2-ES RCP 8.5 (left) and HadGEM2-ES RCP 2.6 (right) are shown in blue.

As expected, the population declines are more severe when the rate of increase in mean temperature is greater. For RCP 2.6, extrapolation of the observed trend suggests a mean population decline of 67.6% for birds and a 43.8% increase in mammal populations by 2100; however, under RCP 8.5 there is a predicted mean population decline of 99.2% for birds and 70.3% for mammals (Figure S2.3).

It is important to note that these extrapolations and the models they are derived from are based purely on statistical correlations between population changes and rates of environmental change. This type of ‘prediction’ has advantages, namely its simplicity and relatively low data requirements. However, these extrapolations are based upon average bird and mammal populations and do not account for the variation in responses of different species in different locations to climate change. These predictions also assume a linear continuation of the observed associations between climate warming and population trends, they do not account for species physiological thermal limits or impact of climate change on species interactions.

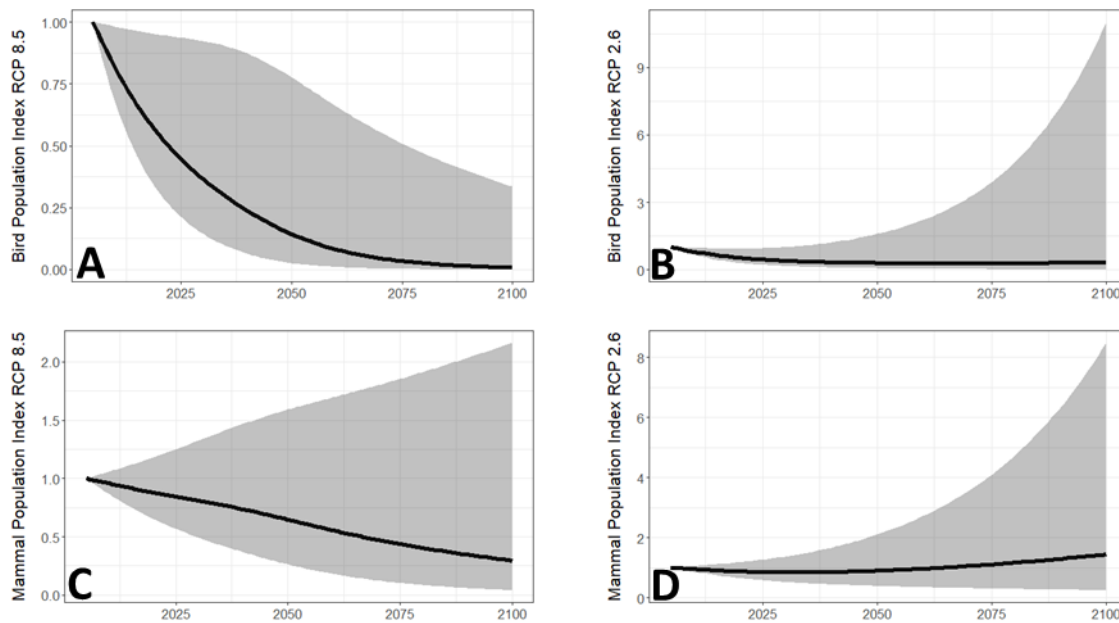


Figure S2.3 Future extrapolations of bird and mammal population indices under two contrasting climate scenarios. Scenario RCP 8.5 (panels A and C) is a “worst-case” scenario based on a continued increase in carbon emissions. The extrapolations show a mean decrease in bird populations (from a 2005 baseline) of 99.2% (panel A) and a decrease of 70.3% for mammal populations (panel C). RCP 2.6 (panels B and D) is a “best-case” scenario whereby emissions peak by 2020 and decrease from then, the extrapolations under this scenario show an average 67.6% decrease in bird populations (panel B) but a 43.8% increase in mammal populations (panel D).

According to the top performing model for birds (RCW + PA) under the RCP 8.5 scenario (5–6°C, 2006–2100) climate warming would lead to an annual population decline of 3.85–4.65% for bird populations and 1.46–1.76% for mammal populations. Accounting for protected area coverage, outside of protected areas I would expect 5.5–6.3% annual population declines for birds and 0.8–1.2% annual population declines for mammals; inside protected areas I would expect a 0.1% increase to 0.7% decrease in bird populations and 0.4–0.7% decrease in mammal populations.

Predictions of species extinctions due to climate change vary widely, estimating that between 0–54% of all species could become extinct due to climate change. A recent meta-analysis estimated that 15.7% of species are likely to become extinct due to climate change, under the RCP 8.5 scenario (Urban, 2015). It is difficult to compare predictions of extinctions and population declines; however, under RCP 8.5 these models suggest very

high declines for average bird populations (99.2%), which would likely lead to much higher levels of species extinctions than the predicted 15.7% (Urban, 2015).

INCLUDING A WIDER SET OF POPULATION TRENDS

The Living Planet population trends used for analysis in Chapter Two were filtered under the following criteria: (i) only populations with a known location were included (many of the population trends in the Living Planet database are nationally aggregated so cannot be spatially linked to environmental data); (ii) only populations where environmental data and body mass data were available were included (see below); (iii) population time series spanning less than 5 years were excluded because longer time series will better reflect environmental changes; and (iv) only population time series that had an $R^2 \geq 0.5$ when fit to the GAM or linear model were included, to ensure interpolated population estimates were reasonable.

Here I relax the last criterion to test whether the findings of Chapter Two still hold when using a broader and lower quality dataset. Populations which fulfilled only the first three criteria were included, thereby increasing the number of populations to 883 bird populations (463 species) and 966 mammal populations (272 species). I ran the same set of models on this expanded set of populations and found that the main results remain similar: populations have declined more rapidly where climate has warmed most quickly, and this is more severe for bird populations. Additionally, I find that within the wider data set body mass is an important predictor for mammal population trends. This means that larger bodied mammals are more likely to have had increasing population trends. I also note a positive impact of protected areas for bird populations, with populations inside of protected areas projected to have a positive population growth rate and those outside protected areas are more likely to have declining populations (Figure S2.4).

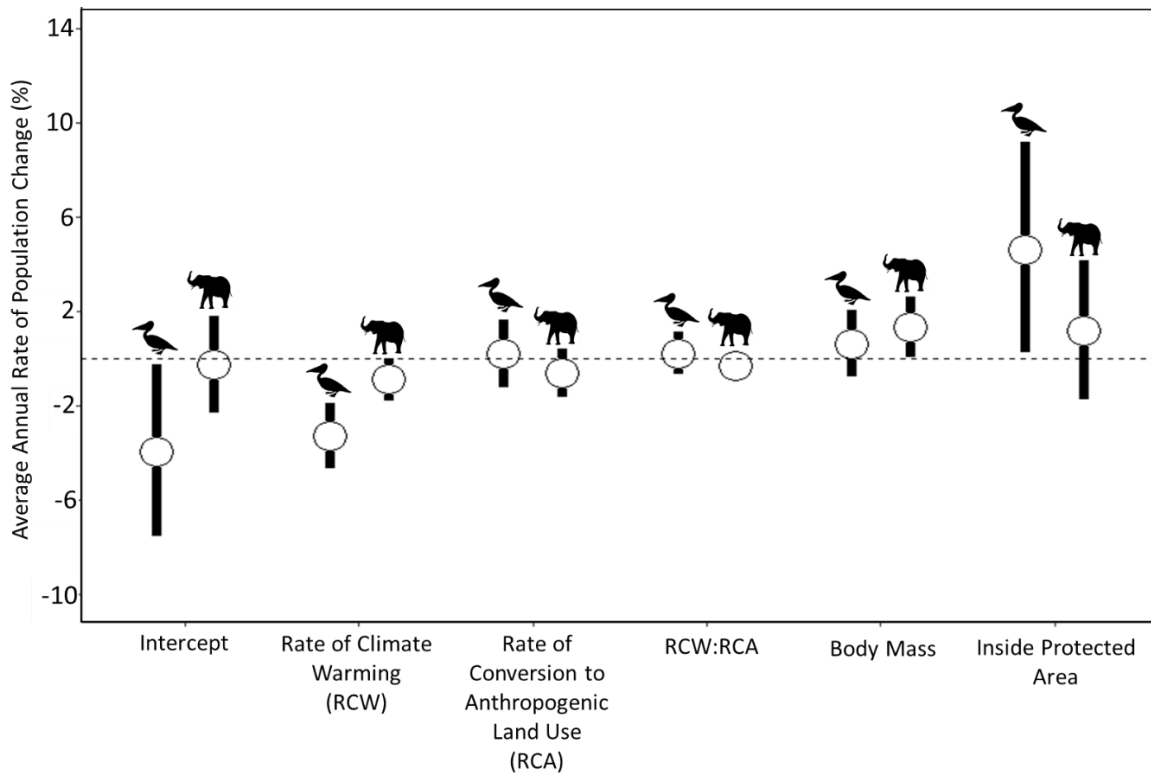


Figure S2.4 The distribution of the coefficients of the average models for both bird and mammal populations. The circles show the estimated coefficient values for each variable and the solid lines show the 2.5 - 97.5% confidence intervals. The intercept shows the distribution of the annual population growth rates in the absence of the effects of explanatory variables. The explanatory variables were scaled and centred, therefore the coefficients show the change in annual population growth rate given a one standard deviation increase in each explanatory variable. When the confidence intervals do not overlap with zero this shows a clear signal of either a positive or negative effect of a variable. Confidence intervals that overlap with zero show that within the averaged model an increase in a given variable has a mixture both positive and negative effect sizes on the rate of population change across different populations.

Results from bird population trends

<i>Model</i>	Δ AIC	Akaike Weight	Marg. R ²	Cond. R ²	Intercept	RCW	RCA	RCW:RCA	Body Mass	Inside Protected Area
<i>RCW+PA</i>	0.00	0.32	0.07	0.64	-4.47 (± 1.71)	-3.26 (± 0.72)				4.59 (± 2.19)
<i>RCW+BM+PA</i>	1.23	0.17	0.07	0.64	-4.74 (± 1.74)	-3.28 (± 0.72)			0.65 (± 0.73)	4.70 (± 2.20)
<i>RCA+RCW+PA</i>	1.95	0.12	0.07	0.64	-4.46 (± 1.71)	-3.27 (± 0.72)	0.21 (± 0.74)			4.58 (± 2.19)
<i>RCW</i>	2.23	0.11	0.04	0.63	-2.03 (± 1.18)	-3.40 (± 0.72)				
<i>RCA+RCW+BM+PA</i>	3.22	0.06	0.07	0.64	-4.74 (± 1.74)	-3.29 (± 0.72)	0.17 (± 0.74)		0.64 (± 0.73)	4.69 (± 2.20)
<i>RCW+BM</i>	3.61	0.05	0.04	0.64	-2.24 (± 1.21)	-3.43 (± 0.72)			0.59 (± 0.73)	
<i>RCA*RCW+PA</i>	3.76	0.05	0.07	0.64	-4.46 (± 1.71)	-3.20 (± 0.74)	0.22 (± 0.74)	0.21 (± 0.45)		4.55 (± 2.19)
<i>RCA+RCW</i>	4.15	0.04	0.04	0.63	-2.03 (± 1.18)	-3.42 (± 0.72)	0.24 (± 0.74)			
<i>RCA*RCW+BM+PA</i>	5.00	0.03	0.07	0.64	-4.74 (± 1.74)	-3.21 (± 0.74)	0.18 (± 0.74)	0.23 (± 0.45)	0.66 (± 0.73)	4.58 (± 2.21)
<i>RCA+RCW+BM</i>	5.56	0.02	0.04	0.64	-2.24 (± 1.21)	-3.44 (± 0.72)	0.20 (± 0.75)		0.57 (± 0.73)	
<i>RCA*RCW</i>	5.90	0.02	0.04	0.63	-2.05 (± 1.18)	-3.33 (± 0.74)	0.26 (± 0.74)	0.24 (± 0.45)		
<i>RCA*RCW+BM</i>	7.27	0.01	0.04	0.64	-2.26 (± 1.21)	-3.35 (± 0.74)	0.22 (± 0.75)	0.26 (± 0.45)	0.60 (± 0.73)	
<i>BM+PA</i>	19.72	<0.01	0.02	0.60	-4.36 (± 1.69)				0.55 (± 0.74)	5.49 (± 2.12)
<i>RCA+PA</i>	20.28	<0.01	0.02	0.59	-4.14 (± 1.66)		0.02 (± 0.71)			5.40 (± 2.11)
<i>RCA+BM+PA</i>	21.76	<0.01	0.07	0.64	-4.36 (± 1.69)		-0.01 (± 0.72)		0.55 (± 0.74)	5.40 (± 2.12)
<i>NULL</i>	22.48	<0.01	0.00	0.59	-1.23 (± 1.15)					
<i>BM</i>	24.09	<0.01	<0.01	0.60	-1.39 (± 1.18)				0.55 (± 0.74)	
<i>RCA</i>	24.50	<0.01	<0.01	0.59	-1.23 (± 1.15)		0.048 (± 0.73)			
<i>RCA+BM</i>	26.12	<0.01	<0.01	0.60	-1.39 (± 1.18)		0.018 (± 0.73)		0.48 (± 0.74)	
				RVI		1.00	0.35	0.10	0.35	0.76

Table S2.4 All competing models used to explain the growth rate of 883 bird populations. The models are ranked in order of performance based on AIC, with higher ranking models listed towards the top of each table. RCW = annual rate of climate warming, RCA = annual rate of conversion to anthropogenic land use, BM = body mass, PA = population inside a protected area. The coefficient values have been transformed into percentage population change. RVI (relative variable importance) is the sum of Akaike weights over all models including the explanatory variable.

Results from mammal population trends

<i>Model</i>	Δ AIC	Akaike Weight	Marg. R ²	Cond. R ²	Intercept	RCW	RCA	RCW:RCA	Body Mass	Inside Protected Area
<i>RCW+BM</i>	0.00	0.17	0.01	0.39	0.11 (±0.66)	-0.85 (±0.46)			1.32 (±0.63)	
<i>RCA+RCW+BM</i>	0.48	0.13	0.02	0.39	0.07 (±0.67)	-0.83 (±0.46)	-0.65 (±0.53)		1.43 (±0.64)	
<i>BM</i>	1.41	0.08	0.01	0.38	0.13 (±0.66)				1.32 (±0.63)	
<i>RCA*RCW+BM</i>	1.59	0.08	0.02	0.39	0.10 (±0.67)	-0.99 (±0.49)	-0.61 (±0.53)	-0.31 (±0.32)	1.41 (±0.64)	
<i>RCW+BM+PA</i>	1.64	0.07	0.02	0.39	-0.58 (±1.31)	-0.89 (±0.46)			1.15 (±0.68)	0.90 (±1.45)
<i>RCA+BM</i>	1.67	0.07	0.01	0.38	0.09 (±0.66)		-0.70 (±0.53)		1.44 (±0.63)	
<i>RCA+RCW+BM+PA</i>	2.10	0.06	0.02	0.39	-0.64 (±1.31)	-0.86 (±0.46)	-0.66 (±0.53)		1.26 (±0.69)	0.92 (±1.45)
<i>RCW</i>	2.23	0.05	<0.01	0.39	-0.19 (±0.66)	-0.86 (±0.46)				
<i>RCW+PA</i>	2.42	0.05	0.01	0.39	-1.50 (±1.19)	-0.93 (±0.46)				1.83 (±1.35)
<i>RCA*RCW+BM+PA</i>	3.22	0.03	0.02	0.39	-0.61 (±1.31)	-1.20 (±0.49)	-0.62 (±0.53)	-0.31 (±0.32)	1.25 (±0.69)	0.92 (±1.45)
<i>BM+PA</i>	3.29	0.03	0.01	0.38	-0.29 (±1.30)				1.22 (±0.68)	0.55 (±1.45)
<i>RCA+RCW</i>	3.36	0.03	0.01	0.40	-0.24 (±0.67)	-0.84 (±0.46)	-0.49 (±0.52)			
<i>RCA+RCW+PA</i>	3.89	0.03	<0.01	0.39	-1.62 (±1.20)	-0.91 (±0.46)	-0.53 (±0.52)			1.90 (±1.35)
<i>RCA+BM+PA</i>	3.54	0.03	0.01	0.38	-0.36 (±1.30)		-0.70 (±0.53)		1.33 (±0.68)	0.59 (±1.44)
<i>NULL</i>	3.69	0.03	0.00	0.39	-0.16 (±0.66)					
<i>RCA*RCW</i>	4.32	0.02	0.01	0.40	-0.21 (±0.67)	-1.01 (±0.49)	-0.45 (±0.52)	-0.34 (±0.33)		
<i>RCA*RCW+PA</i>	4.39	0.02	0.01	0.39	-1.58 (±1.20)	-1.08 (±0.49)	-0.50 (±0.52)	-0.33 (±0.32)		1.90 (±1.35)
<i>RCA</i>	4.69	0.02	<0.01	0.39	-0.22 (±0.66)		-0.53 (±0.52)			
<i>RCA+PA</i>	5.25	0.01	<0.04	0.39	-1.39 (±1.19)		-0.57 (±0.52)			1.63 (±1.34)
				RVI		0.73	0.52	0.14	0.74	0.33

Table S2.5 All competing models used to explain the growth rate of 966 mammal populations. The models are ranked in order of performance based on AIC, with higher ranking models listed towards the top of each table. RCW = annual rate of climate warming, RCA = annual rate of conversion to anthropogenic land use, BM = body mass, PA = population inside a protected area. The coefficient values have been transformed into percentage population change. RVI (relative variable importance) is the sum of Akaike weights over all models including the explanatory variable.

SPATIAL HETEROGENEITY IN THE DATA

The Living Planet database is a comprehensive resource of animal population trends. However, there is spatial bias in the dataset as the populations are not uniformly spatially distributed. Within dataset used in Chapter Two there are 122 (12.4%) populations at a site in the Atlantic Forest, Brazil. To test whether this site was having undue influence on the results I re-ran the analysis excluding these populations (Tables S2.3 and S2.4). I found there were minimal changes to the coefficients and overall results suggesting this site does not disproportionately influence the results.

Results from bird populations

Model	Δ AIC	Akaike Weight	Marg. R ²	Cond. R ²	Intercept	Rate of Climate Warming (RCW)	Rate of Conversion to Anthropogenic Land Use (RCA)	RCW:RCA	Body Mass	Inside Protected Area
RCW+PA	0.00	0.26	0.08	0.79	-6.04 (± 2.66)	-5.12 (± 1.17)				5.51 (± 3.53)
RCW	0.30	0.23	0.06	0.79	-3.33 (± 1.89)	-5.33 (± 1.17)				
RCW+BM+PA	2.06	0.10	0.08	0.79	-6.10 (± 2.72)	-5.12 (± 1.17)			0.13 (± 1.25)	5.53 (± 3.53)
RCA+RCW+PA	2.06	0.10	0.08	0.79	-6.05 (± 2.66)	-5.11 (± 1.18)	-0.09 (± 1.29)			5.52 (± 3.53)
RCW+BM	2.36	0.08	0.06	0.79	-3.35 (± 1.95)	-5.33 (± 1.17)			0.05 (± 1.25)	
RCA+RCW	2.36	0.08	0.06	0.79	-3.33 (± 1.89)	-5.33 (± 1.18)	0.01 (± 1.30)			
RCW*RCA+PA	4.11	0.03	0.08	0.79	-6.03 (± 2.66)	-5.16 (± 1.22)	-0.09 (± 1.29)		-0.12 (± 0.69)	5.50 (± 3.53)
RCA+RCW+BM+PA	4.13	0.03	0.08	0.79	-6.11 (± 2.72)	-5.12 (± 1.18)	-0.10 (± 1.29)		0.14 (± 1.25)	5.54 (± 3.54)
RCA*RCW	4.38	0.03	0.06	0.79	-3.32 (± 1.89)	-5.40 (± 1.22)	0.01 (± 1.30)	-0.15 (± 0.70)		
RCA+RCW+BM	4.43	0.03	0.06	0.79	-3.35 (± 1.95)	-5.33 (± 1.18)	0.00 (± 1.30)		0.05 (± 1.25)	
RCA*RCW+BM+PA	6.20	0.01	0.08	0.79	-6.09 (± 2.73)	-5.17 (± 1.22)	-0.10 (± 1.29)	-0.11 (± 0.69)	0.12 (± 1.25)	5.52 (± 3.54)
RCA*RCW+BM	6.46	0.01	0.06	0.79	-3.33 (± 1.95)	-5.40 (± 1.22)	0.00 (± 1.30)	-0.15 (± 0.70)	0.04 (± 1.25)	
RCA+PA	18.97	<0.01	0.02	0.76	-6.00 (± 2.65)		-0.72 (± 1.27)			7.33 (± 3.48)
Null Model	19.29	<0.01	0.00	0.77	-2.31 (± 1.89)					
BM+PA	19.29	<0.01	0.02	0.76	-5.91 (± 2.71)				-0.08 (± 1.28)	7.25 (± 3.49)
RCA+BM+PA	21.03	<0.01	0.02	0.76	-5.99 (± 2.71)		-0.71 (± 1.27)		-0.03 (± 1.28)	7.32 (± 3.48)
RCA	21.09	<0.01	0.08	0.77	-2.33 (± 1.89)		-0.63 (± 1.29)			
BM	21.32	<0.01	0.07	0.77	-2.25 (± 1.95)				-0.18 (± 1.29)	
RCA+BM	23.13	<0.01	<0.01	0.77	-2.29 (± 1.95)		-0.63 (± 1.29)		-0.15 (± 1.29)	
					RVI	1.00	0.33	0.09	0.26	0.54

Table S2.3 All competing models used to explain the growth rate of bird populations, excluding populations from a heavily surveyed site in the Atlantic Forest. The models are ranked in order of performance based on AIC, with higher ranking models listed towards the top of each table. Models within <2 Δ AIC of the highest ranked model are highlighted with bold text and a grey background. A null model is included for comparison. RCW = annual rate of climate warming, RCA = annual rate of conversion to anthropogenic land use, BM = body mass, PA = population inside a protected area. RVI (relative variable importance) is the sum of Akaike weights over all models including the explanatory variable. P values show the results of an ANOVA comparing each model to the null model, and therefore give the probability that for a given model it is purely chance that it explains more of the variation in population trends than the null model.

Results from mammal populations

Model	Δ AIC	Akaike Weight	Marg. R ²	Cond. R ²	Intercept	Rate of Climate Warming (RCW)	Rate of Conversion to Anthropogenic Land Use (RCA)	RCW:RCA	Body Mass	Inside Protected Area
RCA*RCW+BM	0.00	0.17	0.03	0.44	0.68 (± 0.95)	-2.20 (± 0.73)	-0.75 (± 0.82)	-1.83 (± 1.02)	1.24 (± 0.82)	
RCA*RCW	0.12	0.16	0.02	0.45	0.39 (± 0.95)	-2.23 (± 0.73)	-0.55 (± 0.81)	-1.88 (± 1.02)		
RCW	1.04	0.10	0.01	0.42	0.38 (± 0.93)	-1.72 (± 0.68)				
RCA+RCW+BM	1.18	0.09	0.02	0.42	0.57 (± 0.93)	-1.71 (± 0.68)	-1.18 (± 0.78)		1.28 (± 0.81)	
RCW+BM	1.40	0.08	0.02	0.42	0.64 (± 0.93)	-1.71 (± 0.68)			1.06 (± 0.80)	
RCA+RCW	1.49	0.06	0.02	0.43	0.27 (± 0.93)	-1.73 (± 0.68)	-0.97 (± 0.78)			
RCA*RCW+PA	1.96	0.06	0.02	0.45	-0.36 (± 1.92)	-2.24 (± 0.73)	-0.58 (± 0.82)	-1.86 (± 1.02)		0.96 (± 2.10)
RCA*RCW+BM+PA	2.06	0.04	0.03	0.44	0.82 (± 2.08)	-2.20 (± 0.73)	-0.74 (± 0.82)	-1.83 (± 1.02)	1.27 (± 0.88)	-0.16 (± 2.25)
RCW+PA	2.92	0.03	0.01	0.42	-0.27 (± 1.89)	-1.74 (± 0.69)				0.84 (± 2.09)
RCA+RCW+BM+PA	3.24	0.03	0.02	0.42	0.62 (± 2.07)	-1.71 (± 0.68)	-1.17 (± 0.79)		1.29 (± 0.87)	-0.07 (± 2.25)
RCA+RCW+PA	3.27	0.03	0.02	0.43	-0.59 (± 1.90)	-1.75 (± 0.69)	-1.01 (± 0.78)			1.10 (± 2.10)
RCW+BM+PA	3.45	0.03	0.02	0.42	0.80 (± 2.07)	-1.70 (± 0.69)			1.09 (± 0.89)	-0.19 (± 2.25)
Null Model	5.34	0.01	0.00	0.41	0.41 (± 0.92)					
RCA+PA	5.46	0.01	<0.01	0.41	0.60 (± 0.92)		-1.18 (± 0.79)		1.28 (± 0.80)	
RCA+BM	5.67	0.01	0.01	0.41	0.66 (± 0.92)				1.06 (± 0.80)	
RCA	5.85	0.01	<0.01	0.41	0.31 (± 0.92)		-0.96 (± 0.78)			
RCA+BM+PA	7.44	<0.01	0.01	0.41	1.07 (± 2.05)		-1.17 (± 0.79)		1.37 (± 0.86)	-0.57 (± 2.25)
BM+PA	7.61	<0.01	<0.01	0.41	1.23 (± 2.06)				1.16 (± 0.86)	-0.68 (± 2.26)
RCA+PA	7.78	<0.01	<0.01	0.41	-0.23 (± 1.90)		-0.98 (± 0.78)			0.70 (± 2.10)
					RVI	0.95	0.72	0.45	0.50	0.27

Table S2.4 All competing models used to explain the growth rate of mammal populations, excluding populations from a heavily surveyed site in the Atlantic Forest. The models are ranked in order of performance based on AIC, with higher ranking models listed towards the top of each table. Models within <2 Δ AIC of the highest ranked model are highlighted with bold text and a grey background. A null model is included for comparison. RCW = annual rate of climate warming, RCA = annual rate of conversion to anthropogenic land use, BM = body mass, PA = population inside a protected area. RVI (relative variable importance) is the sum of Akaike weights over all models including the explanatory variable. P values show the results of an ANOVA comparing each model to the null model, and therefore give the probability that for a given model it is purely chance that it explains more of the variation in population trends than the null model.

SPECIES TRAITS

There are many species traits which may influence species population trends, such as generation length and geographic range. The only species trait I considered in Chapter Two was body mass, because it is a correlate of many other species traits (Brook, Sodhi and Bradshaw, 2008; Hilbers *et al.*, 2016). Here I explore the effect of including diet into the models as a fixed effect. Diet has been found to be an important predictor of population density for bird species (Santini, Isaac, Maiorano, et al., 2018), with carnivorous birds typically being found at smaller densities. Carnivorous mammals have undergone large declines in both populations and ranges over the last two centuries (Ripple *et al.*, 2014) and species at higher trophic levels tend to have higher levels of extinction risk (Purvis *et al.*, 2000). Therefore, I hypothesise that populations of carnivorous species will have lower population growth rates than populations of other diet types.

I extracted diet data from the EltonTraits database (Wilman *et al.*, 2014) for both the bird and mammal populations. There were five diet categories for bird species: carnivores of invertebrates (40.4%), carnivores of vertebrates and carrion (23.4%), omnivores (17.2%) plant and seed eaters (15.0%) and frugivores/nectarivores (4.0%). I classified mammal species as either herbivores (84.8%), carnivores (7.7%) or omnivores (7.5%). I did not find any important effects of diet on either bird or mammal population trends, with the coefficients of each dietary group having large standard error values and all models performing worse (in terms of AIC) given the addition of diet as a variable (Tables 3.3 and 3.4). This suggests that, although diet seems to be an important predictor for bird species densities (Santini *et al.*, 2018), it does not have an important effect on population trends.

Results from bird populations

<i>Model</i>	Δ AIC	AIC ω_i	Marg. R^2	Cond. R^2	Intercept	RCW	RCA	RCW:RCA	BM	PA	Diet: Invert	Diet: Omni	Diet: Plant/Seed	Diet: Vert
RCW	0.00	0.24	0.06	0.79	-3.56 (± 1.95)	-5.61 (± 1.20)								
RCW+PA	0.04	0.24	0.08	0.79	-6.16 (± 2.76)	-5.38 (± 1.20)				5.31 (± 3.68)				
RCW+BM	2.05	0.09	0.06	0.79	-3.51 (± 2.02)	-5.61 (± 1.20)			-0.14 (± 1.28)					
RCA+RCW	2.06	0.09	0.06	0.79	-3.56 (± 1.95)	-5.62 (± 1.21)	0.00 (± 1.33)							
RCA+RCW+PA	2.11	0.08	0.08	0.79	-6.17 (± 2.76)	-5.37 (± 1.21)	-0.08 (± 1.32)			5.32 (± 3.69)				
RCW+BM+PA	2.11	0.08	0.08	0.79	-6.13 (± 2.82)	-5.38 (± 1.20)			-0.06 (± 1.28)	5.30 (± 3.69)				
RCA*RCW	4.02	0.03	0.06	0.79	-3.54 (± 1.96)	-5.73 (± 1.25)	-0.00 (± 1.33)	-0.24 (± 0.71)						
RCA*RCW+PA	4.11	0.03	0.08	0.79	-6.13 (± 2.76)	-5.46 (± 1.26)	-0.09 (± 1.32)	-0.20 (± 0.70)		5.28 (± 3.69)				
RCA+RCW+BM	4.12	0.03	0.06	0.79	-3.51 (± 2.02)	-5.61 (± 1.21)	0.01 (± 1.33)		-0.14 (± 1.28)					
RCA+RCW+BM+PA	4.19	0.03	0.08	0.79	-6.14 (± 2.82)	-5.37 (± 1.21)	-0.08 (± 1.32)		-0.06 (± 1.28)	5.31 (± 3.69)				
RCA*RCW+PA	6.08	0.01	0.06	0.79	-3.48 (± 2.02)	-5.72 (± 1.25)	0.01 (± 1.33)	-0.25 (± 0.71)	-0.17 (± 1.28)					
RCA*RCW+BM+PA	6.20	0.01	0.08	0.79	-6.09 (± 2.83)	-5.46 (± 1.26)	-0.08 (± 1.32)	-0.20 (± 0.70)	-0.08 (± 1.28)	5.26 (± 3.69)				
RCW+Diet	6.39	0.01	0.06	0.80	-7.43 (± 4.75)	-5.61 (± 1.20)					4.46 (± 4.36)	5.38 (± 4.80)	2.12 (± 5.11)	4.85 (± 5.03)
RCW+PA+Diet	6.44	0.01	0.09	0.80	-10.14 (± 5.22)	-5.38 (± 1.20)				5.38 (± 3.70)	4.56 (± 4.36)	5.64 (± 4.80)	2.45 (± 5.11)	5.11 (± 5.03)
RCW+BM+Diet	8.48	<0.01	<0.01	0.78	-7.50 (± 4.79)	-5.61 (± 1.20)			-0.20 (± 1.51)		4.51 (± 4.38)	5.51 (± 4.89)	2.36 (± 5.42)	5.12 (± 5.40)
RCA+RCW+Diet	8.50	<0.01	0.06	0.80	-7.42 (± 4.75)	-5.62 (± 1.21)	-0.03 (± 1.35)				4.46 (± 4.36)	5.38 (± 4.80)	2.12 (± 5.12)	4.84 (± 5.04)
RCA+RCW+PA+Diet	8.55	<0.01	0.09	0.80	-10.15 (± 5.23)	-5.37 (± 1.21)	-0.07 (± 1.34)			5.39 (± 3.70)	4.57 (± 4.37)	5.64 (± 4.81)	2.47 (± 5.13)	5.13 (± 5.05)
RCA*RCW+Diet	10.47	<0.01	0.06	0.80	-7.41 (± 4.75)	-5.74 (± 1.25)	-0.03 (± 1.35)	-0.27 (± 0.71)			4.50 (± 4.36)	5.40 (± 4.80)	2.11 (± 5.12)	4.85 (± 5.04)
RCA*RCW+PA+Diet	10.58	<0.01	0.09	0.80	-10.12 (± 5.23)	-5.47 (± 1.26)	-0.07 (± 1.34)	-0.22 (± 0.70)		5.33 (± 3.70)	4.59 (± 4.37)	5.65 (± 4.81)	2.46 (± 5.13)	5.14 (± 5.05)
RCA+RCW+BM+Diet	10.59	<0.01	0.06	0.80	-7.50 (± 4.80)	-5.61 (± 1.21)	0.03 (± 1.35)		-0.20 (± 1.51)		4.51 (± 4.38)	5.51 (± 1.95)	2.36 (± 1.95)	5.11 (± 5.42)
RCA*RCW+BM+Diet	12.57	<0.01	0.07	0.80	-7.50 (± 4.80)	-5.73 (± 1.25)	0.02 (± 1.35)	-0.27 (± 0.71)	-0.23 (± 1.51)		4.55 (± 4.38)	5.54 (± 4.89)	2.38 (± 5.43)	5.16 (± 5.42)
RCA+PA	19.88	<0.01	0.03	0.77	-6.39 (± 2.75)		-0.76 (± 1.30)			7.71 (± 3.63)				
BM+PA	20.19	<0.01	0.02	0.77	-6.22 (± 2.82)				-0.27 (± 1.32)	7.60 (± 3.63)				
Null Model	20.29	<0.01	0.00	0.78	-2.55 (± 1.97)									
RCA+BM+PA	21.92	<0.01	0.03	0.77	-6.30 (± 2.82)		-0.75 (± 1.30)		-0.22 (± 1.32)	7.67 (± 3.63)				
RCA	22.06	<0.01	<0.01	0.78	-2.58 (± 1.97)		-0.70 (± 1.33)							
BM	22.26	<0.01	0.06	0.80	-2.41 (± 2.03)				-0.39 (± 1.32)					
RCA+BM	24.05	<0.01	<0.01	0.78	-2.45 (± 2.03)		-0.67 (± 1.33)		-0.35 (± 1.32)					
RCA+PA+Diet	26.27	<0.01	0.03	0.78	-10.45 (± 5.40)		-0.77 (± 1.31)			7.79 (± 3.64)	4.38 (± 4.57)	5.91 (± 5.02)	2.48 (± 5.35)	5.44 (± 5.26)
RCA+Diet	28.47	<0.01	<0.01	0.78	-6.46 (± 4.94)		-0.69 (± 1.34)				4.21 (± 4.57)	5.55 (± 5.03)	1.95 (± 5.36)	5.04 (± 5.27)
BM+Diet	28.60	<0.01	<0.01	0.78	-6.55 (± 4.99)				-0.58 (± 1.57)		4.31 (± 4.58)	5.85 (± 5.12)	2.44 (± 5.68)	5.61 (± 5.66)
RCA+BM+Diet	30.43	<0.01	<0.01	0.78	-6.70 (± 4.99)		-0.69 (± 1.34)		-0.59 (± 1.56)		4.35 (± 4.58)	5.93 (± 5.12)	2.65 (± 5.69)	5.83 (± 5.67)

Table S2.5 All competing models used to explain the growth rate of bird populations. The models are ranked in order of performance based on AIC, with higher ranking models listed towards the top of each table. A null model is included for comparison. RCW = annual rate of climate warming, RCA = annual rate of conversion to anthropogenic land use, BM = body mass, PA = population inside a protected area. RVI (relative variable importance) is the sum of Akaike weights over all models including the explanatory variable.

Results from mammal populations

<i>Model</i>	Δ AIC	AIC ω_i	Marg. R ²	Cond. R ²	Intercept	RCW	RCA	RCW:RCA	BM	PA	Diet: Herb	Diet: Omni
<i>RCA*RCW</i>	0.00	0.14	0.02	0.48	0.57 (± 1.05)	-2.28 (± 0.77)	-0.44 (± 0.88)	-1.87 (± 1.04)				
<i>RCW</i>	0.29	0.12	0.01	0.45	0.58 (± 1.02)	-1.80 (± 0.73)						
<i>RCA*RCW+BM</i>	0.86	0.09	0.03	0.47	0.88 (± 1.06)	-2.25 (± 0.77)	-0.58 (± 0.88)	-1.81 (± 1.04)	1.04 (± 0.92)			
<i>RCA+RCW</i>	1.16	0.08	0.02	0.45	0.48 (± 1.02)	-1.81 (± 0.73)	-0.90 (± 0.84)					
<i>RCW+BM</i>	1.25	0.08	0.02	0.44	0.86 (± 1.04)	-1.79 (± 0.73)			0.96 (± 0.90)			
<i>RCA*RCW+PA</i>	1.69	0.06	0.02	0.48	-0.45 (± 2.00)	-2.30 (± 0.77)	-0.50 (± 0.88)	-1.84 (± 1.04)		1.34 (± 2.20)		
<i>RCA+RCW+BM</i>	1.79	0.06	0.02	0.44	0.80 (± 1.03)	-1.80 (± 0.73)	-1.04 (± 0.84)		1.11 (± 0.90)			
<i>RCW+PA</i>	2.00	0.05	0.01	0.45	-0.40 (± 1.97)	-1.83 (± 0.73)				1.28 (± 2.18)		
<i>RCA+RCW+PA</i>	2.73	0.04	0.02	0.45	-0.69 (± 1.99)	-1.85 (± 0.73)	-0.96 (± 0.84)			1.54 (± 2.19)		
<i>RCA*RCW+BM+PA</i>	2.87	0.03	0.03	0.47	0.43 (± 2.21)	-2.26 (± 0.77)	-0.59 (± 0.89)	-1.80 (± 1.04)	0.95 (± 0.99)	0.55 (± 2.36)		
<i>RCW+BM+PA</i>	3.26	0.03	0.02	0.44	0.45 (± 2.18)	-1.80 (± 0.73)			0.88 (± 0.97)	0.51 (± 2.35)		
<i>RCA*RCW+Diet</i>	3.45	0.03	0.02	0.48	-1.56 (± 2.99)	-2.31 (± 0.77)	-0.45 (± 0.88)	-1.93			2.31 (± 3.15)	3.10 (± 3.98)
<i>RCA+RCW+BM</i>	3.77	0.02	0.02	0.44	0.24 (± 2.18)	-1.82 (± 0.73)	-1.05 (± 0.85)		1.00 (± 0.97)	0.68 (± 2.36)		
<i>RCW+Diet</i>	3.94	0.02	0.01	0.45	-1.19 (± 2.93)	-1.82 (± 0.73)					1.95 (± 3.08)	2.33 (± 3.91)
<i>RCA*RCW+BM+Diet</i>	4.22	0.02	0.03	0.47	-0.56 (± 3.05)	-2.28 (± 0.77)	-0.57 (± 0.88)	-1.90 (± 1.05)	1.17 (± 1.00)		1.41 (± 3.18)	3.45 (± 3.94)
<i>Null Model</i>	4.40	0.02	0.00	0.43	0.59 (± 1.01)							
<i>RCA+RCW+Diet</i>	4.77	0.01	0.02	0.45	-1.42 (± 2.93)	-1.84 (± 0.73)	-0.93 (± 0.84)				2.12 (± 3.08)	2.36 (± 3.91)
<i>RCW+BM+Diet</i>	4.89	0.01	<0.01	0.43	-0.30 (± 3.00)	-1.80 (± 0.73)			1.06 (± 0.98)		1.14 (± 3.13)	2.67 (± 3.89)
<i>RCA*RCW+PA+Diet</i>	5.15	0.01	0.02	0.48	-2.51 (± 3.39)	-2.33 (± 0.77)	-0.50 (± 0.88)	-1.91 (± 1.05)		1.37 (± 2.22)	2.20 (± 3.14)	3.21 (± 3.97)
<i>BM</i>	5.28	0.01	0.02	0.44	0.88 (± 1.02)				0.98 (± 0.89)			
<i>RCA</i>	5.36	0.01	<0.01	0.43	0.50 (± 1.02)		-0.87 (± 0.84)					
<i>RCA+RCW+BM+Diet</i>	5.41	0.01	0.02	0.44	-0.42 (± 2.99)	-1.81 (± 0.73)	-1.04 (± 0.84)		1.21 (± 0.98)		1.20 (± 3.11)	2.75 (± 3.87)
<i>RCW+PA+Diet</i>	5.66	0.01	0.01	0.45	-2.09 (± 3.33)	-1.85 (± 0.73)				1.29 (± 2.20)	1.84 (± 3.08)	2.44 (± 3.91)
<i>RCA+BM</i>	5.88	0.01	0.01	0.42	0.82 (± 1.01)		-1.02 (± 0.85)		1.13 (± 0.89)			
<i>RCA+RCW+PA+Diet</i>	6.37	0.01	0.02	0.45	-2.49 (± 3.34)	-1.87 (± 0.73)	-0.98 (± 0.84)			1.53 (± 2.21)	2.00 (± 3.07)	2.50 (± 3.90)
<i>RCA+PA</i>	7.12	<0.01	<0.01	0.43	-0.39 (± 1.99)		-0.92 (± 0.85)			1.16 (± 2.20)		
<i>BM+PA</i>	7.33	<0.01	<0.01	0.43	0.84 (± 2.18)				0.97 (± 0.96)	0.05 (± 2.36)		
<i>RCA+BM+PA</i>	7.93	<0.01	0.01	0.42	0.65 (± 2.17)		-1.02 (± 0.85)		1.10 (± 0.96)	0.21 (± 2.36)		
<i>BM+Diet</i>	8.93	<0.01	<0.01	0.42	0.14 (± 2.97)				1.13 (± 0.97)		0.65 (± 3.10)	2.40 (± 3.87)
<i>RCA+Diet</i>	9.12	<0.01	<0.01	0.43	-1.01 (± 2.90)		-0.89 (± 0.84)				1.64 (± 3.05)	2.05 (± 3.88)
<i>RCA+BM+Diet</i>	9.53	<0.01	0.01	0.42	0.03 (± 2.94)		-1.03 (± 0.85)		1.28 (± 0.97)		0.70 (± 3.06)	2.47 (± 3.84)
<i>RCA+PA+Diet</i>	10.90	<0.01	<0.01	0.43	-1.83 (± 3.32)		-0.93 (± 0.85)			1.18 (± 2.22)	1.55 (± 3.04)	2.15 (± 3.88)

Table S2.6 All competing models used to explain the growth rate of mammal populations. The models are ranked in order of performance based on AIC, with higher ranking models listed towards the top of each table. A null model is included for comparison. RCW = annual rate of climate warming, RCA = annual rate of conversion to anthropogenic land use, BM = body mass, PA = population inside a protected area.

ALTERNATIVE LAND USE CHANGE DATA

In Chapter Two I did not find the rate of conversion to anthropogenic land use (RCA) to be an important predictor of either bird or mammal population trends. This was unexpected as habitat loss is a major threat to biodiversity. It is possible I did not find RCA to be important because I used the HYDE land use dataset which is both spatially and temporally coarse. I used the HYDE database as it provides the greatest temporal coverage of all freely available land use datasets. This was necessary as I required data from 1950, the first year in which trends from the Living Planet database are available. Here I explore the use of the ESA CCI data set (Bontemps *et al.*, 2013), which provides global land cover maps of 36 land cover classes, available annually from 1992-2015 at 300m spatial resolution. I repeat the analysis from Chapter Two but use the ESA CCI dataset to quantify the RCA. This allows me to explore whether RCA is an important predictor of bird and mammal population trends at a finer spatiotemporal scale.

The ESA CCI data covers a considerably shorter timespan than the HYDE data. Consequently, this truncates the population trends to 1992 onwards and limits analysis to population trends at least five years in length available from 1992 or after. There were 481 populations (birds = 278, mammals = 203) available for this analysis. I recalculated average rates of warming and population growth rates for each truncated population trend. There are 36 land cover classes in the ESA CCI dataset, I reclassified the classes into either anthropogenic or natural (Table 3.5). For each population I calculated the percentage of anthropogenic land cover in a 3 km buffer for each year 1992-2015. I used this to calculate a rate of change in anthropogenic land cover for each population.

<i>CCI Land Cover Category</i>	<i>Model Category</i>
<i>Cropland, rainfed</i>	Anthropogenic
<i>Urban areas</i>	Anthropogenic
<i>Cropland, irrigated or post-flooding</i>	Anthropogenic
<i>Mosaic cropland (>50%)/natural vegetation (tree, shrub, herbaceous cover) (<50%)</i>	Anthropogenic
<i>Mosaic natural vegetation (tree, shrub, herbaceous cover) (>50%)/ cropland (<50%)</i>	Natural
<i>Tree cover, broadleaved, evergreen, closed to open (>15%)</i>	Natural
<i>Tree cover, broadleaved, deciduous, closed (>40%)</i>	Natural
<i>Tree cover, broadleaved, deciduous, closed (>40%)</i>	Natural
<i>Tree cover, broadleaved, deciduous, open (15-40%)</i>	Natural
<i>Tree cover, needleleaved, evergreen, closed to open (>15%)</i>	Natural
<i>Tree cover, needleleaved, evergreen, closed (>40%)</i>	Natural
<i>Tree cover, needleleaved, evergreen, open (15-40%)</i>	Natural
<i>Tree cover, needleleaved, deciduous, closed to open (>15%)</i>	Natural
<i>Tree cover, needleleaved, deciduous, closed (>40%)</i>	Natural
<i>Tree cover, needleleaved, deciduous, open (15-40%)</i>	Natural
<i>Tree cover, mixed leaf type (broadleaved and needleleaved)</i>	Natural
<i>Mosaic tree and shrub (>50%)/herbaceous cover (<50%)</i>	Natural
<i>Mosaic herbaceous cover (>50%)/tree and shrub (<50%)</i>	Natural
<i>Shrubland</i>	Natural
<i>Evergreen shrubland</i>	Natural
<i>Deciduous shrubland</i>	Natural
<i>Grassland</i>	Natural
<i>Lichens and mosses</i>	Natural
<i>Sparse vegetation (tree, shrub, herbaceous cover) (<15%)</i>	Natural
<i>Sparse shrub (<15%)</i>	Natural
<i>Sparse herbaceous cover (<15%)</i>	Natural
<i>Tree cover, flooded, fresh or brackish water</i>	Natural
<i>Tree cover, flooded, saline water</i>	Natural
<i>Shrub or herbaceous cover, flooded, fresh/saline/brackish water</i>	Natural
<i>Bare areas</i>	Natural
<i>Consolidated bare areas</i>	Natural
<i>Unconsolidated bare areas</i>	Natural
<i>Water bodies</i>	Natural
<i>Permanent snow and ice</i>	Natural
<i>Herbaceous cover</i>	Natural
<i>Tree or shrub cover</i>	Natural

Table S2.7 Land cover categories in the ESA CCI database and the reclassification categories I assigned to calculate rate of conversion to anthropogenic land use for each population.

I used the same selection of models and model averaging method as in Chapter Two. When using ESA CCI to quantify RCA I found that RCA and protected area coverage are important predictors for bird population trends. This finding suggests that the impacts of land use change on population trends are more detectable at higher spatiotemporal resolutions. This result shows that within this selection of population trends bird population

declines are higher where RCA has been more rapid. I also found that bird populations inside protected areas have higher population growth rates than those outside (Figure 3.3). This suggests that protected areas are effective for conserving bird populations. However, it is difficult to state this with certainty as only 16.3% of the bird species in this study are found both inside and outside protected areas, therefore these two sets of populations are not directly comparable. Additionally, protected area coverage appears to be the most important variable in explaining the variation in the bird population trends as it is in each of the top performing models (Table 3.6) and each of these models have relatively high marginal R^2 values (>10%).

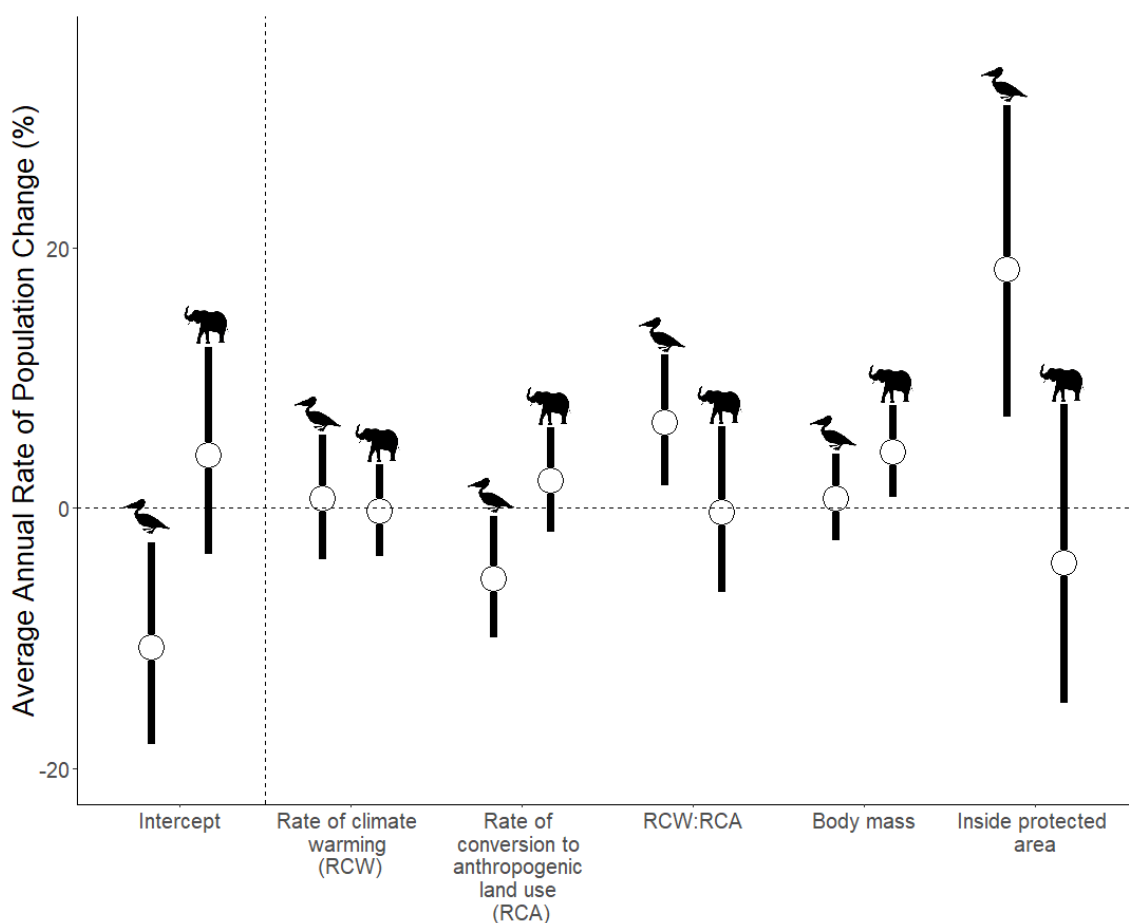


Figure S2.5 The distribution of the coefficients of the average models for both bird and mammal populations. The circles show the estimated coefficient values for each variable and the solid lines show the 2.5 - 97.5% confidence intervals. The intercept shows the distribution of the annual population growth rates in the absence of the effects of explanatory variables. The explanatory variables were scaled and centred, therefore the coefficients show the change in annual population growth rate given a one standard deviation increase in each explanatory variable. When the confidence intervals do not overlap with zero this shows a clear signal of either a positive or negative effect of a variable. Confidence intervals that overlap with zero show that within the averaged model an increase in a given variable has a mixture both positive and negative effect sizes on the rate of population change across different populations.

For mammal populations I found only body mass to be important for explaining population trends, with population growth rates tending to be higher for larger mammal species (Figure 3.3). Body mass features in each of the top performing models for mammal populations, but marginal R^2 values are relatively low ($\geq 3\%$) and few models outperform the null model. As in Chapter Two, the mammal population growth rates are more difficult to explain than the bird population growth rates, using the variables I have selected. I do not find RCW to be an important variable for predicting population growth rates in either bird or mammal populations (Figure S2.5). This is surprising as it was a key variable in explaining both bird and mammal population growth rates in Chapter Two. It is possible that it is no longer important because I use a considerably shorter time-period here, and that longer time-periods are required to detect the impacts of climate warming.

Results from bird populations

<i>Model</i>	Δ AIC	Akaike Weight	Marg. R ²	Cond. R ²	Intercept	RCW	RCA	RCW:RCA	Body Mass	Inside Protected Area
<i>RCA*RCW+PA</i>	0.00	0.17	0.17	0.82	-11.16 (\pm 4.22)	0.60 (\pm 1.97)	-4.83 (\pm 1.97)	4.51 (\pm 1.66)		18.24 (\pm 5.22)
<i>RCA*RCW+BM+PA</i>	0.48	0.13	0.17	0.82	-10.51 (\pm 4.46)	0.60 (\pm 1.97)	-4.91 (\pm 1.97)	4.55 (\pm 1.66)	-1.51 (\pm 3.00)	18.42 (\pm 5.24)
<i>RCA+PA</i>	1.43	0.08	0.12	0.81	-10.63 (\pm 4.30)		-3.14 (\pm 1.90)			18.22 (\pm 5.92)
<i>RCA+RCW+PA</i>	1.60	0.07	0.14	0.82	-11.19 (\pm 4.36)	2.70 (\pm 1.88)	-3.35 (\pm 1.92)			18.79 (\pm 5.40)
<i>RCW+PA</i>	1.64	0.07	0.11	0.82	-11.14 (\pm 4.37)	2.44 (\pm 1.89)				18.15 (\pm 5.41)
<i>RCA+BM+PA</i>	1.69	0.07	0.12	0.82	-10.18 (\pm 4.55)		-3.18 (\pm 1.91)		1.08 (\pm 3.05)	18.36 (\pm 5.34)
<i>RCA+RCW+BM+PA</i>	2.11	0.06	0.13	0.83	-10.69 (\pm 4.59)	2.72 (\pm 1.89)	-3.41 (\pm 1.93)		1.19 (\pm 3.02)	18.95 (\pm 5.43)
<i>BM+PA</i>	2.22	0.05	0.09	0.81	-10.30 (\pm 4.56)				0.74 (\pm 3.06)	17.74 (\pm 5.34)
<i>RCW+BM+PA</i>	2.42	0.05	0.11	0.82	-10.80 (\pm 4.60)	2.45 (\pm 1.89)			0.83 (\pm 3.04)	18.25 (\pm 5.43)
<i>RCA*RCW</i>	3.23	0.03	0.07	0.82	-1.35 (\pm 2.90)	0.48 (\pm 2.02)	-4.59 (\pm 2.02)	4.55 (\pm 1.70)		
<i>RCA*RCW+BM</i>	3.31	0.03	0.07	0.83	-0.76 (\pm 3.35)	0.48 (\pm 2.02)	-4.65 (\pm 2.03)	4.58 (\pm 1.70)	1.09 (\pm 3.09)	
<i>RCA</i>	3.36	0.03	0.02	0.82	-0.76 (\pm 2.94)		-2.88 (\pm 1.95)			
<i>Null Model</i>	3.39	0.03	0.00	0.81	-1.01 (\pm 2.94)					
<i>RCA+RCW</i>	3.56	0.03	0.03	0.83	-1.08 (\pm 2.98)	2.60 (\pm 1.93)	-3.10 (\pm 1.97)			
<i>RCW</i>	3.70	0.03	0.01	0.82	-1.32 (\pm 2.98)	2.35 (\pm 1.93)				
<i>RCA+BM</i>	4.32	0.02	0.02	0.82	-0.39 (\pm 3.41)		-2.91 (\pm 1.96)		0.67 (\pm 3.14)	
<i>BM</i>	4.40	0.02	<0.01	0.81	-0.80 (\pm 3.40)				0.38 (\pm 3.15)	
<i>RCA+RCW+BM</i>	4.70	0.02	0.03	0.83	-0.65 (\pm 3.43)	2.62 (\pm 1.93)	-3.13 (\pm 1.98)		0.79 (\pm 3.11)	
<i>RCW+BM</i>	5.27	0.01	0.01	0.82	-1.07 (\pm 3.42)	2.36 (\pm 1.93)			0.48 (\pm 3.13)	
				RVI		0.91	0.94	0.80	0.29	0.98

Table S3.7 All competing models used to explain the growth rate of bird populations. The models are ranked in order of performance based on AIC, with higher ranking models listed towards the top of each table. A null model is included for comparison. RCW = annual rate of climate warming, RCA = annual rate of conversion to anthropogenic land use, BM = body mass, PA = population inside a protected area. RVI (relative variable importance) is the sum of Akaike weights over all models including the explanatory variable.

Results from mammal populations

<i>Model</i>	Δ AIC	Akaike Weight	Marg. R ²	Cond. R ²	Intercept	RCW	RCA	RCW:RCA	Body Mass	Inside Protected Area
<i>BM</i>	0.00	0.26	0.03	0.58	-1.76 (± 2.96)				5.51 (± 2.26)	
<i>RCA+BM</i>	0.92	0.17	0.03	0.58	-2.58 (± 3.05)		5.71 (± 5.17)		5.91 (± 2.27)	
<i>BM+PA</i>	1.52	0.12	0.03	0.58	1.68 (5.45)				6.09 (± 2.36)	-4.57 (± 6.17)
<i>RCW+BM</i>	2.10	0.09	0.03	0.58	-1.78 (± 2.97)	-0.35 (± 2.41)			5.46 (± 2.27)	
<i>RCA+BM+PA</i>	2.52	0.07	0.04	0.58	0.67 (± 5.51)		5.57 (± 5.17)		6.46 (± 2.38)	-4.31 (± 6.14)
<i>RCA+RCW+BM</i>	3.05	0.06	0.03	0.58	-2.58 (± 3.05)	-0.22 (± 2.40)	5.69 (± 5.18)		5.89 (± 2.29)	
<i>Null Model</i>	3.24	0.05	0.00	0.61	2.49 (± 2.30)					
<i>RCW+BM+PA</i>	3.66	0.04	0.03	0.58	1.65 (± 5.49)	-0.16 (± 2.42)			6.06 (± 2.39)	-4.51 (± 6.21)
<i>RCA+RCW+BM+PA</i>	4.68	0.03	0.04	0.58	0.67 (± 5.54)	-0.03 (± 2.41)	5.56 (± 5.17)		6.45 (± 2.41)	-4.30 (± 6.18)
<i>RCA</i>	4.81	0.02	<0.01	0.61	2.09 (± 2.35)		3.85 (± 5.29)			
<i>RCA*RCW+BM</i>	5.18	0.02	0.03	0.58	-2.70 (± 3.10)	-0.20 (± 2.39)	5.09 (± 5.87)	-2.25 (± 11.40)	6.02 (± 2.37)	
<i>RCW</i>	5.18	0.02	<0.01	0.61	2.39 (± 2.31)	-0.95 (± 2.44)				
<i>RCA+RCW</i>	6.79	0.01	<0.01	0.61	2.01 (± 2.37)	-0.89 (± 2.44)	3.77 (± 5.29)			
<i>RCA*RCW+BM+PA</i>	6.86	0.01	0.04	0.58	0.54 (± 5.68)	-0.03 (± 2.41)	5.27 (± 5.87)	-1.15 (± 11.52)	6.51 (± 2.46)	-4.21 (± 6.25)
<i>RCA+PA</i>	6.92	0.01	<0.01	0.61	2.66 (± 5.64)		3.81 (± 5.31)			-0.68 (± 6.05)
<i>RCW+PA</i>	7.29	0.01	<0.01	0.61	3.04 (± 5.61)	-0.92 (± 2.45)				-0.79 (± 6.06)
<i>RCA*RCW</i>	8.79	<0.01	0.01	0.61	2.06 (± 2.36)	-0.89 (± 2.44)	4.92 (± 6.07)	4.24 (± 11.34)		
<i>RCA+PCW+PA</i>	8.93	<0.01	<0.01	0.61	2.42 (± 5.67)	-0.87 (± 2.44)	3.74 (± 5.31)			-0.50 (± 6.06)
<i>RCA*RCW+PA</i>	10.93	<0.01	0.01	0.61	2.89 (± 5.79)	-0.85 (± 2.44)	4.96 (± 6.07)	4.61 (± 11.61)		-1.00 (± 6.19)
				RVI		0.73	0.52	0.14	0.74	0.33

Table S3.8 All competing models used to explain the growth rate of mammal populations. The models are ranked in order of performance based on AIC, with higher ranking models listed towards the top of each table. A null model is included for comparison. RCW = annual rate of climate warming, RCA = annual rate of conversion to anthropogenic land use, BM = body mass, PA = population inside a protected area. RVI (relative variable importance) is the sum of Akaike weights over all models including the explanatory variable.

CHAPTER THREE APPENDIX

<i>Species</i>	Model	Mean AUC	Std Dev.
Alpine ibex (<i>Capra ibex</i>)	Bioclim	0.369	0.045
	GAM	0.922	0.023
	Random Forest	0.939	0.009
Blue wildebeest (<i>Connochaetes taurinus</i>)	Bioclim	0.586	0.004
	GAM	0.841	0.007
	Random Forest	0.869	0.026
Brown bear (<i>Ursus arctos</i>)	Bioclim	0.949	0.018
	GAM	0.984	0.011
	Random Forest	0.995	0.003
Common warthog (<i>Phacochoerus africanus</i>)	Bioclim	0.710	0.009
	GAM	0.805	0.004
	Random Forest	0.815	0.004
Giraffe (<i>Giraffa Camelopardalis</i>)	Bioclim	0.766	0.026
	GAM	0.945	0.004
	Random Forest	0.949	0.007
Hartebeest (<i>Alcelaphus buselaphus</i>)	Bioclim	0.674	0.016
	GAM	0.838	0.003
	Random Forest	0.875	0.010
Plain's zebra (<i>Equus burchellii</i>)	Bioclim	0.655	0.012
	GAM	0.849	0.007
	Random Forest	0.874	0.007
Polar bear (<i>Ursus maritimus</i>)	Bioclim	0.949	0.018
	GAM	0.984	0.011
	Random Forest	0.995	0.003
Pyrenean chamois (<i>Rupicapra pyrenaica</i>)	Bioclim	0.970	0.002
	GAM	0.984	0.001
	Random Forest	0.984	0.001
Red deer (<i>Cervus elaphus</i>)	Bioclim	0.610	0.007
	GAM	0.880	0.006
	Random Forest	0.940	0.004
Reindeer (<i>Rangifer tarandus</i>)	Bioclim	0.658	0.012
	GAM	0.911	0.008
	Random Forest	0.947	0.006
Roe deer (<i>Capreolus capreolus</i>)	Bioclim	0.547	0.008
	GAM	0.749	0.001
	Random Forest	0.842	0.002
Snowshoe hare (<i>Lepus americanus</i>)	Bioclim	0.791	0.019
	GAM	0.872	0.013
	Random Forest	0.930	0.008
Waterbuck (<i>Kobus ellipsiprymnus</i>)	Bioclim	0.632	0.027
	GAM	0.776	0.009
	Random Forest	0.784	0.007
White-tailed deer (<i>Odocoileus virginianus</i>)	Bioclim	0.670	0.011
	GAM	0.880	0.004
	Random Forest	0.930	0.001
Wolverine (<i>Gulo gulo</i>)	Bioclim	0.786	0.164
	GAM	0.858	0.133
	Random Forest	0.886	0.114

Table S3.1 AUC scores for the three types of habitat suitability model built for each species. For each species the three models were combined into a weighted ensemble model based on the AUC scores.

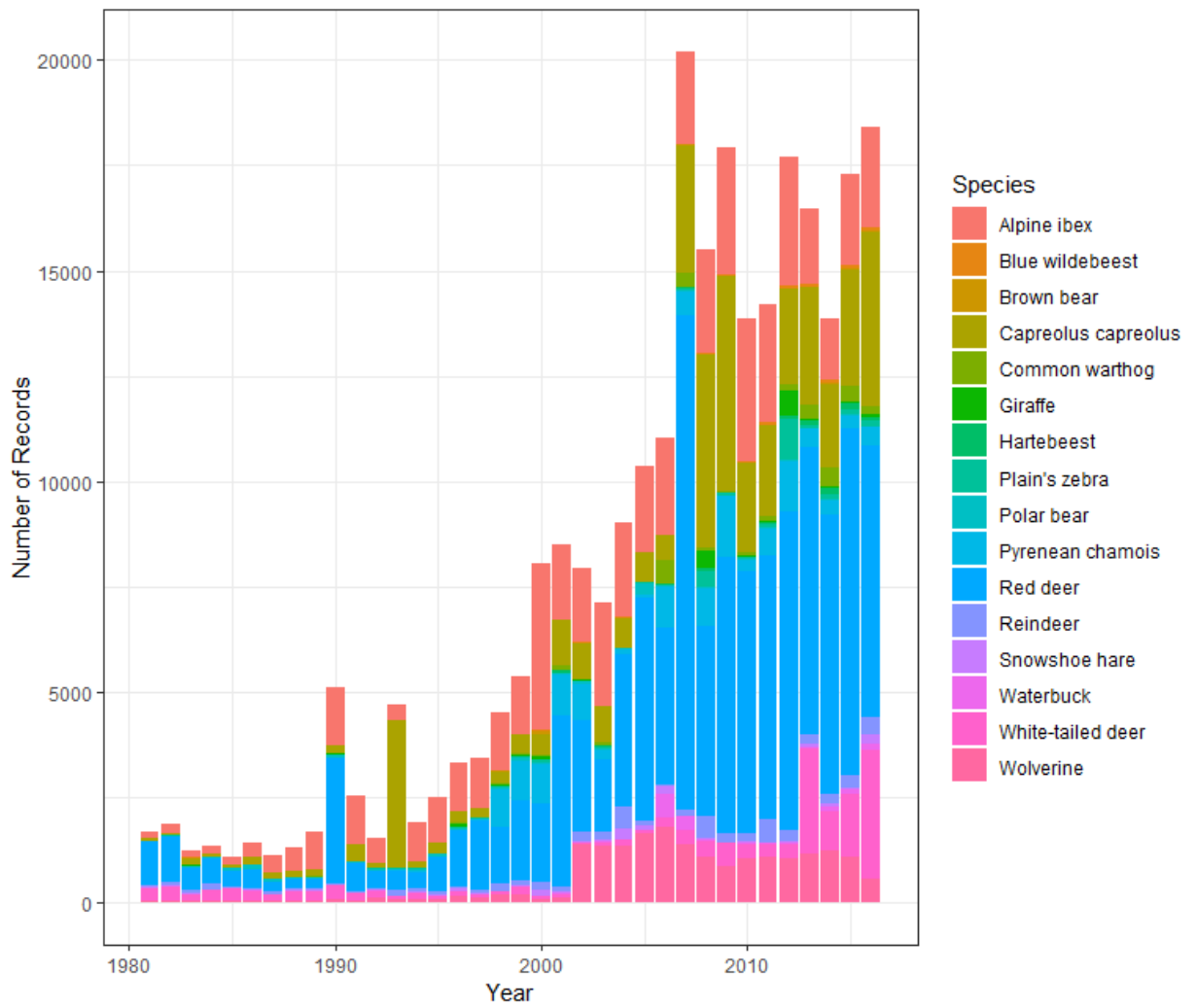


Figure S3.1 The number of occurrence records available (1980-2016) on GBIF for each species. I used data from 2006-2016 as most (61.6%) of the occurrence data is record from 2006 onwards and 2016 was the last complete year when the study began.

<i>Modelled Species</i>	Target Background Species	Distribution Intersection with Modelled Species (%)
Alpine ibex (<i>Capra ibex</i>)	Chamois (<i>Rupicapra rupicapra</i>)	88.8
	Red deer (<i>Cervus elaphus</i>)	88.9
	Alpine marmot (<i>Marmota marmota</i>)	99.9
	Mountain hare (<i>Lepus timidus</i>)	95.9
	Stoat (<i>Mustela erminea</i>)	96.4
	Rock ptarmigan (<i>Lagopus mutus</i>)	86.3
	Rock partridge (<i>Alectoris graeca</i>)	79.3
Blue wildebeest (<i>Connochaetes taurinus</i>)	African pipit (<i>Anthus cinnamomeus</i>)	99.4
	African fish eagle (<i>Haliaeetus vocifer</i>)	100
	Lilac-breasted roller (<i>Coracias caudatus</i>)	99.9
Brown bear (<i>Ursus arctos</i>)	American black bear (<i>Ursus americanus</i>)	64.2
	Coyote (<i>Canis latrans</i>)	81.6
	Stoat (<i>Mustela erminea</i>)	99.3
	Canada lynx (<i>Lynx canadensis</i>)	73.15
	Snowshoe hare (<i>Lepus americanus</i>)	64.9
	American beaver (<i>Castor canadensis</i>)	65.4
Common warthog (<i>Phacochoerus africanus</i>)	Serval (<i>Leptailurus serval</i>)	89.2
	African fish eagle (<i>Haliaeetus vocifer</i>)	96.6
	Hartebeest (<i>Alcelaphus buselaphus</i>)	55.2
Giraffe (<i>Giraffa camelopardalis</i>)	Serval (<i>Leptailurus serval</i>)	81.9
	Common warthog (<i>Phacochoerus africanus</i>)	69.3
	Cape buffalo (<i>Syncerus caffer</i>)	63.5
	African fish eagle (<i>Haliaeetus vocifer</i>)	84.2
	Hartebeest (<i>Alcelaphus buselaphus</i>)	59.2
Hartebeest (<i>Alcelaphus buselaphus</i>)	Serval (<i>Leptailurus serval</i>)	84.6
	Common warthog (<i>Phacochoerus africanus</i>)	80.0
	Cape buffalo (<i>Syncerus caffer</i>)	63.4
	African fish eagle (<i>Haliaeetus vocifer</i>)	98.4
Plain's zebra (<i>Equus burchellii</i>)	Serval (<i>Leptailurus serval</i>)	92.0
	Common warthog (<i>Phacochoerus africanus</i>)	71.3
	African fish eagle (<i>Haliaeetus vocifer</i>)	90.9
	Waterbuck (<i>Kobus ellipsiptymnus</i>)	71.5
Polar bear (<i>Ursus maritimus</i>)	Arctic fox (<i>Vulpes lagopus</i>)	92.9
	Reindeer (<i>Rangifer tarandus</i>)	78.0
	Wolverine (<i>Gulo gulo</i>)	66.4
	Snowy owl (<i>Bubo scandiacus</i>)	89.8
Pyrenean chamois (<i>Rupicapra pyrenaica</i>)	Common blackbird (<i>Turdus merula</i>)	100
	Common starling (<i>Sturnus vulgaris</i>)	99.2
Red deer (<i>Cervus elaphus</i>)	European badger (<i>Meles meles</i>)	99.5
	Common starling (<i>Sturnus vulgaris</i>)	65.7
Reindeer - Europe (<i>Rangifer tarandus</i>)	Brown bear (<i>Ursus arctos</i>)	89.9
	Eurasian lynx (<i>Lynx lynx</i>)	85.8
	Wolverine (<i>Gulo gulo</i>)	98.4
	Sable (<i>Martes zibellina</i>)	74.0
	Peregrine Falcon (<i>Falco peregrinus</i>)	98.6
Reindeer - North America (<i>Rangifer tarandus</i>)	American black bear (<i>Ursus americanus</i>)	62.0
	Coyote (<i>Canis latrans</i>)	55.1
	Stoat (<i>Mustela erminea</i>)	83.3
	Canada lynx (<i>Lynx canadensis</i>)	68.3
	Snowshoe hare (<i>Lepus americanus</i>)	61.0

	American beaver (<i>Castor canadensis</i>)	59.8	
Roe deer (<i>Capreolus capreolus</i>)	Common blackbird (<i>Turdus merula</i>)	95.8	
	Common starling (<i>Sturnus vulgaris</i>)	99.1	
	American black bear (<i>Ursus americanus</i>)	95.5	
Snowshoe hare (<i>Lepus americanus</i>)	Red fox (<i>Vulpes vulpes</i>)	97.8	
	Coyote (<i>Canis latrans</i>)	84.1	
	Grey wolf (<i>Canis lupus</i>)	79.6	
	Stoat (<i>Mustela erminea</i>)	94.8	
	Canada lynx (<i>Lynx canadensis</i>)	79.5	
	Brown bear (<i>Ursus arctos</i>)	64.9	
	American beaver (<i>Castor canadensis</i>)	95.9	
	Black-capped chickadee (<i>Poecile atricapillus</i>)	67.9	
	Waterbuck (<i>Kobus ellipsiprymnus</i>)	Hartebeest (<i>Alcelaphus buselaphus</i>)	57.4
		Cape buffalo (<i>Syncerus caffer</i>)	58.5
African fish eagle (<i>Haliaeetus vocifer</i>)		95.4	
Serval (<i>Leptailurus serval</i>)		55.4	
Common warthog (<i>Phacochoerus africanus</i>)		76.8	
White-tailed deer (<i>Odocoileus virginianus</i>)	Red-eyed vireo (<i>Vireo olivaceus</i>)	82.0	
	Cattle egret (<i>Bubulcus ibis</i>)	80.2	
Wolverine - Europe (<i>Gulo gulo</i>)	Sable (<i>Martes zibellina</i>)	60.0	
	Peregrine Falcon (<i>Falco peregrinus</i>)	91.3	
Wolverine - North America (<i>Gulo gulo</i>)	American black bear (<i>Ursus americanus</i>)	64.4	
	Coyote (<i>Canis latrans</i>)	81.6	
	Stoat (<i>Mustela erminea</i>)	99.3	
	Canada lynx (<i>Lynx canadensis</i>)	73.1	
	Brown bear (<i>Ursus arctos</i>)	100	
	American beaver (<i>Castor canadensis</i>)	65.4	

Table S3.2 For each species habitat suitability model I identified mammal and bird species with similar ranges to the modelled species and used their occurrence data as target-background points. I only used species occurrence data as target-background points if their range covered at least 50% of the modelled species range.

CHAPTER FOUR APPENDIX

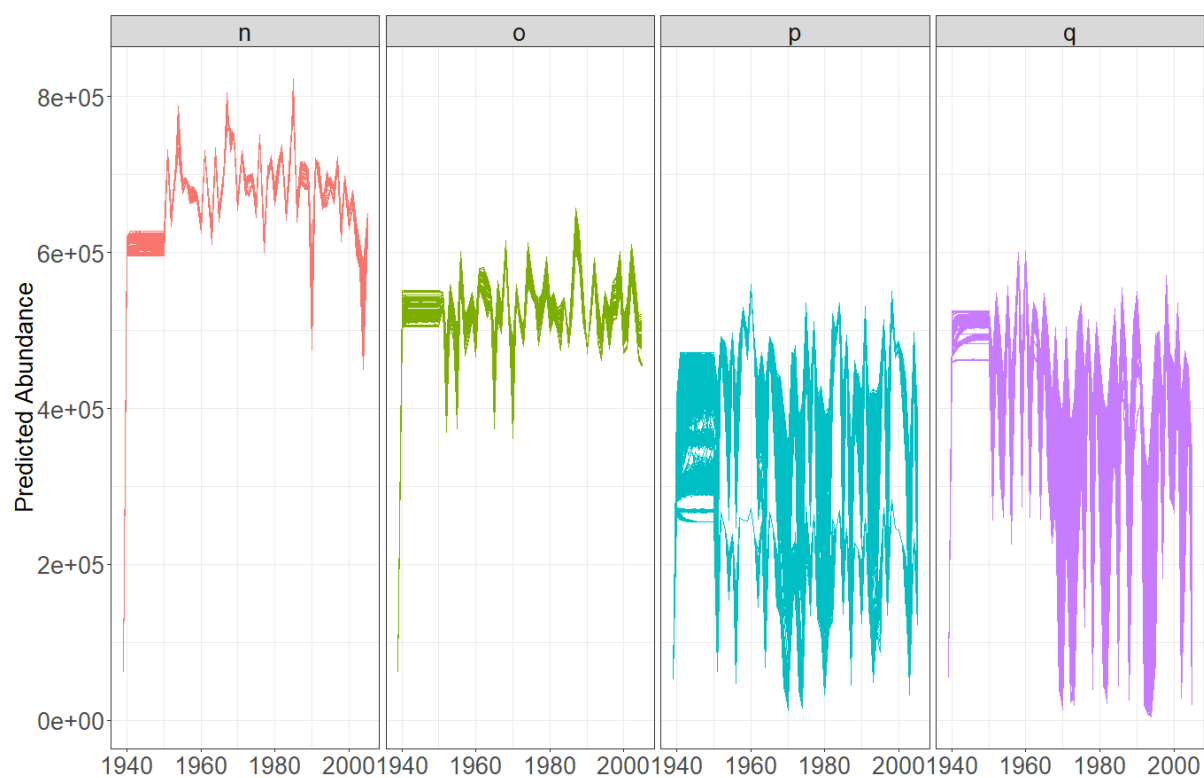


Figure S4.1 Each panel shows all the predicted abundance trends for a red deer population over the years 1939-2005. The burn-in period was from 1939-1949, the predicted abundance quickly stabilises after the first few years. The annually changing habitat suitability maps are initiated in 1950.

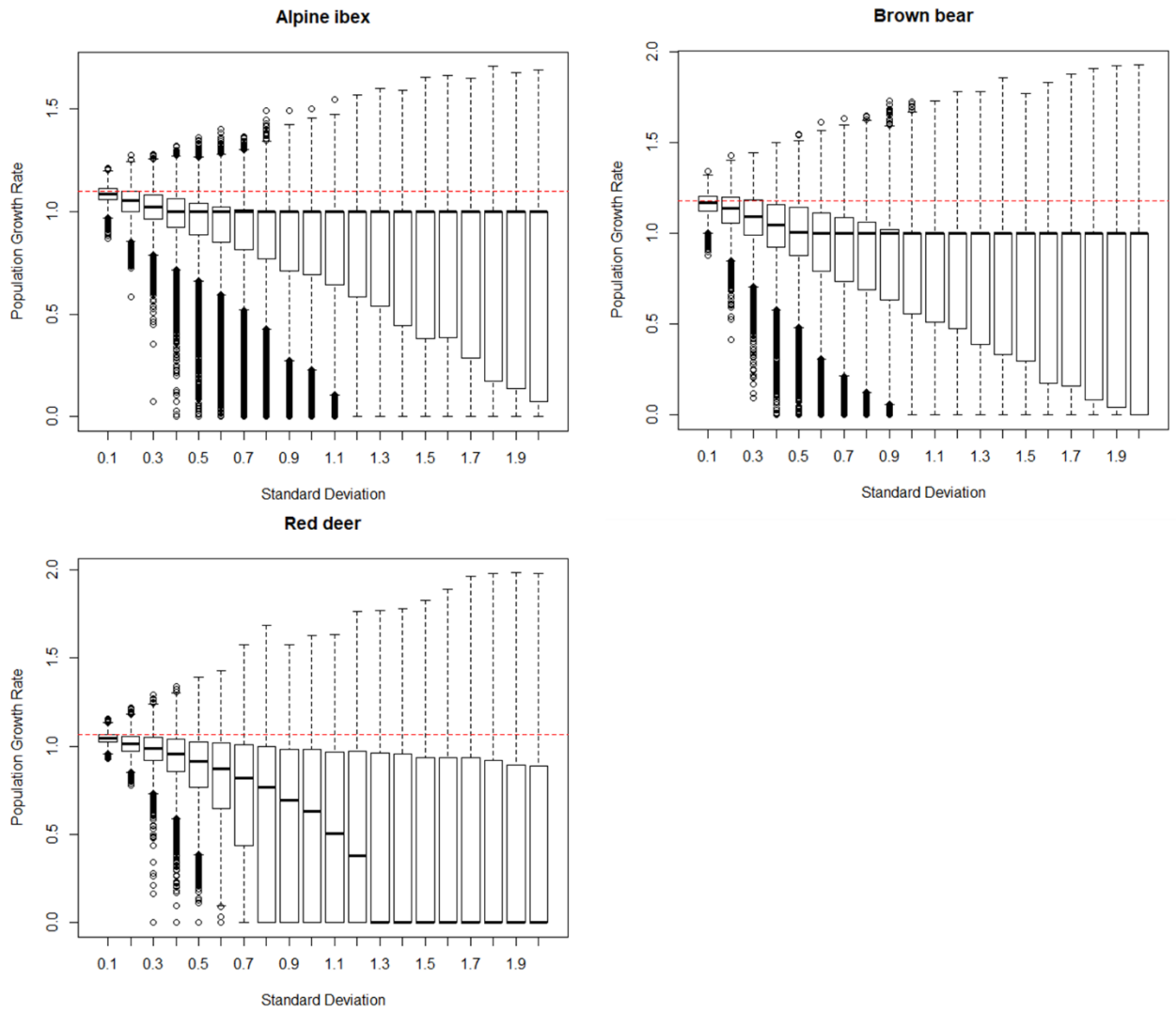


Figure S4.2 The distribution of population growth rates over a range of increasing levels of stochasticity, for each species. For each species a transition matrix was gathered from COMADRE. For each species I sampled from a normal distribution with the mean as the transition matrix and the standard deviation as a value between 0.1 and 2, at 0.1 intervals. For each interval I sampled the normal distribution 10,000 times and calculated the population growth rate for the resulting transition matrix.

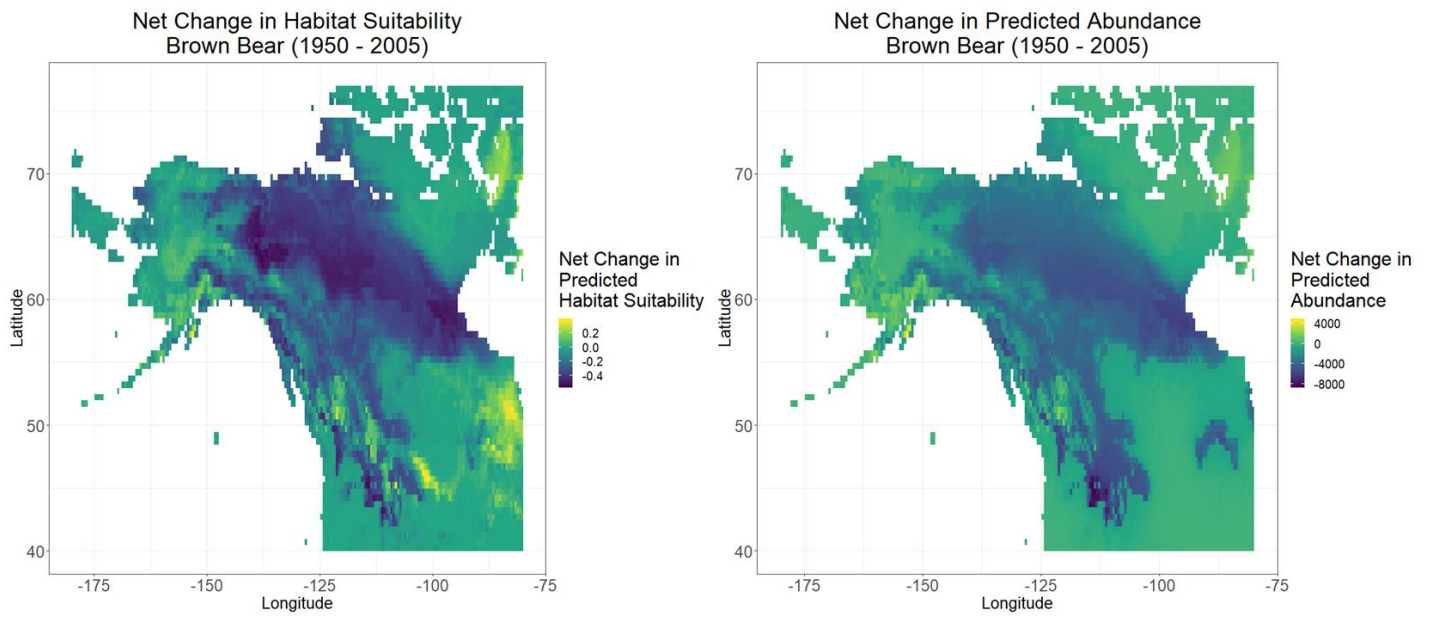
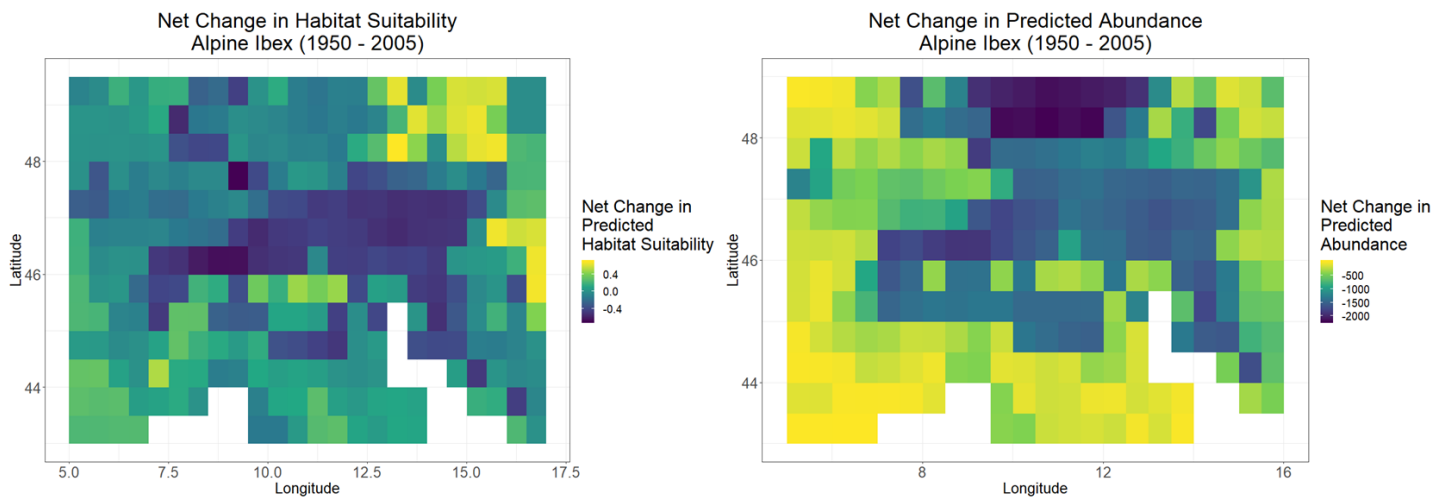


Figure S4.3 Maps of the net change in predicted habitat suitability and average net change in predicted abundance for brown bear between 1950-2005.



FigureS 4.4 Maps of the net change in predicted habitat suitability and average net change in predicted abundance for Alpine ibex between 1950-2005.

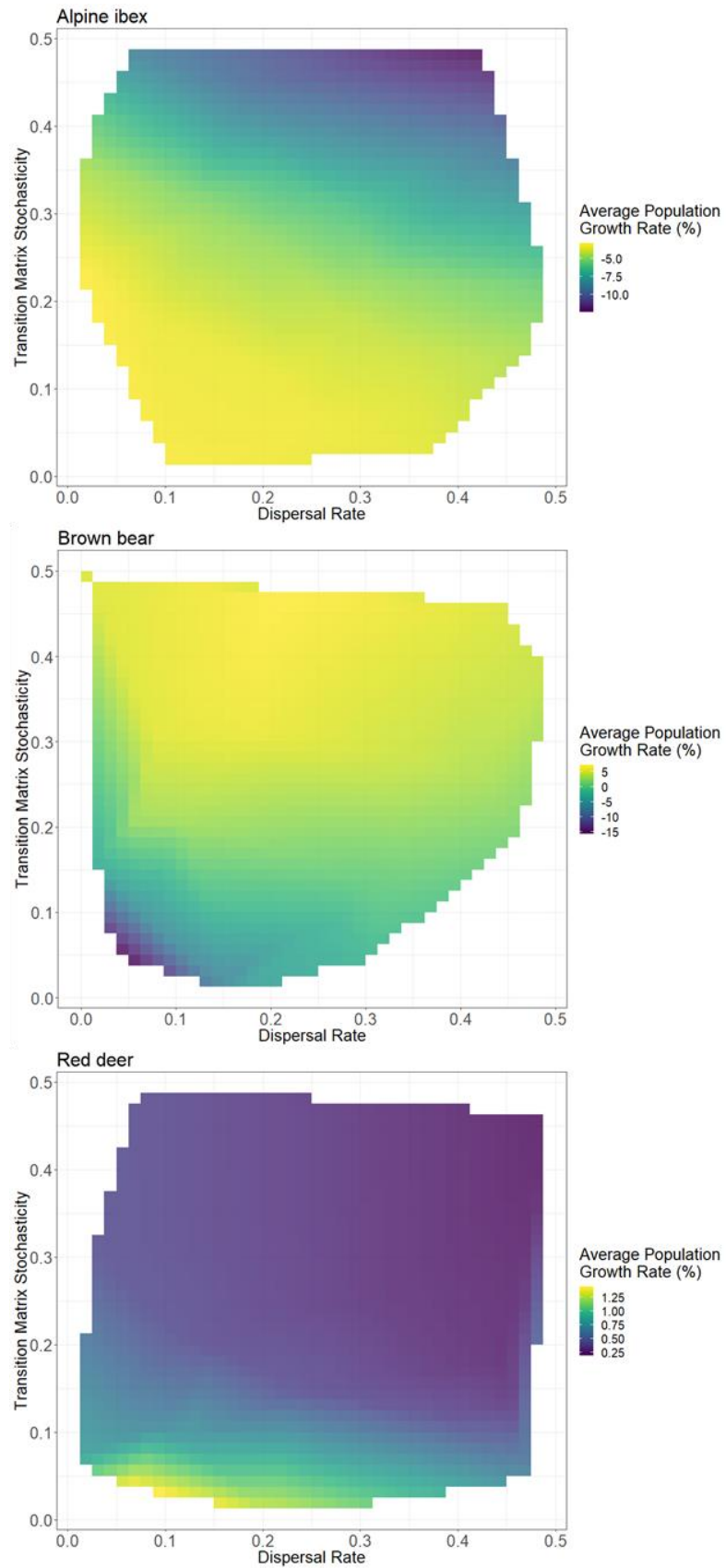


Figure S4.5 The variation in the average population growth rate for each species across the sample space for the dispersal rate and transition matrix stochasticity parameters. Each panel shows a different species, with a corresponding legend.

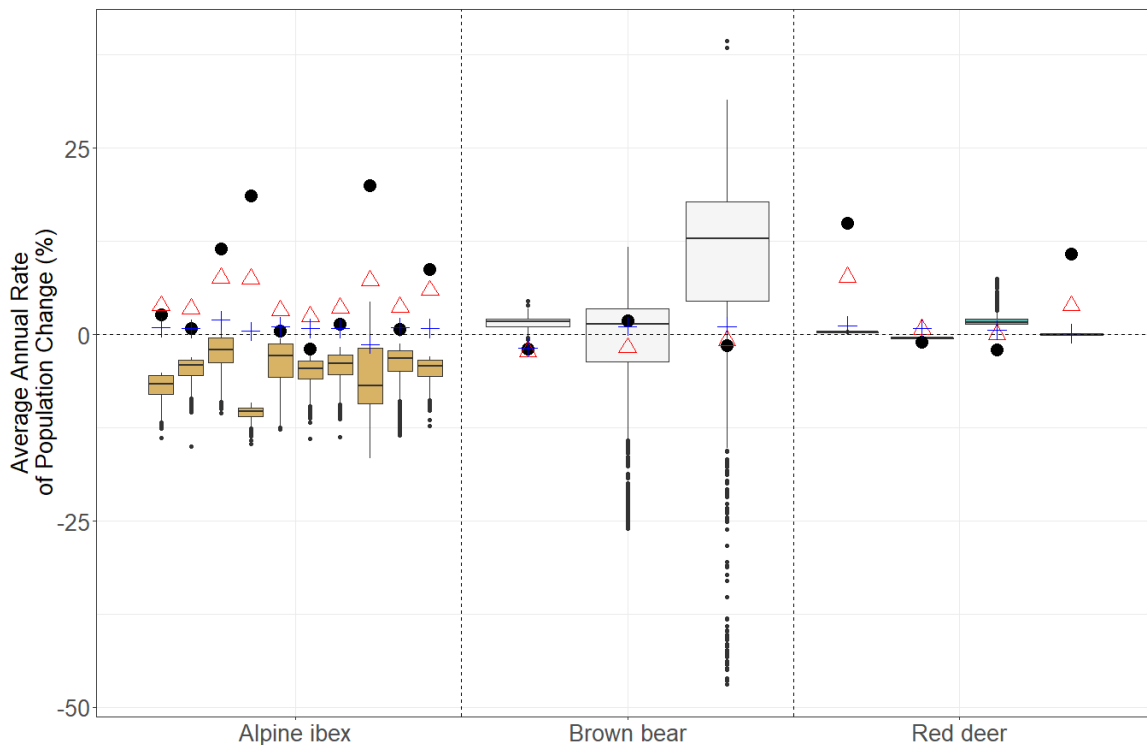


Figure S4.6 Each boxplot shows the distribution of the predicted average annual rate of change for each population. The red triangles show the fitted values for the top performing model for mammals from Chapter Two, with both the fixed and random effects. The blue crosses show the fitted values for the same model using predictions made with only fixed effects. The explanatory variables of this model are: rate of conversion to anthropogenic land use (RCA); rate of climate warming (RCW); the interaction between RCA and RCW; and species body mass. The black dots show the observed average annual rate of population change for each population. Values below zero indicate population decline and values above zero indicate growing populations. The letters a-q are for the identification of individual populations.

R CODE USED FOR COUPLED NICHE-DEMOGRAPHIC MODELS

FUNCTION TO CREATE THE DISPERSAL KERNEL

```
demoniche_create_csv<-function (Populations, Nichemap = "oneperiod",dispersal_constants
= c(50, 100))
{
  require(LaplacesDemon)
  require(sp)
  if (exists("BEMDEM"))
    rm(BEMDEM, inherits = TRUE)
  if (is.vector(Populations))
    print("There must be at least two populations!")
  if (is.vector(Nichemap) | (Nichemap == "oneperiod")[1]) {
    min_dist <- sort(unique(dist(Populations[, 2:3])))[1]
    extent <- expand.grid(X = seq(min(Populations[, "X"]),
                                max(Populations[, "X"]), by = min_dist), Y = seq(min(
Populations[, "Y"]), max(Populations[, "Y"]), by = min_dist))

    Nichemap <- cbind(HScoreID = 1:nrow(extent), extent,
                     matrix(1, ncol = length(Nichemap), nrow = nrow(extent),
```

```

dimnames = list(NULL, paste(Nichemap)))
}
if (is.vector(Nichemap[, -c(1:3)])) {
  Nichemap <- Nichemap[Nichemap[, -c(1:3)] != 0, ]
} else {
  Nichemap <- Nichemap[rowSums(Nichemap[, -c(1:3)]) != 0, ]
}
years_projections <- colnames(Nichemap)[4:ncol(Nichemap)]
if ((ncol(Nichemap) - 3) != length(years_projections))
  print("Number of years of projections is not equal to the number of habitat scores!")
")
colnames(Populations) <- c("PatchID", "XCOORD", "YCOORD",
                          "area_population")
colnames(Nichemap) <- c("HScoreID", "XCOORD", "YCOORD", years_projections)
if (max(Nichemap[, 4:ncol(Nichemap)]) > 100) {
  Nichemap[, 4:ncol(Nichemap)] <- Nichemap[, 4:ncol(Nichemap)]/1000
}
if (max(Nichemap[, 4:ncol(Nichemap)]) > 10) {
  Nichemap[, 4:ncol(Nichemap)] <- Nichemap[, 4:ncol(Nichemap)]/100
}
Niche_ID <- data.frame(matrix(0, nrow = nrow(Nichemap), ncol = 4))
Niche_ID[, 1:3] <- Nichemap[, 1:3]
colnames(Niche_ID) <- c("Niche_ID", "X", "Y", "PopulationID")
rownames(Niche_ID) <- Nichemap[, 1]
destination_Nicherows <- 1:nrow(Populations)
for (pxs in 1:nrow(Populations)) {
  rows <- which(spDistsN1(as.matrix(Nichemap[, 2:3], ncol = 2),
                        matrix(as.numeric(Populations[pxs, 2:3]), ncol = 2),
                        longlat = TRUE) == min(spDistsN1(as.matrix(Nichemap[, 2:3],
                        ncol = 2), matrix(as.numeric(Populations[pxs, 2:3]), ncol =
                        2), longlat = TRUE)))
  Niche_ID[rows, 4] <- Populations[pxs, 1]
  destination_Nicherows[pxs] <- rows[1]
}
Niche_values <- as.matrix(Nichemap[, 4:(length(years_projections) + 3)], ncol = length
h(years_projections))
dist_populations <- spDists(as.matrix(Niche_ID[, 2:3]), longlat = TRUE)
dimnames(dist_populations) <- list(Niche_ID[, 1], Niche_ID[,1])
disp_prob<-function(x){
  data4<-dist_populations[x,]
  dispersal_probabilities_row<-dhalfcauchy(data4, scale=dispersal_constants[1], log
=FALSE)
  dispersal_probabilities_row[data4 > dispersal_constants[2]]<-0
  return(dispersal_probabilities_row)
}

disp_prob_out<-lapply(1:nrow(dist_populations), disp_prob)
disp_prob_out_m<-do.call("rbind", disp_prob_out)
diag(disp_prob_out_m)<-0
sea<-which(Nichemap[,4] == - 1)
disp_prob_out_m[,sea]<-0

scale_1dd<-function(x){
  dispersal_probs<-disp_prob_out_m[x, ]/sum(disp_prob_out_m[x, ])
  return(dispersal_probs)
}

rep_scale_1dd<-lapply(1:nrow(disp_prob_out_m), scale_1dd)
dispersal_probabilities<-do.call(rbind,rep_scale_1dd)

write.table(dispersal_probabilities, "disp_probs_hc_max.csv", row.names = FALSE,
col.names = FALSE)
}

```

FUNCTION TO SETUP THE COUPLED NICHE-DEMOGRAPHIC MODEL

```

demoniche_setup_csv<-function (modelname, Populations, stages, Nichemap = "oneperiod",
                                matrices, matrices_var = FALSE,
                                prob_scenario = c(0.5, 0.5), proportion_initial,
                                density_individuals, transition_affected_niche = FALSE,
                                transition_affected_env = FALSE,
                                transition_affected_demogr = FALSE,
                                env_stochas_type = "normal", noise = 1,
                                fraction_SDD = FALSE,
                                fraction_LDD = FALSE, dispersal_constants = c(50, 100),
                                no_yrs, Ktype = "ceiling", K = NULL, Kweight = FALSE,
                                sumweight = FALSE, spin_years = spin_years,
                                dispersal_probabilities)
{
  require(sp)
  if (exists("BEMDEM"))
    rm(BEMDEM, inherits = TRUE)
  if (is.vector(matrices)) {
    matrices <- matrix(matrices, ncol = 2, nrow = length(matrices))
    print("You are carrying out deterministic modelling.")
    colnames(matrices) <- c("matrixA", "matrixA")
  }
  if (length(proportion_initial) != length(stages))
    print("Number of stages or proportions is wrong!")
  if (nrow(matrices)%length(stages) != 0)
    print("Number of rows in matrix is not a multiple of stages name vector!")
  if (is.vector(Populations))
    print("There must be at least two populations!")
  if (sum(proportion_initial) > 1.02 | sum(proportion_initial) <
      0.99)
    print("Your 'proportion_initial' doesn't add to one...")
  if (is.numeric(sumweight)) {
    if (length(sumweight) != length(stages))
      print("Length of sumweight does not correpond to length of stages!")
  }
  list_names_matrices <- list()
  for (i in 1:ncol(matrices)) {
    M_name_one <- paste(colnames(matrices)[i], sep = "_")
    list_names_matrices <- c(list_names_matrices, list(M_name_one))
  }
  if (is.vector(Nichemap) | (Nichemap == "oneperiod")[1]) {
    min_dist <- sort(unique(dist(Populations[, 2:3]))) [1]
    extent <- expand.grid(X = seq(min(Populations[, "X"]),
                                  max(Populations[, "X"]), by = min_dist),
                          Y = seq(min(Populations[, "Y"]),
                                  max(Populations[, "Y"]), by = min_dist))
    Nichemap <- cbind(HScoreID = 1:nrow(extent), extent,
                     matrix(1, ncol = length(Nichemap), nrow = nrow(extent),
                              dimnames = list(NULL, paste(Nichemap))))
  }
  if (is.vector(Nichemap[, -c(1:3)])) {
    Nichemap <- Nichemap[Nichemap[, -c(1:3)] != 0, ]
  } else {
    Nichemap <- Nichemap[rowSums(Nichemap[, -c(1:3)]) != 0, ]
  }
  years_projections <- colnames(Nichemap)[4:ncol(Nichemap)]
  if ((ncol(Nichemap) - 3) != length(years_projections))
    print("Number of years of projections is not equal to the number of habitat scores!")
  colnames(Populations) <- c("PatchID", "XCOORD", "YCOORD",
                            "area_population")
  colnames(Nichemap) <- c("HScoreID", "XCOORD", "YCOORD", years_projections)

  if (max(Nichemap[, 4:ncol(Nichemap)]) > 100) {

```



```

NicheID[, 4:ncol(NicheID)] <- NicheID[, 4:ncol(NicheID)]/1000
}
if (max(NicheID[, 4:ncol(NicheID)]) > 10) {
  NicheID[, 4:ncol(NicheID)] <- NicheID[, 4:ncol(NicheID)]/100
}
NicheID <- data.frame(matrix(0, nrow = nrow(NicheID), ncol = 4))
NicheID[, 1:3] <- NicheID[, 1:3]
colnames(NicheID) <- c("Niche_ID", "X", "Y", "PopulationID")
rownames(NicheID) <- NicheID[, 1]
if (length(density_individuals) == 1) {
  density_individuals <- rep(density_individuals, times = nrow(Populations))
}
n0_all <- matrix(0, nrow = nrow(NicheID), ncol = length(stages))
destination_Nicherows <- 1:nrow(Populations)
for (pxs in 1:nrow(Populations)) {
  rows <- which(spDistsN1(as.matrix(NicheID[, 2:3], ncol = 2),
    matrix(as.numeric(Populations[pxs, 2:3]), ncol = 2),
    longlat = TRUE) == min(spDistsN1(as.matrix(
    NicheID[, 2:3], ncol = 2),
    matrix(as.numeric(Populations[pxs, 2:3]), ncol = 2),
    longlat = TRUE)))
  NicheID[rows, 4] <- Populations[pxs, 1]
  n0_all[rows[1], ] <- n0_all[rows[1], ] + (Populations[pxs, 4] * proportion_initial *
  density_individuals[pxs])
  destination_Nicherows[pxs] <- rows[1]
}
Niche_values <- as.matrix(NicheID[, 4:(length(years_projections) +
  3)], ncol = length(years_projections))
if (is.numeric(K)) {
  populationmax_all <- matrix(mean(K), ncol = length(years_projections),
    nrow = nrow(NicheID))
  colnames(populationmax_all) <- years_projections
  rownames(populationmax_all) <- NicheID[, "Niche_ID"]
}
if (length(K) == 1) {
  populationmax_all <- matrix(K, ncol = length(years_projections),
    nrow = nrow(NicheID))
}
if (length(K) == nrow(Populations)) {
  populationmax_all <- matrix(0, ncol = length(years_projections),
    nrow = nrow(NicheID))
  for (rx in 1:length(destination_Nicherows)) {
    populationmax_all[destination_Nicherows[rx], ] <- populationmax_all[destination_N
    icherows[rx],
    ] + K[rx]
  }
  populationmax_all[populationmax_all == 0] <- mean(K)
}
if (length(K) == length(years_projections)) {
  populationmax_all[rowSums(n0_all) == 0, ] <- matrix(K,
    ncol = length(years_projections),
    nrow = nrow(NicheID) - nrow(Populations))
  populationmax_all[rowSums(n0_all) > 0, ] <- matrix(K,
    ncol = length(years_projections), nrow = nrow(Populations), byrow = TRUE)
}
if (length(dim(K)) == 2) {
  populationmax_all[, ] <- matrix(colMeans(K), ncol = length(years_projections),
    nrow = nrow(NicheID), byrow = TRUE)
  populationmax_all[rowSums(n0_all) > 0, ] <- K }
if (is.null(K)) {
  populationmax_all <- matrix("no_K", ncol = length(years_projections),
    nrow = nrow(NicheID))
}
dist_latlong <- round(as.matrix(dist(NicheID[1:(length(unique(NicheID[, 2]))+2), 2:3
  ])), 1)

```

```

neigh_index <- sort(unique(as.numeric(dist_latlong[1,])))[2:3] #distance two closest
cells
if (sumweight[1] == "all_stages")
  sumweight <- rep(1, length(proportion_initial))
if (Kweight[1] == "FALSE")
  Kweight <- rep(1, length(proportion_initial))
if (transition_affected_env[1] == "all")
  transition_affected_env <- which(matrices[, 1] > 0)
if (transition_affected_niche[1] == "all")
  transition_affected_niche <- which(matrices[, 1] > 0)
if (transition_affected_demogr[1] == "all")
  transition_affected_demogr <- which(matrices[, 1] > 0)
if (any(matrices < 0))
  print("There are some negative rates in the transition matrices!")
if (any(matrices_var < 0))
  print("There are some negative rates in the standard deviation transition matrices!")
")
if (max(transition_affected_niche) > nrow(matrices)) {
  print("Stages affected by Habitat suitability values does not comply with the size
of matrix! Not that the matrix is made with 'byrow = FALSE")
}
if (max(transition_affected_env) > nrow(matrices)) {
  print("Stages affected by environmental stochasticity does not comply with the size
of matrix! Note that the matrix is made with 'byrow = FALSE")
}
if (max(transition_affected_demogr) > nrow(matrices)) {
  print("Stages affected by demographic stochasticity does not comply with the size o
f matrix! Note that the matrix is made with 'byrow = FALSE")
}
BEMDEM <- list(Orig_Populations = Populations, Niche_ID = Niche_ID,
  Niche_values = Niche_values, years_projections = years_projections,
  matrices = matrices, matrices_var = matrices_var,
  prob_scenario = prob_scenario, noise = noise, stages = stages,
  proportion_initial = proportion_initial,
  density_individuals = density_individuals,
  fraction_LDD = fraction_LDD, fraction_SDD = fraction_SDD,
  dispersal_probabilities = dispersal_probabilities,
  dist_latlong = dist_latlong, neigh_index = neigh_index,
  no_yrs = no_yrs, K = K, Kweight = Kweight,
  populationmax_all = populationmax_all,
  n0_all = n0_all, list_names_matrices = list_names_matrices,
  sumweight = sumweight,
  transition_affected_env = transition_affected_env,
  transition_affected_niche = transition_affected_niche,
  transition_affected_demogr = transition_affected_demogr,
  env_stochas_type = env_stochas_type,
  dispersal_probabilities = dispersal_probabilities )
assign(modelname, BEMDEM, envir = .GlobalEnv)
eval(parse(text = paste("save(", modelname, ", file='", modelname,
  ".rda'", sep = "")))
}

```

FUNCTION TO RUN THE DEMOGRAPHIC MODEL

```

demoniche_population_function<-function (Matrix_projection, Matrix_projection_var, n, p
opulationmax,
  K = NULL, Kweight = BEMDEM$Kweight, onepopulation_Niche,
  sumweight, noise, prob_scenario, prev_mx, transition_affected_demogr,
  transition_affected_niche, transition_affected_env, env_stochas_type,
  yx_tx)
{

```

```

prob_scenario_noise <- c(prob_scenario[prev_mx[yx_tx]] *
                        noise, 1 - (prob_scenario[prev_mx[yx_tx]] * noise))
rand_mxs <- sample(1:2, 1, prob = prob_scenario_noise, replace = TRUE)

one_mxs <- Matrix_projection[, rand_mxs]
prev_mx[yx_tx + 1] <- rand_mxs
if (Matrix_projection_var[1] != FALSE) {
  one_mxs_var <- one_mxs * (Matrix_projection_var[, rand_mxs])
  if (is.numeric(transition_affected_niche)) {
    one_mxs[transition_affected_niche] <- one_mxs[transition_affected_niche] *
      onepopulation_Niche
  }
  if (is.numeric(transition_affected_env)) {
    switch(EXPR = env_stochas_type, normal = one_mxs[transition_affected_env] <- rnorm(
length(one_mxs[transition_affected_env]),
mean = one_mxs[transition_affected_env], sd = one_mxs_var[transition_affected_env]),
lognormal = one_mxs[transition_affected_env] <- rlnorm(length(one_mxs[tran
sition_affected_env]),
meanlog = one_mxs[t
ransition_affected_env],
sdlog = one_mxs_var
[transition_affected_env]))
  }
}
one_mxs[one_mxs < 0] <- 0 #changing any negative values to zero
A <- matrix(one_mxs, ncol = length(n), nrow = length(n),
byrow = FALSE)
Atest <- A
Atest[1, ][-1] <- 0 #getting fertility values
if (sum(colSums(Atest) > 1)) { #picking out survival scores higher than 1
  for (zerox in which(colSums(Atest) > 1)) {
    Atest[, zerox] <- Atest[, zerox]/sum(Atest[, zerox])
  }
  A[-1, ] <- Atest[-1, ] #changing survival values
}
n[is.na(n)] <- 0
n <- as.vector(A %% n) #n is the number of ibex in each stage of the matrix - a r
ow from n0s which is all of the populations - here it is multiplied by the matrix
n <- floor(n)

if (sum(n) > 0) {
  if (is.numeric(populationmax)) {
    if (sum(n * Kweight) > populationmax) {
      n <- n * (populationmax/sum(n * sumweight)) #where carrying capacity comes in
- brings n back down to carrying capacity
    }
  }
}
print(sum(n))
return(n)
}

```

FUNCTION TO RUN THE DISPERSAL MODEL

```

dispersal_faster_csv <- function (seeds_per_population, fraction_LDD, fraction_SDD,
dispersal_probabilities, dist_latlong, neigh_index,
niche_values, stages)
{
  seeds_per_population_migrate_LDD <- round(seeds_per_population * fraction_LDD)
  seeds_per_population_migrate_SDD <- round(seeds_per_population * fraction_SDD)
  seeds_per_population_new_SDD <- seeds_per_population_new_LDD <- matrix(0, nrow = nrow
(seeds_per_population), ncol = ncol(seeds_per_population))
}

```

```

if (fraction_SDD > 0) {
  source_patches <- which(colSums(seeds_per_population_migrate_SDD) > 0)
  for (px_orig in source_patches) {
    for (pxdisp_new in 1:length(seeds_per_population_migrate_SDD[1,])) {
      if (dist_latlong[pxdisp_new, px_orig] == neigh_index[1]) {
        seeds_per_population_new_SDD[,pxdisp_new] <- round(seeds_per_population_new_S
DD[,pxdisp_new] + (seeds_per_population_migrate_SDD[,px_orig] * 0.2))
      }
      if (length(neigh_index) == 2) {
        if (dist_latlong[pxdisp_new, px_orig] == neigh_index[2]) {
          seeds_per_population_new_SDD[,pxdisp_new] <- round(seeds_per_population_new
_SDD[,pxdisp_new] + (seeds_per_population_migrate_SDD[,px_orig] * 0.05))
        }
      }
    }
  }
}

if (fraction_LDD > 0) {

  source_patches_ldd<-which(colSums(seeds_per_population_migrate_LDD)>0)

  disp_prob<-dispersal_probabilities

  sample_ages<-function(x, dp){
    new_patches<-sample(1:length(dp),x,prob=dp, replace =TRUE)
    return(new_patches)
  }

  disp_out<-function(stg,seeds_new, stage_out){

    a<-data.frame(table(stage_out[[stg]])) #slowness
    a$Var1<-as.numeric(as.character(a$Var1))
    a$Freq<-as.numeric(as.character(a$Freq))

    if (nrow(a)>0){
      seeds_new[stg,a$Var1]<-seeds_new[stg,a$Var1] +a$Freq
    } else {
      seeds_new[stg,]<-seeds_new[stg,]
    }
    return(seeds_new[stg,])
  }

  dispersal<-function(j, seeds_ldd, disp_prob){

    dp<-disp_prob[j,]
    print(j)
    ages<-matrix(seeds_ldd[,j], ncol = 1)
    stage_out<-lapply(X = ages, FUN = sample_ages, dp = dp )
    st<-as.matrix(1:length(stage_out))

    if(length(stage_out)>0){
      seeds_new_out<-sapply( X = st,FUN = disp_out, seeds_new = seeds_new, stage_
out = stage_out)
      #seeds_newt<-t(seeds_new_out)

      return(seeds_new_out)

    } else {

      return(seeds_new)

    }
  }
}

```

```

seeds_new<-seeds_per_population_new_LDD

source_patches<-as.matrix(source_patches_ldd, ncol = 1)

check_disp<-apply(X = source_patches,1, FUN = dispersal, seeds_ldd = seeds_per_population_migrate_LDD, disp_prob = disp_prob)

seeds_per_population_new_LDD<-matrix(rowSums(check_disp), ncol = ncol(seeds_per_population_new_LDD) , nrow = length(stages), byrow = T)

print(paste("no. source_patches ", length(source_patches_ldd), sep=""))
print(paste("no. to migrate ",sum(colSums(seeds_per_population_migrate_LDD)), sep=""))
print(paste("no. which migrated ", sum(colSums(seeds_per_population_new_LDD)), sep=""))

}

seeds_stay <- (seeds_per_population - seeds_per_population_migrate_SDD - #seeds that migrate must go out of the cell and are taken off the total
seeds_per_population_migrate_LDD)
print(sum(seeds_stay+ seeds_per_population_new_SDD + seeds_per_population_new_LDD))

return(seeds_stay + seeds_per_population_new_SDD + seeds_per_population_new_LDD)
}

```

FUNCTION TO RUN THE COUPLED NICHE-DEMOGRAPHIC MODEL

```

demoniche_model_csv<-function (modelname, Niche, Dispersal, repetitions, foldername)
{
  BEMDEM <- get(modelname, envir = .GlobalEnv)
  require(popbio)
  require(lattice)
  Projection <- array(0, dim = c(BEMDEM$no_yrs, length(BEMDEM$stages),
                                nrow(BEMDEM$Niche_ID),
                                length(BEMDEM$years_projections)),
                      dimnames = list(paste("timesliceyear",
                                             1:BEMDEM$no_yrs,sep = "_"),
                                       c(paste(BEMDEM$stages),
                                         BEMDEM$Niche_ID[, "Niche_ID"],
                                         paste(BEMDEM$years_projections)))

  eigen_results <- vector(mode = "list", length(BEMDEM$list_names_matrices))
  names(eigen_results) <- unlist(BEMDEM$list_names_matrices)
  yrs_total <- BEMDEM$no_yrs * length(BEMDEM$years_projections)
  population_sizes <- array(NA, dim = c(yrs_total,
                                         length(BEMDEM$list_names_matrices),repetitions),
                            dimnames = list(paste("year", 1:yrs_total,sep = ""),
                                             BEMDEM$list_names_matrices,
                                             paste("rep", 1:repetitions, sep = "_")))

  population_results <- array(1:200, dim = c(yrs_total, 4,
                                             length(BEMDEM$list_names_matrices)),
                              dimnames = list(paste("year", 1:yrs_total, sep = ""),
                                              c("Meanpop", "SD", "Max", "Min"),
                                              paste(BEMDEM$list_names_matrices)))

  metapop_results <- array(NA, dim = c(yrs_total,
                                       length(BEMDEM$list_names_matrices), repetitions),
                           dimnames = list(paste("year", 1:yrs_total,sep = ""),
                                             BEMDEM$list_names_matrices, paste("rep", 1:repetitions,
                                             sep = "_")))

  simulation_results <- array(NA, dim = c(length(BEMDEM$list_names_matrices),
                                           7 + length(BEMDEM$years_projections)),
                              dimnames = list(BEMDEM$list_names_matrices,
                                              c("lambda", "stoch_lambda", "mean_perc_ext_final",

```

```

        "initial_population_area",initial_population",
        "mean_final_pop", "mean_no_patches_final",
        paste("EMA", BEMDEM$years_projections)))
EMA <- array(0, dim = c(repetitions, length(BEMDEM$list_names_matrices),
        length(BEMDEM$years_projections), 2), dimnames = list(
        paste("rep", 1:repetitions, sep = "_"),
        BEMDEM$list_names_matrices,BEMDEM$years_projections,
        c("EMA", "No_populations")))
population_Niche <- rep(1, nrow(BEMDEM$Niche_ID))
simulation_results[, "initial_population_area"] <- sum(BEMDEM$Orig_Populations
[, "area_population"])
simulation_results[, "initial_population"] <- round(sum(colSums(BEMDEM$n0_all)
* BEMDEM$sumweight), 0)
dir.create(paste(getwd(), "/", foldername, sep = ""), showWarnings = FALSE)
for (rx in 1:repetitions) {
  print(paste("Starting projections for repetition:", rx),
        quote = FALSE)
  for (mx in 1:length(BEMDEM$list_names_matrices)) {
    print(paste("Projecting for scenario/matrix:",
    (BEMDEM$list_names_matrices)[mx]),
        quote = FALSE)
    yx_tx <- 0
    Matrix_projection <- cbind(BEMDEM$matrices[, 1],
        (BEMDEM$matrices[, mx]))
    if (BEMDEM$matrices_var[1] != FALSE) {
      if (ncol(BEMDEM$matrices_var) > 1) {
        Matrix_projection_var <- cbind(BEMDEM$matrices_var[, 1],
        (BEMDEM$matrices_var[, mx]))
      } else {
        Matrix_projection_var <- cbind(BEMDEM$matrices_var[,1],
        (BEMDEM$matrices_var[, 1]))
      }
    } else {
      Matrix_projection_var <- FALSE
    }
    prev_mx <- rep(1, times = yrs_total + 1)
    for (tx in 1:length(BEMDEM$years_projections)) {
      # print(tx)
      if (Niche == TRUE) {
        population_Niche <- BEMDEM$Niche_values[, tx]
      }
      for (yx in 1:BEMDEM$no_yrs) {
        yx_tx <- yx_tx + 1
        if (tx == 1 && yx == 1) {
          n0s <- BEMDEM$n0_all[rowSums(BEMDEM$n0_all) >
          0, ]
          n0s_ID <- which(rowSums(BEMDEM$n0_all) >
          0)
        } else {
          if (tx != 1 && yx == 1) {
            ###added by me###
            paste(sum(is.na(Projection[BEMDEM$no_yrs, , , tx - 1])), " NAs")
            Projection[BEMDEM$no_yrs, , , tx - 1][is.na(Projection[BEMDEM$no_y
rs, , , tx - 1])<-0
            #####
            n0s <- t(Projection[BEMDEM$no_yrs, , colSums(Projection[BEMDEM$no_
yrs, , , tx - 1]) > 0, tx - 1])
            n0s_ID <- which(colSums(Projection[BEMDEM$no_yrs, , , tx - 1]) > 0
)
          } else {
            n0s <- t(Projection[yx - 1, , colSums(Projection[yx - 1, , , tx]) >
0, tx])
            n0s_ID <- which(colSums(Projection[yx - 1, , , tx]) > 0)
          }
        }
      }
    }
  }
  population_Niche_short <- population_Niche[n0s_ID]

```

```

    if (nrow(n0s) > 0) {
      for (px in 1:nrow(n0s)) {
        n <- as.vector(n0s[px, ])
        populationmax <- BEMDEM$populationmax_all[n0s_ID[px], tx]
        #added by FS
        populationmax[is.na(populationmax)] <- min(BEMDEM$populationmax_all)
        ##
        Projection[yx, , n0s_ID[px], tx] <- demoniche_population_function(
Matrix_projection = Matrix_projection, Matrix_projection_var = Matrix_projection
_var, n = n, populationmax = populationmax, onepopulation_Niche = population_Nic
he_short[px], sumweight = BEMDEM$sumweight, Kweight = BEMDEM$Kweight, prob_scena
rio = BEMDEM$prob_scenario, noise = BEMDEM$noise, prev_mx = prev_mx, transition_
affected_demogr = BEMDEM$transition_affected_demogr, transition_affected_niche =
BEMDEM$transition_affected_niche, transition_affected_env = BEMDEM$transition_a
ffected_env, env_stochas_type = BEMDEM$env_stochas_type, yx_tx = yx_tx)
      }
    }
    metapop_results[yx_tx, mx, rx] <- length(intersect(which(colSums(Proje
ction[yx, , , tx]) > 1), n0s_ID))
    if (sum(Projection[yx, , , tx]) > 0) {
      if (Dispersal == TRUE) {
        if (Niche == TRUE) {
          population_Niche <- BEMDEM$Niche_values[, tx]
        }
        print(paste("Year ", tx+1849, sep=""))
        disp <- dispersal_faster_csv(seeds_per_population =
Projection[yx,, , tx], fraction_LDD = BEMDEM$fraction_LDD,
dispersal_probabilities = BEMDEM$dispersal_probabilities,
dist_latlong = BEMDEM$dist_latlong,
neigh_index = BEMDEM$neigh_index,
fraction_SDD = BEMDEM$fraction_SDD,
niche_values = population_Niche, stages = BEMDEM$stages)
        Projection[yx, , , tx] <- disp #age here 0 years/seed
      }
    }
    population_sizes[yx_tx, mx, rx] <- sum(rowSums(Projection[yx,, , tx])
* BEMDEM$sumweight)
  }
  EMA[rx, mx, tx, 1] <- min(apply((Projection[, , , tx] * BEMDEM$sumweight
), 1, sum))
  EMA[rx, mx, tx, 2] <- sum(colSums(Projection[yx, , , tx]) > 1)
  simulation_results[mx, 7 + tx] <- mean(EMA[, mx, tx, 1])
}
pop <- data.frame(cbind(BEMDEM$Niche_ID[, 2:3], (colSums(Projection[yx,,,]
* BEMDEM$sumweight))))

print(sum(pop))
write.csv(pop, paste(getwd(), "/", foldername, "/", BEMDEM$list_names_matri
ces[mx], "_pop_output.csv", sep=""))
}
}
rm(Projection)
print("Calculating summary values", quote = FALSE)
for (mx in 1:length(BEMDEM$list_names_matrices)) {
  for (yx_tx in 1:yrs_total) {
    population_results[yx_tx, "Meanpop", mx] <- mean(population_sizes[yx_tx,
mx, ])
    population_results[yx_tx, "SD", mx] <- sd(population_sizes[yx_tx,
mx, ])
    population_results[yx_tx, "Min", mx] <- min(population_sizes[yx_tx,
mx, ])
    population_results[yx_tx, "Max", mx] <- max(population_sizes[yx_tx,
mx, ])
  }
}
return(population_results)
}

```